

An Adaptive Model Selection Framework for Demand Forecasting under Horizon-Induced Degradation to Support Business Strategy and Operations

Adolfo González^{1*}

Víctor Parada^{2*}

^{1,2} Department of Computer Engineering and Informatics, Faculty of Engineering,
University of Santiago Chile

Abstract

Business environments characterized by structural demand intermittency, high variability, and multi-step planning horizons require robust and reproducible model selection mechanisms. Empirical evidence shows that no forecasting model is universally dominant and that relative rankings vary across error metrics, demand regimes, and forecast horizons, generating ambiguity in multi-SKU decision contexts. This study proposes AHSIV (Adaptive Hybrid Selector for Intermittency and Variability), a horizon-aware and regime-conditioned model selection framework designed to address horizon-induced ranking instability. The proposed approach integrates scaled and absolute error metrics adjusted through a Metric Degradation by Forecast Horizon (MDFH) procedure, structural demand classification, multi-objective Pareto dominance, and hierarchical bias refinement within a unified decision architecture. The empirical evaluation is conducted on the Walmart, M3, M4, and M5 datasets under multiple train–test partition schemes and twelve-step forecasting horizons. Results indicate that AHSIV achieves statistical equivalence with the strongest monometric baseline in terms of aggregated performance while increasing the frequency of horizon-specific best-model selection. The findings demonstrate that model selection in heterogeneous demand environments cannot be treated as a static ranking problem, and that horizon-consistent, structurally adaptive mechanisms provide a principled, operationally coherent solution for multi-SKU forecasting.

Keywords: Model selection; Forecast horizon degradation; Intermittent demand; Multi-SKU forecasting; Inventory strategy

* Corresponding author

1 E-Mail: adolfo.gonzalez.c@usach.cl; <https://orcid.org/0009-0008-4452-1285>

2 E-Mail: victor.parada@usach.cl; <https://orcid.org/0000-0002-8649-5694>

1. Introduction

In increasingly competitive and volatile business environments, the ability to anticipate future demand behavior has become central to strategic decision-making. In line with Porter's (1998) competitive strategy framework, sustained competitive advantage depends on coherent operational decisions aligned with strategic positioning. Within this context, demand forecasting transcends purely statistical estimation and operates as a critical mechanism for inventory planning, capital allocation, and integrated supply chain coordination (Bassiouni, Chakrabortty, Sallam, & Hussain, 2024; Huber, Gossmann, & Stuckenschmidt, 2017; Garred, Oger, & Lauras, 2026). Empirical evidence consistently demonstrates that the quality of forecasting processes directly affects operational efficiency, financial performance, and strategic stability, particularly in environments characterized by demand volatility, structural disruptions, and asymmetric cost structures associated with overstocking and stockouts (Abolghasemi, Beh, Tarr, & Gerlach, 2020; Goltzos, Syntetos, Glock, & Ioannou, 2022; Silver, Pyke, Peterson, & others, 1998; Theodorou, Spiliotis, & Assimakopoulos, 2025). Consequently, improving forecast accuracy is not merely a technical objective but a strategic imperative that influences working capital exposure, service levels, and long-term organizational performance.

From a managerial standpoint, forecasted demand represents a forward-looking commitment of financial resources. Consequently, deviations between predicted and realized volumes generate differentiated economic impacts that affect working capital, service levels, and supply stability. While traditional accuracy metrics such as MAE, RMSE, and RMSSE quantify local predictive precision, they do not necessarily capture aggregate volumetric coherence between projected and observed demand. To address this strategic dimension, this study incorporates the Global Relative Accuracy (GRA) metric, which evaluates the relative alignment between total forecasted and realized demand volumes, thereby linking predictive performance with inventory investment efficiency (Badulescu, Hameri, & Cheikhrouhou, 2021; Nowotarski & Weron, 2015; Theodorou, Spiliotis, & Assimakopoulos, 2025).

Despite the recognized importance of forecast accuracy, selecting an appropriate forecasting model for each SKU remains a complex methodological challenge. Large-scale empirical evidence from forecasting competitions demonstrates that no single model consistently dominates across datasets, structural conditions, and planning horizons (Makridakis, Spiliotis, & Assimakopoulos, 2018; Makridakis, Spiliotis, & Assimakopoulos, 2022; Nowotarski & Weron, 2015). Moreover, different performance metrics frequently produce conflicting model rankings, complicating objective and reproducible selection processes (Badulescu, Hameri, & Cheikhrouhou, 2021; Poler & Mula, 2011). In practice, organizations are often compelled to adopt a single model even when evaluation indicators provide ambiguous signals, leading to decisions influenced by heuristics rather than systematic criteria (Petropoulos, Kourentzes, Nikolopoulos, & Siemsen, 2018; Aidoo-Anderson, Polychronakis, Sapountzis, & Kelly, 2025).

This problem is further amplified in multi-step forecasting contexts. Forecast error typically increases with the length of the prediction horizon due to the accumulation of innovations and structural uncertainty (Hyndman & Athanasopoulos, 2021; Chatfield, 2000). Importantly, model rankings may vary substantially across horizons, revealing the horizon-dependent nature of predictive performance (Tashman, 2000). Evaluations based solely on short-term test windows may therefore generate

optimistic or misleading conclusions when models are deployed for longer planning horizons. Furthermore, inference about projected differences and scenario comparisons requires structural invariance conditions to hold, as violations of invariance may invalidate horizon-based extrapolations (Hendry & Pretis, 2023). Consequently, model selection cannot be treated as a static ranking problem; it must explicitly account for the degradation in predictive accuracy as the forecast horizon extends.

Although prior research has proposed multicriteria and automated selection approaches (Poler & Mula, 2011; Wang, Hyndman, Li, & Kang, 2023; Abdallah et al., 2025), existing frameworks typically evaluate models using fixed-horizon metrics and incorporate structural characteristics descriptively rather than embedding them within adaptive, reproducible decision mechanisms. In addition, the presence of structural breaks, demand intermittency, and regime shifts, such as those observed during major disruptions, further complicates the stability of forecasting models and challenges traditional evaluation paradigms (Riachy et al., 2025; Santa Cruz & Corrêa, 2017). There remains a methodological gap in integrating (i) horizon-dependent error behavior, (ii) structural properties of demand series such as intermittency and variability (Santa Cruz & Corrêa, 2017), and (iii) business-oriented volumetric coherence criteria within a unified selection framework.

In response to this gap, the present study proposes the Adaptive Hybrid Selector for Intermittency and Variability (AHSIV), a multicriteria, structure-adaptive model selection strategy explicitly designed for multi-horizon demand forecasting. The proposed framework operates on performance metrics adjusted via the Metric Degradation by Forecast Horizon (MDFH) procedure, which projects test-based error measures to future planning horizons to ensure coherent inter-model comparison under horizon extension while preserving structural consistency conditions (Hendry & Pretis, 2023). By combining horizon-adjusted accuracy metrics, structural regime identification, and volumetric coherence assessment, AHSIV aims to identify, for each SKU, the forecasting model that balances local precision, structural stability, and planning consistency across the decision horizon.

Through this approach, model selection is repositioned as a structured decision problem grounded in adaptive performance evaluation rather than as a purely statistical ranking exercise. The proposed methodology contributes to the literature by formalizing horizon-aware model comparison, integrating business-aligned aggregate accuracy criteria, and providing a reproducible multicriteria framework suitable for heterogeneous demand environments.

The present study contributes to the forecasting and model selection literature by reframing model selection as a horizon-aware, structurally adaptive decision problem rather than a static ranking task evaluated at a single test horizon. While prior research has documented metric inconsistency, horizon dependence, and the absence of universally dominant forecasting models, a formal integration of these elements within a unified selection framework remains underdeveloped. Specifically, this study makes three primary contributions. First, it formalizes the Metric Degradation by Forecast Horizon (MDFH) procedure, which projects out-of-sample error metrics toward future decision horizons under structural stability constraints, thereby enabling consistent inter-model comparison across multi-step contexts. Second, it proposes the Adaptive Hybrid Selector for Intermittency and Variability (AHSIV), which integrates structural demand classification with multi-objective dominance logic and conservative, scaled-error minimization under high-interruption regimes. Third, it incorporates systematic bias minimization as a lexicographic refinement criterion, directly linking

predictive evaluation with asymmetric inventory cost implications. Through this integration, model selection is repositioned as a structured, regime-sensitive, and horizon-consistent decision mechanism suitable for heterogeneous multi-SKU environments.

2. Literature Review

Demand forecasting has been widely recognized as a critical component of operational and financial efficiency in organizations, particularly in contexts where inventory management represents a significant proportion of working capital. The literature has demonstrated that the quality of forecasting processes directly affects key performance indicators such as logistics costs, service levels, and overall profitability, contributing to better alignment between inventory policies and operational and strategic objectives (Mentzer & Moon, 2004). In this regard, forecasting transcends its purely technical character and consolidates as a fundamental tool for efficient purchasing planning, replenishment, and resource allocation, directly impacting supply chain efficiency and organizational competitiveness (González, 2020; Goltzos, Syntetos, Glock, & Ioannou, 2022; Sousa & Miguéis, 2025; Garred, Oger, & Lauras, 2026; Theodorou, Spiliotis, & Assimakopoulos, 2025; Efendigil & Kahraman, 2009). Recent studies in industrial and retail environments confirm that marginal improvements in forecast accuracy may translate into significant reductions in inventory costs and sustained improvements in service levels, particularly in large-scale multi-SKU systems (Hammam, El-Kharbotly, & Sadek, 2025; Paranthaman, Perera, Thalagala, & Kosgoda, 2025; Theodorou, Spiliotis, & Assimakopoulos, 2025).

From the perspective of operations theory, the relationship between forecast accuracy and organizational performance is reinforced by asymmetric cost structures in inventory systems, where holding, obsolescence, and stockout costs exert differentiated effects on operational efficiency. Empirical evidence shows that overestimation and underestimation errors generate economically and operationally asymmetric consequences, affecting supply chain performance and service level fulfillment (Ulrich, Jahnke, Langrock, Pesch, & Senge, 2022; Erjiang, Yu, Tian, & Tao, 2022; Silver, Pyke, Peterson, & others, 1998). In environments characterized by high volatility and uncertainty, even marginal deviations between actual and estimated demand may amplify along the supply chain, leading to persistent economic inefficiencies and sustained degradation of service levels (Goodwin, Hoover, Makridakis, Petropoulos, & Tashman, 2023; Riachy et al., 2025). This has motivated the development of forecasting approaches explicitly oriented toward decision-making and the economic evaluation of forecast error (Kumar, Maheswari, Raman, Iniyavan, & Hashim, 2025; Hammam, El-Kharbotly, & Sadek, 2025; Garred, Oger, & Lauras, 2026).

The literature converges on the view that no demand forecasting model is universally superior or optimal across all contexts, time series types, and planning horizons. Large-scale comparative studies, particularly the M competitions, have shown that the relative performance of models varies significantly depending on the forecasting horizon, the statistical structure of the series, and the metric used to evaluate error, generating unstable rankings among statistical, machine learning, and deep learning approaches (Makridakis, Spiliotis, & Assimakopoulos, 2018; Makridakis & Petropoulos, 2020; Makridakis, Spiliotis, & Assimakopoulos, 2022; Makridakis et al., 2025; Hendry & Pretis, 2023). Subsequent studies in real business contexts confirm that these approaches may exhibit divergent behavior even on the same dataset, depending on demand patterns, evaluation criteria, and operational objectives (Petropoulos, Wang, & Disney, 2019; Negre, Alonso, Prieto, García, & de-la-

Fuente-Valentín, 2024; Wang, Hyndman, Li, & Kang, 2023; Flyckt & Lavesson, 2025; Giannopoulos, Dasaklis, Tsantilis, & Patsakis, 2025; Peláez-Rodríguez, Pérez-Aracil, Fister, Torres-López, & Salcedo-Sanz, 2024).

A central aspect of forecasting model selection is the diversity of performance metrics used to evaluate predictive accuracy, as measures such as MAE, RMSE, MAPE, and R^2 capture distinct dimensions of error and exhibit different sensitivities to outliers, scale, and series variability (Hyndman & Athanasopoulos, 2021). Consequently, the same model may be considered optimal under one criterion and suboptimal under another, generating inconsistent rankings and decision ambiguity, a phenomenon extensively documented in both methodological and empirical literature (Badulescu, Hameri, & Cheikhrouhou, 2021; Nowotarski & Weron, 2015; Makridakis, Spiliotis, & Assimakopoulos, 2018; Makridakis & Petropoulos, 2020; Makridakis, Spiliotis, & Assimakopoulos, 2022). Empirical studies indicate that this inconsistency persists even when advanced models and extensive metric sets are employed, highlighting the absence of universally stable selection criteria and reinforcing the need for more structured and systematic selection approaches (Pesendorfer, Schiraldi, & Silva-Junior, 2023; Wang, Hyndman, Li, & Kang, 2023; Aidoo-Anderson, Polychronakis, Sapountzis, & Kelly, 2025).

Complementarily, the literature documents the use of Mean Absolute Error (MAE) and Mean Absolute Scaled Error (MASE) as operational criteria for discriminating and selecting demand forecasting models, particularly in contexts characterized by structural heterogeneity and intermittent demand. Unlike quadratic metrics, MAE penalizes errors linearly, facilitating direct interpretation of the expected average deviation in the same units as the analyzed system—a characteristic particularly valued in operational and managerial contexts (Katrinos & Daskalaki, 2015; Mancuso & Werner, 2019; Bandeira, Alcalá, Vita, & Barbosa, 2020). Empirical evidence shows that MAE-based rankings may differ substantially from those derived from RMSE, particularly in high-variability or outlier-prone scenarios, where the economic impact of error is approximately proportional to its absolute magnitude (Santa Cruz & Corrêa, 2017; Doszyń & Dudek, 2024).

In multi-SKU (Stock Keeping Unit) and multi-series settings, where comparison across demands of different scales is critical, MASE has been proposed as a natural extension of MAE, normalizing error relative to a naïve benchmark model and enabling consistent cross-series comparisons (Hyndman & Athanasopoulos, 2021). Empirical findings suggest that selection criteria based on MAE or MASE lead to more stable and robust decisions than those grounded in quadratic metrics, especially in multi-series contexts where economic impact is directly associated with accumulated absolute error (Bandeira, Alcalá, Vita, & Barbosa, 2020; Makridakis, Spiliotis, & Assimakopoulos, 2018; Makridakis & Petropoulos, 2020; Song, Chang, Gao, Huang, & Ye, 2025).

Beyond error magnitude, the literature distinguishes metrics that capture the systematic direction of forecast error. While metrics such as MAE, RMSE, or sMAPE quantify forecast accuracy, they do not identify persistent tendencies toward overestimation or underestimation. To address this dimension, bias-related metrics such as BIAS or Mean Forecast Error (MFE) have been proposed to detect systematic errors and their dominant direction (Hyndman & Koehler, 2006). Empirical evidence documents that forecast bias has direct operational and economic implications, as sustained overestimation increases the risk of overstocking, whereas recurrent underestimation elevates the

probability of stockouts and service level degradation (Carboneau, Laframboise, & Vahidov, 2008; Sanders & Graman, 2016; Zhao, Xie, Ai, Yang, & Zhang, 2023).

The complexity of predictive performance evaluation intensifies in multi-SKU contexts, where heterogeneity in scale and variability patterns complicates direct comparison among models. To mitigate this issue, scaled metrics such as RMSSE and MASE have been widely adopted in forecasting competitions to enable cross-series comparisons across different magnitudes (Makridakis, Spiliotis, & Assimakopoulos, 2018). Nevertheless, empirical evidence reveals persistent contradictions among evaluation criteria and inconsistent rankings across different forecasting horizons, leading to the conclusion that no single metric is sufficient to comprehensively capture predictive performance and that multidimensional evaluation approaches are recommended (Petropoulos et al., 2022; Giannopoulos, Dasaklis, Tsantilis, & Patsakis, 2025; Hendry & Pretis, 2023).

The literature further establishes that forecast error depends explicitly on the forecasting horizon, tending to increase as projections extend into unobserved future periods, particularly in series exhibiting temporal dependence, heteroscedasticity, or structural changes (Hyndman & Athanasopoulos, 2021; Makridakis & Petropoulos, 2020; Riachy et al., 2025). This error growth is often described through nonlinear relationships or power-law-type approximations, reflecting progressive degradation of predictive capacity at longer horizons (Chatfield, 2000). Accordingly, explicit mechanisms for adjusting or degrading metrics such as RMSE, RMSSE, or MAE as a function of the future horizon have been proposed to avoid overly optimistic interpretations based on short-term evaluations (Petropoulos et al., 2022; Lazcano, Sandubete, & Jaramillo-Morán, 2025; Hendry & Pretis, 2023).

From an inventory management perspective, the literature recognizes that demand forecasts translate directly into inventory volumes acquired in advance to satisfy future demand (Mentzer & Moon, 2004). In this context, several studies argue that predictive performance evaluation should not be limited to local error measures but should incorporate an aggregated perspective considering the coherence between total projected volume and total observed volume, particularly when purchasing and replenishment decisions are executed in consolidated form (Sepúlveda-Rojas, Rojas, Valdés-González, & San Martín, 2015; Ulrich, Jahnke, Langrock, Pesch, & Senge, 2022; Kumar, Maheswari, Raman, Iniyavan, & Hashim, 2025; Theodorou, Spiliotis, & Assimakopoulos, 2025). Within this framework, aggregated metrics aimed at capturing the global economic impact of forecasting and its alignment with inventory planning have been proposed (Nowotarski & Weron, 2015; Goltzos, Syntetos, Glock, & Ioannou, 2022; Abdallah et al., 2025), which should be complemented with traditional error metrics for comprehensive evaluation.

Finally, the literature identifies the inherent structure of the demand series as a determinant factor in forecasting model performance, particularly in series characterized by intermittency, high variability, or structural changes, which pose significant challenges for traditional approaches (Syntetos & Boylan, 2005; Syntetos, Boylan, & Croston, 2005; Makridakis, Spiliotis, & Assimakopoulos, 2018). Although research emphasizes the need to explicitly characterize these properties to adapt model selection and evaluation criteria (Petropoulos et al., 2022; Shi, Ding, Qu, & Xie, 2026), evidence suggests that such characteristics are often incorporated descriptively or ex post, rather than

systematically integrated into formal, adaptive, and reproducible model selection processes (Paranthaman, Perera, Thalagala, & Kosgoda, 2025; Giannopoulos, Dasaklis, Tsantilis, & Patsakis, 2025; Aidoo-Anderson, Polychronakis, Sapountzis, & Kelly, 2025).

In summary, the specialized literature indicates that no universally dominant demand forecasting model exists; that evaluation metrics yield contradictory signals; that predictive performance depends on both the forecasting horizon and the underlying series structure; and that forecasting decisions carry direct economic implications for inventory management. However, a systematic, adaptive, and replicable framework capable of selecting, at the level of each individual demand series, a forecasting model that coherently balances technical accuracy, structural stability, and business-oriented efficiency remains absent. In response to this gap, the present study introduces the Adaptive Hybrid Selector for Intermittency and Variability (AHSIV) as a methodological proposal to structure and strengthen forecasting model selection processes in business environments characterized by high demand heterogeneity and operational complexity.

3. Materials and Methods

This section systematically describes the methodological design employed to evaluate and compare different model selection criteria for demand forecasting in business environments characterized by high structural heterogeneity and strong dependence on the forecasting horizon. The datasets used, the training–testing partition schemes considered, and the set of forecasting models evaluated are detailed. Furthermore, the metrics employed to quantify predictive performance are presented, along with the procedures for future-horizon adjustment and the statistical methods applied for inferential analysis. Finally, the selection criteria analyzed, including monometric, multicriteria, and adaptive approaches, are formalized, establishing the methodological framework underpinning the empirical results reported in subsequent sections.

3.1. Predictive Performance Evaluation Metrics

The evaluation of demand forecasting models is grounded in quantitative metrics that assess discrepancies between observed and predicted values from different perspectives. Since each metric emphasizes distinct properties of forecast error, the specialized literature recommends their combined use to ensure more robust and consistent model selection, particularly in multi-series and extended-horizon contexts (Hyndman & Koehler, 2006; Makridakis, Spiliotis, & Assimakopoulos, 2018).

The Mean Absolute Error (MAE) is defined as:

$$\text{MAE} = \frac{1}{n} \sum_{t=1}^n |y_t - \hat{y}_t| \quad (1)$$

This metric quantifies the average absolute error in the same units as the variable of interest, providing a direct and easily interpretable measure of forecast accuracy (Hyndman & Athanasopoulos, 2021).

The Root Mean Squared Error (RMSE) is expressed as:

$$\text{RMSE} = \sqrt{\frac{1}{n} \sum_{t=1}^n (y_t - \hat{y}_t)^2} \quad (2)$$

RMSE penalizes large errors more severely, making it particularly relevant in scenarios where extreme deviations generate high operational costs (Hyndman & Koehler, 2006).

To enable consistent comparisons across series with different scales and variability, the Root Mean Squared Scaled Error (RMSSE) is used, defined as:

$$\text{RMSSE} = \sqrt{\frac{\frac{1}{h} \sum_{t=1}^h (y_t - \hat{y}_t)^2}{\frac{1}{T-1} \sum_{t=2}^T (y_t - y_{t-1})^2}} \quad (3)$$

This metric normalizes the model's squared error relative to a naïve benchmark, and has been widely used in forecasting competitions and cross-series evaluation of demand prediction models (Makridakis & Petropoulos, 2020; Makridakis, Spiliotis, & Assimakopoulos, 2022).

The Mean Absolute Percentage Error (MAPE) is defined as:

$$\text{MAPE} = \frac{100}{n} \sum_{t=1}^n \left| \frac{y_t - \hat{y}_t}{y_t} \right| \quad (4)$$

MAPE expresses prediction error as a percentage, facilitating interpretation and communication. However, the literature has highlighted important limitations when actual values are close to zero, as the metric may produce significant distortions in model comparison (Hyndman & Koehler, 2006; Kolassa & Schütz, 2007).

The Symmetric Mean Absolute Percentage Error (sMAPE) is defined as:

$$\text{sMAPE} = \frac{1}{n} \sum_{t=1}^n \frac{2 |y_t - \hat{y}_t|}{|y_t| + |\hat{y}_t|} \quad (5)$$

sMAPE provides a relative percentage-based measure of error in symmetric form, partially mitigating the limitations of traditional MAPE. Nevertheless, it may exhibit instability when actual or predicted values approach zero (Hyndman & Koehler, 2006).

The coefficient of determination (R^2) is expressed as:

$$R^2 = 1 - \frac{\sum_{t=1}^n (y_t - \hat{y}_t)^2}{\sum_{t=1}^n (y_t - \bar{y})^2} \quad (6)$$

This indicator measures the proportion of variance explained by the model relative to a historical mean benchmark. Although commonly used as a complementary criterion to evaluate overall explanatory capacity, it was not originally designed as an out-of-sample predictive accuracy metric (Hyndman & Athanasopoulos, 2021).

The BIAS metric is incorporated and defined as:

$$\text{BIAS} = \frac{1}{n} \sum_{t=1}^n (y_t - \hat{y}_t) \quad (7)$$

BIAS identifies the presence of systematic forecast errors, indicating whether the model persistently overestimates or underestimates demand. Positive BIAS values reflect systematic underestimation, whereas negative values indicate recurrent overestimation. This dimension is not captured by magnitude-based error metrics but is critical in operational contexts, as sustained overestimation tends to generate overstock and elevated holding costs, while recurrent underestimation increases the risk of stockouts and lost sales (Hyndman & Koehler, 2006; Carboneau, Laframboise, & Vahidov, 2008; Sanders & Graman, 2016; Zhao, Xie, Ai, Yang, & Zhang, 2023). Empirical studies highlight that explicit bias control improves ranking stability and inventory decision efficiency, particularly in intermittent and slow-moving demand scenarios (Doszyń & Dudek, 2024).

Taken together, these metrics capture complementary dimensions of forecast accuracy. Their integrated use constitutes a recommended practice for model selection in expert decision-support systems, consistent with the specialized literature on forecasting and predictive analytics.

3.2. Metric Degradation

In multi-step forecasting model evaluation, the literature has consistently established that forecast error increases with the prediction horizon due to the accumulation of innovations and the propagation of structural model errors (Box, Jenkins, Reinsel, & Ljung, 2015; Hyndman & Athanasopoulos, 2021; Chatfield, 2000). However, this growth is neither uniform nor necessarily guaranteed, as it critically depends on the structural stability of the future forecast trajectory and the absence of structural breaks, systematic bias, or explosive behavior (Clements & Hendry, 1998; Clements & Hendry, 2005; Armstrong, 2001).

Within this context, the degradation of metrics such as the MAE, RMSE and RMSSE must satisfy two fundamental principles: theoretical consistency, meaning that expected error should increase with the forecasting horizon, and structural control, such that error extrapolation is only valid when the trajectory of the process exhibits stable and non-erratic behavior (Clements & Hendry, 2005; Hyndman & Athanasopoulos, 2021).

Let $E_m(h)$ denote an error metric associated with model m , evaluated up to forecast horizon h . In general terms, error growth can be modeled through a horizon-dependent power law:

$$E_m(h) \propto h^{\alpha_m}, \alpha_m \in (0,1] \quad (8)$$

where h represents the number of future steps considered and α_m is a degradation parameter controlling the rate of error growth for model m . This formulation is supported by classical results showing that, for correctly specified processes, forecast error variance grows approximately proportionally with the horizon, implying sublinear growth of RMSE, with $\alpha \approx 0.5$ as a theoretical baseline associated with noise-type accumulation (Box, Jenkins, Reinsel, & Ljung, 2015; Chatfield, 2000).

Nevertheless, not every forecast trajectory permits valid extrapolation of errors. Clements and Hendry (1998) demonstrate that in the presence of systematic bias or explosive behavior, the error observed in the test set ceases to be informative regarding future error. For this reason, error degradation is formulated as a function conditional on the structural regime of the process:

$$E_m(h_{\text{future}}) = E_m(h_{\text{test}}) \left[\gamma \left(\frac{h_{\text{future}}}{h_{\text{test}}} \right)^{\alpha_m} + (1 - \gamma) \right], \gamma \in \{0,1\} \quad (9)$$

where h_{test} corresponds to the horizon used in the out-of-sample evaluation phase, h_{future} to the future forecasting horizon, and γ is an indicator variable acting as a structural activation mechanism. Specifically, $\gamma = 1$ indicates that the process exhibits a stable regime, allowing error extrapolation, whereas $\gamma = 0$ represents biased or explosive behavior, in which case observed error is not extrapolated (Clements & Hendry, 2005; Armstrong, 2001)

The structural regime of the process is diagnosed using all available observed information up to the last known time point, that is, the union of the training and test sets, explicitly excluding any unobserved future values. Based on this complete observed series, indicators derived from successive differences are employed, following widely used practices in structural characterization of demand series (Syntetos & Boylan, 2005; Syntetos, Boylan, & Croston, 2005).

First, the relative variability of increments is considered, defined through the coefficient of variation of the absolute changes in the observed series:

$$CV_{\Delta} = \frac{\text{sd}(|\Delta y_t|)}{\text{mean}(|\Delta y_t|)}, \Delta y_t = y_t - y_{t-1} \quad (10)$$

where y_t denotes the observed value of the series at time t , with $t = 1, \dots, T$, and T representing the last period with real available information. The coefficient CV_{Δ} measures the relative dispersion of process increments and allows identification of excessively volatile series relative to their average magnitude, a criterion widely used to characterize structural forecasting difficulty in demand series (Syntetos & Boylan, 2005; Syntetos, Boylan, & Croston, 2005).

Additionally, the average magnitude of second differences is evaluated:

$$\text{mean}(|\Delta^2 y_t|), \Delta^2 y_t = \Delta y_t - \Delta y_{t-1} \quad (11)$$

which captures abrupt changes in trajectory slope and allows detection of structural discontinuities. This criterion is consistent with empirical stability analyses of exponential smoothing methods, in which smoother trajectories exhibit more controlled error growth across horizons, whereas irregular trajectories tend to amplify error in a nonlinear manner (Gardner Jr, 2006).

Based on these indicators, the structural regime of the process is classified as:

$$\text{regime} = \begin{cases} \text{Stable,} & \text{if } CV_{\Delta} < 0.2 \wedge \text{mean}(|\Delta^2 y_t|) < 0.1 \cdot \text{mean}(|\Delta y_t|) \\ \text{Biased,} & \text{if } CV_{\Delta} < 0.5 \\ \text{Explosive,} & \text{otherwise} \end{cases} \quad (12)$$

The stability thresholds are deliberately conservative. In particular, the condition $CV_{\Delta} < 0.2$ is adopted as a low-variability criterion, aligned with coefficient-of-variation-based demand categorisation frameworks in the intermittent demand literature (Syntetos & Boylan, 2005). Rather

than replicating a specific classification boundary, this threshold functions as a structural safeguard preventing unjustified error extrapolation under irregular forecast trajectories.

When the test set is sufficiently informative, the degradation parameter α_m is estimated empirically using temporal blocks:

$$\alpha_m = \frac{\log(\tilde{e}_K/\tilde{e}_1)}{\log(h_K/h_1)} \quad (13)$$

where \tilde{e}_k represents the aggregated (median) error of block k , h_k is the mean horizon associated with that block, and K is the total number of blocks. To avoid numerical instability or overfitting induced by small sample sizes, weak regularization is applied:

$$\alpha_m \leftarrow \text{clip}(\alpha_m, 0.3, 0.9) \quad (14)$$

In the absence of sufficient empirical evidence, the baseline value $\alpha_m = 0.5$ is adopted, corresponding to the theoretical noise-accumulation case (Box, Jenkins, Reinsel, & Ljung, 2015; Hyndman & Athanasopoulos, 2021; Chatfield, 2000).

Within this framework, the error metrics MAE, RMSE, and RMSSE, defined theoretically as functions of the forecasting horizon, are not recalculated using unobserved future values. Instead, they are operationally approximated through the degradation function when comparing models across future horizons. In particular, under the stable regime:

$$\text{MAE}_m(h_{\text{future}}) \approx \text{MAE}_m(h_{\text{test}}) \left(\frac{h_{\text{future}}}{h_{\text{test}}} \right)^{\alpha_m} \quad (15)$$

$$\text{RMSE}_m(h_{\text{future}}) \approx \text{RMSE}_m(h_{\text{test}}) \left(\frac{h_{\text{future}}}{h_{\text{test}}} \right)^{\alpha_m} \quad (16)$$

$$\text{RMSSE}_m(h_{\text{future}}) \approx \text{RMSSE}_m(h_{\text{test}}) \left(\frac{h_{\text{future}}}{h_{\text{test}}} \right)^{\alpha_m} \quad (17)$$

In summary, metric degradation is modeled through a horizon-dependent power law activated exclusively under structurally stable regimes. This approach prevents optimistic extrapolation of forecast error and provides a coherent, controlled, and theoretically grounded evaluation of predictive performance in multi-step forecasting contexts.

The degradation mechanism defined above constitutes the Metric Degradation by Forecast Horizon (MDFH) algorithm. MDFH provides a regime-conditioned, horizon-adjusted projection of out-of-sample error metrics from the evaluation horizon to any future decision horizon, without using unobserved realizations. This algorithm serves as the foundational adjustment procedure employed in all subsequent model selection mechanisms.

3.3. Model Selectors

To evaluate and compare different model selection criteria for demand forecasting over future horizons, this section presents three selection approaches that differ in their methodological complexity, degree of adaptation to the statistical structure of demand, and the dimensionality of the

performance metrics considered. These selectors range from simple monometric criteria to adaptive and multivariate mechanisms, enabling a systematic analysis of the advantages and limitations of each approach in contexts characterized by heterogeneity, intermittency, and structural variability.

Let $M = \{m_1, m_2, \dots, m_K\}$ (18)

denote the set of candidate models evaluated on the same demand series. For each model $m \in M$, out-of-sample performance metrics and a future forecast trajectory defined over a horizon h are available. These elements serve as the basis for applying the selection criteria presented below.

3.3.1. RMSSE Evaluated at Forecast Horizon h Selector

The RMSSE evaluated at forecast horizon h selector (RMSSE_h) is a monometric model selection criterion designed to identify the forecasting model that exhibits the lowest expected scaled error when projections are extended to a future horizon h . This selector relies on the RMSSE as its primary metric, which serves as the conceptual foundation for the official WRMSSE metric used in the M5 Accuracy Competition (Makridakis, Spiliotis, & Assimakopoulos, 2022). RMSSE enables performance comparison across a series of different magnitudes by scaling the error relative to a naïve benchmark model, making it particularly suitable for multi-series and multi-SKU contexts.

For each model $m \in M$, out-of-sample predictions are available, as well as a future forecast trajectory defined over horizon h , represented by the vector:

$$\hat{y}_{t+1:t+h}^{(m)} = (\hat{y}_{t+1}^{(m)}, \hat{y}_{t+2}^{(m)}, \dots, \hat{y}_{t+h}^{(m)}) \quad (19)$$

Given that the literature consistently shows that forecast error tends to increase as the prediction horizon extends due to the accumulation of innovations and the propagation of structural errors (Hyndman & Athanasopoulos, 2021), the present study incorporates an explicit horizon adjustment via the MDFH algorithm. Accordingly, for each model m , the RMSSE adjusted to the future horizon h is defined as:

$$\text{RMSSE}_m^{(h)} = \text{MDFH}(\hat{y}^{(m)}, \text{RMSSE}_m, h_{\text{test}},) \quad (20)$$

where the MDFH function projects the expected error from the evaluation (test) horizon to the considered future horizon, reflecting the structural degradation of predictive performance as the forecast extends. Under this criterion, the optimal model is selected by directly minimizing the scaled error adjusted to the future horizon:

$$m^* = \arg \min_{m \in M} \text{RMSSE}_m^{(h)} \quad (21)$$

This procedure defines a simple, transparent, and reproducible monometric baseline, particularly appropriate as a comparative reference against more complex selectors. Although the use of a single scaled metric mitigates the limitations of unscaled errors in heterogeneous environments, the literature has shown that rankings based exclusively on a single metric may become sensitive to the structural regime of demand and to the forecasting horizon, especially in the presence of intermittency and high variability (Doszyń & Dudek, 2024; Giannopoulos, Dasaklis, Tsantilis, & Patsakis, 2025). This observation motivates its systematic comparison with adaptive and multivariate selection approaches, as presented in the following sections.

3.3.2. Adaptive Hybrid Selector for Intermittency and Variability

The Adaptive Hybrid Selector for Intermittency and Variability (AHSIV) is a forecasting model selection mechanism designed for heterogeneous demand environments. Its objective is to identify the model with the best relative performance given the time series' underlying statistical structure. This approach is grounded in empirical and theoretical evidence demonstrating that forecasting performance depends not only on the algorithm employed but also on the degree of intermittency, variability, structural stability of demand, and the forecasting horizon considered (Hyndman & Athanasopoulos, 2021; Makridakis, Spiliotis, & Assimakopoulos, 2018). Recent studies confirm that, in highly disaggregated multi-SKU contexts, the coexistence of intermittent, lumpy, and highly volatile demand patterns precludes the existence of a universally dominant model, reinforcing the need for structurally informed and adaptive selection mechanisms (Khan & Al Hanbali, 2025; Flyckt & Lavesson, 2025; Giannopoulos, Dasaklis, Tsantilis, & Patsakis, 2025).

All horizon-dependent error metrics employed by AHSIV are previously adjusted using the MDFH algorithm. Specifically, the scaled and absolute error measures used for model comparison at future horizon h correspond to:

$$\text{RMSSE}_m^{(h)} := \text{RMSSE}_m^{\text{MDFH}}(h) \quad (22)$$

$$\text{MAE}_m^{(h)} := \text{MAE}_m^{\text{MDFH}}(h) \quad (23)$$

where the MDFH procedure projects the out-of-sample evaluation error from the test horizon to the decision horizon without using unobserved future realizations. This projection is conditional on the series's structural stability regime and follows the horizon-dependent power-law formulation defined previously.

Consequently, all Pareto comparisons and minimization rules within AHSIV operate over MDFH-conditioned metrics rather than raw test errors. Metrics lacking a theoretically supported horizon-dependent variance-propagation structure, such as BIAS and sMAPE, are not subject to MDFH adjustment, as their statistical behavior does not support a stable power-law extrapolation framework.

For each model $m \in M$, a set of performance metrics evaluated at a future forecasting horizon h is available:

$$e_m^{(h)} = (\text{RMSSE}_m^{(h)}, \text{MAE}_m^{(h)}, \text{sMAPE}_m, \text{BIAS}_m) \quad (24)$$

The joint inclusion of absolute, scaled, and bias-related metrics aligns with well-established recommendations in the forecasting evaluation literature, which emphasize that no single metric is sufficient to fully characterize predictive performance (Hyndman & Koehler, 2006; Makridakis & Petropoulos, 2020). Recent research on intermittent demand has shown that rankings based on a single metric may become unstable or inconsistent, particularly in the presence of structural zeros and outliers, thereby justifying multivariate evaluation and scale-invariant measures (Doszyń & Dudek, 2024; Song, Chang, Gao, Huang, & Ye, 2025; Giannopoulos, Dasaklis, Tsantilis, & Patsakis, 2025).

AHSIV classifies each demand series into a structural regime using two global descriptors. The demand frequency, denoted by p , is defined as the proportion of periods with strictly positive demand relative to the total number of observations. The relative variability of the complete series, denoted by c , is defined as the ratio between the standard deviation and the mean of historical demand. These descriptors form the foundation of multiple intermittent-demand classification schemes and have been widely used to differentiate regular patterns from sporadic or highly variable ones (Syntetos & Boylan, 2005; Syntetos, Boylan, & Croston, 2005). Recent evidence confirms that prior structural segmentation consistently improves model selection and predictive performance in real industrial settings, even when advanced machine learning approaches are employed (Shi, Ding, Qu, & Xie, 2026; Giannopoulos, Dasaklis, Tsantilis, & Patsakis, 2025).

Based on these descriptors, two thresholds are defined:

$$p^* \in (0,1), c^* > 0 \quad (25)$$

inducing the following structural partition:

$$R(p, c) = \begin{cases} \text{Regular - stable regime,} & \text{if } p \geq p^* \wedge c < c^*, \\ \text{Intermittent or highly variable regime,} & \text{otherwise.} \end{cases} \quad (26)$$

This classification reflects the fundamental distinction between series with frequent demand and bounded variability, for which multi-objective optimization schemes are appropriate, and series characterized by high intermittency or variability, for which metrics may become unstable and composite criteria may degrade. Empirical evidence indicates that model rankings vary substantially across intermittency regimes, even when advanced machine learning, deep learning, or large language models are employed, reinforcing the need for regime-conditioned decision rules (Makridakis, Spiliotis, & Assimakopoulos, 2018; Flyckt & Lavesson, 2025).

When the series exhibits sufficiently frequent demand and bounded variability, AHSIV operates under a multi-objective scheme, considering scaled and absolute errors as primary minimization objectives:

$$z_m = (\text{RMSSE}_m^{(h)}, \text{MAE}_m^{(h)}) \quad (27)$$

A model m_i Pareto-dominates another model m_j if:

$$\text{RMSSE}_i^{(h)} \leq \text{RMSSE}_j^{(h)}, \text{MAE}_i^{(h)} \leq \text{MAE}_j^{(h)} \quad (28)$$

with at least one inequality being strict. Let $P \subset M$ denote the Pareto front induced by z_m . The use of Pareto dominance avoids arbitrary metric aggregation and represents a well-established practice in multi-objective selection problems with potentially conflicting objectives (Deb, 2011; Coello, 2006). Recent applications in intermittent forecasting show that this approach improves selection stability compared to linear metric aggregation or composite rankings, particularly in highly heterogeneous environments (Song, Chang, Gao, Huang, & Ye, 2025; Giannopoulos, Dasaklis, Tsantilis, & Patsakis, 2025).

A hierarchical refinement is subsequently applied to the set P , selecting the model that lexicographically minimizes systematic bias and relative percentage error:

$$m^* = \arg \min_{m \in P} (|\text{BIAS}_m|, \text{sMAPE}_m) \quad (29)$$

where lexicographic ordering prioritizes bias minimization over sMAPE minimization. This decision aligns with the literature, which emphasizes that systematic bias has direct operational implications in inventory contexts, as persistent overestimation and underestimation generate asymmetric costs associated with overstock and stockouts (Hyndman & Koehler, 2006). Empirical studies confirm that bias correction has a direct financial impact on inventory value and lost sales, particularly for slow-moving and highly intermittent products (Doszyń & Dudek, 2024; Zhao, Xie, Ai, Yang, & Zhang, 2023).

When the series exhibits high intermittency or variability, AHSIV adopts a conservative strategy, avoiding multi-objective combinations that may induce instability or spurious rankings. In this regime, the selected model is obtained through direct minimization of scaled error:

$$m^* = \arg \min_{m \in M} \text{RMSSE}_m^{(h)} \quad (30)$$

The exclusive use of RMSSE in this context is justified by its scale invariance and its demonstrated robustness when comparing models across series with heterogeneous magnitudes and irregular patterns, particularly across multiple horizons (Makridakis, Spiliotis, & Assimakopoulos, 2018; Hyndman & Athanasopoulos, 2021). Recent evidence confirms that RMSSE maintains comparative stability even under extreme intermittency and long horizons, where other metrics tend to degrade or yield inconsistent rankings (Giannopoulos, Dasaklis, Tsantilis, & Patsakis, 2025).

Once the optimal model m^* is identified, AHSIV constructs a total ranking of candidate models by assigning:

$$\text{Rank}_{\text{AHSIV}}(m^*) = 1, \text{Rank}_{\text{AHSIV}}(m \in \{2, \dots, K\}, m \neq m^*) \quad (31)$$

and ordering the remaining models accordingly. From this ranking, the normalized function is defined as:

$$F_{\text{AHSIV}}(m) = \frac{\text{Rank}_{\text{AHSIV}}(m) - 1}{K - 1} \in [0, 1] \quad (32)$$

Lower values of F_{AHSIV} indicate superior relative performance, enabling consistent, reproducible comparison independent of the number of evaluated models. This normalization facilitates integration of the selector into automated evaluation and model selection pipelines, as used in modern decision-support systems for supply chains, smart manufacturing, and inventory planning (Song, Chang, Gao, Huang, & Ye, 2025; Shi, Ding, Qu, & Xie, 2026; Taghiyeh, Lengacher, & Handfield, 2020).

In summary, AHSIV can be interpreted as a regime-dependent piecewise decision function. By combining structural classification, multi-objective optimization, explicit bias control, and robust decision rules, the selector aligns model selection with the statistical properties of demand. In doing so, AHSIV mitigates the adverse effects of intermittency and high variability on predictive performance evaluation, providing a more stable and coherent selection criterion for demand

forecasting applications in complex business environments, consistent with current developments in intermittent forecasting and applied machine learning research (Giannopoulos, Dasaklis, Tsantilis, & Patsakis, 2025; Khan & Al Hanbali, 2025).

3.3.3. Equilibrium Ranking Aggregation Selector

The Equilibrium Ranking Aggregation (ERA) is proposed as a multivariate forecasting model selector that identifies the model with the best global performance balance, thereby avoiding the isolated optimization of a single metric. This approach is grounded in recent empirical evidence indicating that metrics such as Mean Absolute Error (MAE), Root Mean Squared Error (RMSE), and the coefficient of determination (R^2) capture complementary dimensions of predictive quality. In particular, while MAE reflects average forecast accuracy, RMSE penalizes large errors more severely, and R^2 evaluates the overall explanatory capacity of the model. Consequently, a robust evaluation of predictive performance should simultaneously consider these dimensions (Kumar, Maheswari, Raman, Iniyavan, & Hashim, 2025).

For each model M_i , out-of-sample performance metrics evaluated at a future horizon h are considered and defined as:

$$\mathbf{e}_i^{(h)} = (\text{MAE}_i^{(h)}, \text{RMSE}_i^{(h)}, R_i^2) \quad (33)$$

where $\text{MAE}_i^{(h)}$ and $\text{RMSE}_i^{(h)}$ correspond to error metrics explicitly adjusted to the future horizon through the MDFH algorithm, reflecting the expected degradation of error as the forecasting horizon extends, and R_i^2 represents the model's global explanatory capacity.

From a mathematical perspective, the selection logic proposed by Kumar et al. (2025) can be interpreted as the search for a model satisfying a joint optimality condition, consisting of simultaneously minimizing absolute and quadratic errors while maximizing explained variance:

$$M^* = \arg \min_{M_i \in \mathcal{M}} \{\text{MAE}_i^{(h)}, \text{RMSE}_i^{(h)}\} \text{ and } \max_{M_i \in \mathcal{M}} R_i^2 \quad (34)$$

This condition may be interpreted as a form of total dominance under a partial order defined as:

$$M_a < M_b \Leftrightarrow (\text{MAE}_a^{(h)} \leq \text{MAE}_b^{(h)}) \wedge (\text{RMSE}_a^{(h)} \leq \text{RMSE}_b^{(h)}) \wedge (R_a^2 \geq R_b^2) \quad (35)$$

where a model dominates another if it exhibits lower projected error at the future horizon and greater explanatory capacity.

In practice, since this strict condition is rarely satisfied exactly in real-world contexts, the ERA approach operationalizes this equilibrium logic through a ranking aggregation procedure. For each metric, an independent ordinal ranking is constructed-minimizing $\text{MAE}^{(h)}$ and $\text{RMSE}^{(h)}$, and maximizing R^2 . These rankings are subsequently aggregated through vectorized summation and normalized to obtain an equilibrium score:

$$\text{ERA}_i \in [0,1] \quad (36)$$

where higher values indicate a superior global trade-off among future predictive accuracy, error stability, and explanatory capacity. The selected model is the one maximizing the ERA score, thereby defining a coherent, reproducible, and conceptually balanced multivariate selector aligned with contemporary approaches to forecasting evaluation and operational decision optimization.

3.4. Strategic Quality Metric for Demand Forecasting

From a business perspective, the forecasting process is not limited to minimizing statistical error; rather, it serves as a critical input for strategic and tactical decision-making in purchasing planning, replenishment, and inventory management. In this context, predicted demand may be interpreted as the inventory volume that the organization decides to acquire in advance to serve the future market, thereby committing financial resources, logistical capacity, and service levels (Sepúlveda-Rojas, Rojas, Valdés-González, & San Martín, 2015; Ulrich, Jahnke, Langrock, Pesch, & Senge, 2022; Kumar, Maheswari, Raman, Iniyavan, & Hashim, 2025; Sayed, Gabbar, & Miyazaki, 2009; Peng et al., 2024; Nguyen et al., 2026). Consequently, forecast quality should be assessed not only in terms of temporal accuracy but also in terms of its aggregate coherence with the actual realized demand volume.

The comparison between total projected volume and realized demand allows identification of discrepancies that translate directly into economic and operational inefficiencies. Systematic overestimation of demand tends to generate overstock, increasing holding costs, obsolescence, and immobilized working capital, whereas persistent underestimation increases the risk of stockouts, lost sales, and service level deterioration (Goltsos, Syntetos, Glock, & Ioannou, 2022; Goodwin, Hoover, Makridakis, Petropoulos, & Tashman, 2023; Erjiang, Yu, Tian, & Tao, 2022; Sayed, Gabbar, & Miyazaki, 2009; Demizu, Fukazawa, & Morita, 2023; Nguyen et al., 2026). These implications reinforce the need to incorporate metrics that capture forecasting performance from a volumetric and strategic perspective.

To synthesize these discrepancies at an aggregated level, the Global Relative Accuracy (GRA) metric is proposed, inspired by prior approaches to global predictive performance evaluation and cumulative volume comparison (Nowotarski & Weron, 2015; Badulescu, Hameri, & Cheikhrouhou, 2021; Sayed, Gabbar, & Miyazaki, 2009; Peng et al., 2024). GRA evaluates the relative proximity between the total forecasted demand volume and the total actual demand volume over a given evaluation horizon, formally defined as:

$$\text{GRA} = 1 - \frac{|\sum_{t=1}^T \hat{y}_t - \sum_{t=1}^T y_t|}{\sum_{t=1}^T y_t} \quad (37)$$

where y_t denotes the observed demand at time t , \hat{y}_t the predicted demand, and T the evaluation horizon. This formulation allows GRA to be interpreted as a bounded, dimensionless measure, with values close to 1 indicating high coherence between the total forecasted volume and the effectively realized demand.

From a strategic standpoint, a high GRA value reflects more efficient allocation of financial resources, greater stability in supply processes, and improved alignment between purchasing decisions and actual market behavior (Ulrich, Jahnke, Langrock, Pesch, & Senge, 2022; Goltsos, Syntetos, Glock,

& Ioannou, 2022; Peng et al., 2024; Nguyen et al., 2026; Demizu, Fukazawa, & Morita, 2023). Unlike traditional pointwise error metrics such as MAE or RMSE, GRA does not directly penalize temporal redistribution of error; rather, it captures the net impact of the forecast on the total managed volume, which is particularly relevant in business environments where the economic cost of aggregate error outweighs isolated deviations.

In this sense, GRA does not aim to replace classical accuracy metrics but rather to complement them by providing an additional *ex post* evaluation dimension focused on the strategic quality of forecasting. Its incorporation enables predictive performance to be analyzed from an aggregated business perspective, assessing the alignment between generated forecasts and key operational objectives, such as inventory efficiency, cost reduction, and achieved service levels. In doing so, GRA contributes to improved interpretation and feedback of forecasting processes in environments characterized by high demand heterogeneity and operational complexity (Sayed, Gabbar, & Miyazaki, 2009; Demizu, Fukazawa, & Morita, 2023; Nguyen et al., 2026).

3.5. Backtesting Strategy

For each demand series, the complete set of available historical observations is initially considered, represented as a discrete time series $\{y_t\}_{t=1}^T$, where y_t denotes the observed demand at period t , and T corresponds to the total number of available observations. From this set, the last H temporal cycles are reserved as the future evaluation horizon, with $H \in \mathbb{N}^+$, in order to reproduce a strictly out-of-sample operational forecasting scenario. Accordingly, the series is partitioned as:

$$\{y_t\}_{t=1}^T = \{y_t\}_{t=1}^{T-H} \cup \{y_t\}_{t=T-H+1}^T \quad (38)$$

where the final segment $\{y_t\}_{t=T-H+1}^T$ is exclusively allocated to predictive performance evaluation.

The definition of a temporal cycle is adapted to the intrinsic frequency of each series, which may correspond to daily, weekly, monthly, or annual periods, ensuring that the evaluation horizon H remains consistent with the effective planning and decision-making unit associated with the analyzed demand. Under this approach, H represents a multi-step forecasting horizon whose length is defined according to the operational context and the temporal granularity of the series, without imposing a priori restrictions on its magnitude.

This evaluation scheme aligns with temporal validation protocols widely employed in empirical multi-step forecasting studies, where predictive performance is assessed over fixed future horizons using either fixed-origin or rolling-origin evaluation frameworks. In the specific case of a fixed-origin evaluation, the forecasting model $f(\cdot)$ is trained exclusively on the historical information $\{y_t\}_{t=1}^{T-H}$ and generates multi-step predictions of the form:

$$\hat{y}_{T+k} = f(y_1, y_2, \dots, y_{T-H}), k = 1, \dots, H \quad (39)$$

thereby strictly preserving the temporal structure of the data and preventing any leakage of future information (Tashman, 2000; Kourentzes_1, Barrow, & Crone, 2014; Semenoglou, Spiliotis, Makridakis, & Assimakopoulos, 2021).

This procedure corresponds to a fixed-origin evaluation framework, in which the final segment of the series is retained as the test set, while prior data are used exclusively for model estimation and validation. Such an approach has been widely recognized in the forecasting literature as an appropriate practice for out-of-sample predictive performance assessment, as it prevents contamination by future information and yields realistic estimates of forecast error over horizons relevant to decision-making (Tashman, 2000; Hyndman & Koehler, 2006).

The use of a clearly defined evaluation horizon, separated at the end of the series, is particularly pertinent in demand forecasting contexts, where forecasts serve as direct inputs to operational planning, inventory management, and resource allocation processes. In this sense, the explicit retention of a future segment for evaluation is consistent with methodological principles of temporal validation and out-of-sample assessment consistently discussed in the specialized literature (Armstrong, 2001; Makridakis, Spiliotis, & Assimakopoulos, 2022).

3.6. Experimental Design

To evaluate the effectiveness of AHSIV, an experimental framework is defined to systematically compare its performance with that of alternative model selection criteria, specifically the monometric selector based on RMSSE and the multivariate ERA approach. The evaluation is conducted under controlled conditions, considering a common set of candidate models and out-of-sample performance metrics adjusted to future forecasting horizons. The objective is to determine whether AHSIV consistently improves by explicitly integrating predictive accuracy, error stability, and systematic bias, while incorporating structural information on demand intermittency and variability.

Figure 1 illustrates the experimental process, highlighting the main stages of the study: dataset preparation, evaluation of candidate models, application of different model selectors, including AHSIV, and subsequent comparison of the results. This experimental design enables systematic validation of the proposed approach and establishes a clear methodological foundation for its comparison with baseline selection criteria.

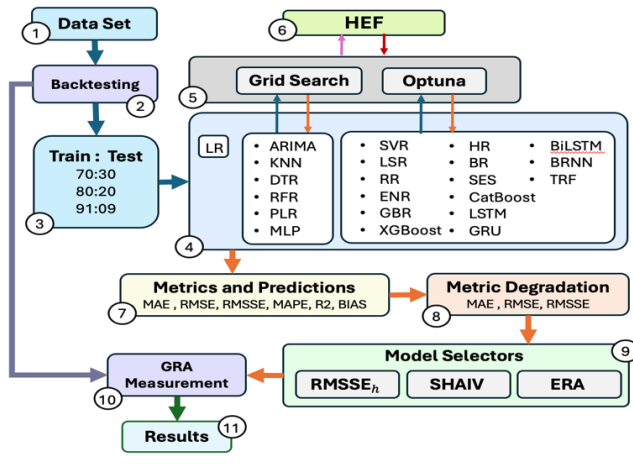


Figure 1. Experimental Framework.

3.6.1. Stage 1: Dataset

In this stage, the datasets used in the experiments were processed. These datasets originate from widely recognized sources in the forecasting literature, including Walmart (Yasser, 2021), M3

(Makridakis & Hibon, 2000), M4 (Makridakis, Spiliotis, & Assimakopoulos, 2018), and M5 (Makridakis, Spiliotis, & Assimakopoulos, 2022). Table 1 summarizes their main characteristics, including the number of series, observations, and frequency. For the M5 dataset, the last n months were selected, and filtering procedures were applied to exclude products with no recent sales or with high structural intermittency. For the M3 and M4 datasets, missing values were removed, and the last n periods, defined according to their respective frequencies, were extracted in order to construct complete and continuous product-level time series.

Table 1. Datasets used in the experiments.

Dataset	Frequency	# Time Series	# Observations	Annual Frequency
Walmart	Weekly	46	64.35	52
M5	Diary	1.454	1.054.150	365
M4	Weekly	294	28.224	52
M3	Monthly	1.428	34.272	12
Total	-	3.222	1.116.646	-

For the experimental analysis, a stratified random sample was drawn from each dataset to ensure statistical representativeness while preserving the heterogeneity of the original population. The sample size was determined under the finite population assumption, considering a 99% confidence level, a 5% margin of error, and a conservative expected proportion of $p = 0.5$. The characterization of the resulting samples is presented in Table 2.

Table 2. Randomly stratified data set.

Dataset	Frequency	# Time Series	# Observations	Annual Frequency
Walmart	Weekly	46	6435	52
M5	Diary	650	471.250	365
M4	Weekly	204	19.584	52
M3	Monthly	454	10.896	12
Total	-	1.354	508.165	-

The Walmart, M3, M4, and M5 datasets were selected because they represent demand scenarios exhibiting different degrees and forms of non-stationarity documented in the literature, which pose significant challenges for forecasting model generalization (Makridakis, Spiliotis, & Assimakopoulos, 2018; Petropoulos, Wang, & Disney, 2019; Makridakis, Spiliotis, & Assimakopoulos, 2022). Collectively, these datasets encompass a heterogeneous spectrum of temporal behaviors, including seasonality and non-stationary trends (M3), structural heterogeneity and regime changes (M4), as well as intermittency, temporal irregularity, heteroscedasticity, and exogenous effects typical of real retail environments (Walmart and M5). This diversity enables evaluation of selection methods under realistic conditions of increasing structural complexity.

3.6.2. Stage 2: Backtesting

In this stage, the temporal backtesting scheme defined in the previous methodological section is applied in order to evaluate the predictive performance of the models under a strictly out-of-sample scenario, in accordance with temporal evaluation protocols recommended in the forecasting literature (Tashman, 2000; Hyndman & Koehler, 2006).

For the Walmart, M3, M4, and M5 datasets, a future evaluation horizon of $H = 12$ cycles is established, where the definition of a cycle is adapted to the intrinsic temporal frequency of each series. Accordingly, the evaluation horizon is 12 weeks for weekly series, 12 months for monthly

series, and 12 daily periods for daily series. This definition ensures operational consistency with the demand planning unit and guarantees comparability across datasets with different temporal granularities.

The adopted evaluation procedure corresponds to a fixed-origin scheme, in which historical data preceding the evaluation horizon are used for model estimation and validation, while the final cycles are reserved exclusively for out-of-sample predictive performance assessment. This approach prevents future information leakage and provides realistic estimates of forecast error over multi-step horizons relevant to decision-making in non-stationary demand environments (Kourentzes_1, Barrow, & Crone, 2014; Semenoglou, Spiliotis, Makridakis, & Assimakopoulos, 2021; Makridakis, Spiliotis, & Assimakopoulos, 2022).

3.6.3. Stage 3: Training and Test Separation

The empirical evaluation was conducted using the Walmart, M5, M4, and M3 datasets, each partitioned into three training–testing configurations (91:9, 80:20, and 70:30).

3.6.4. Stage 4: Demand Forecasting Models

The forecasting models employed range from traditional statistical approaches to modern machine learning techniques and deep neural networks, enabling a comprehensive evaluation of methods with different modeling capabilities, as detailed in Appendix A.

The models are classified into two groups: Exhaustive Search (ES), which performs an exhaustive exploration over discrete and finite parameter spaces (ARIMA, KNN, DTR, RFR, PLR, and MLP); and Search in Continuous Space (SCS), which includes parameterized models optimized through hyperparameter search techniques in high-dimensional continuous spaces (SVR, LSR, RR, ENR, GBR, XGBoost, HR, BR, SES, CatBoost, LSTM, GRU, BiLSTM, BRNN, and TRF). This classification distinguishes the groups to which specific optimization techniques are applied, according to the structural specifications of each model.

3.6.5. Stage 5: Optimizers

To optimize the parameters and hyperparameters of the evaluated models, two complementary approaches were employed, selected according to the nature of the search space and the computational complexity of the models.

Grid Search: This approach was applied to models in the Exhaustive Search (ES) group, which performs a complete exploration of all possible combinations within a discrete, finite search space. This guarantees identification of the best configuration within the predefined domain.

Optuna: This approach was applied to the models classified under Stochastic Continuous Search (SCS). Optuna is an optimization framework based on Bayesian methods that employs Tree-structured Parzen Estimators (TPE) and early-pruning mechanisms to discard unpromising configurations during the search, enabling efficient exploration of high-dimensional continuous parameter spaces.

3.6.6. Stage 6: HEF

The Hierarchical Evaluation Function (HEF) (González & Parada, 2026) was employed as the objective function in the optimization process. This function guided the selection of parameters and hyperparameters for the evaluated models within the considered optimization frameworks.

3.6.7. Stage 7: Metrics and Predictions

At this stage, once the models have been trained and evaluated using the previously defined temporal partitioning scheme, considering the 91:9, 80:20, and 70:30 splits, multi-step forecasts are generated for future horizons $H \in \{1, 2, \dots, 12\}$ cycles. The metrics MAE, RMSE, RMSSE, MAPE, R^2 , and BIAS are computed during the training and evaluation process over the training and testing sets defined by these partitions. Subsequently, future projections for the different values of H are generated using the trained models, enabling analysis of forecast behavior over increasing horizons without introducing future information into the estimation process.

3.6.8. Stage 8: Metric Degradation

The Metric Degradation by Forecast Horizon (MDFH) procedure is introduced to explicitly model the expected degradation of error metrics when a forecasting model, evaluated over a finite test horizon, is projected toward longer future prediction horizons. MDFH is grounded in evidence from the multi-step forecasting literature, which shows that metrics such as MAE, RMSE, and RMSSE tend to increase with the prediction horizon due to the accumulation of innovations and the propagation of structural model errors.

Under this framework, MDFH adjusts these metrics only when the trajectory of future forecasts exhibits structurally stable behavior, as identified through analysis of the relative variability of successive forecast increments. In such cases, error degradation is modeled as a power-law relationship between the test and future horizons, controlled by a robustly estimated degradation exponent. When the forecast exhibits signs of instability, systematic bias, or explosive behavior, or when the metric does not correspond to an absolute or squared error measure, the procedure applies no adjustment and retains the original metric value, thereby avoiding unjustified extrapolations.

The operational implementation of this adjustment is formalized in Algorithm A1, which summarizes the steps required for consistent application of MDFH as a function of the forecasting horizon.

Algorithm A1 exhibits linear time complexity $O(n + m)$, where n corresponds to the length of the trajectory used for structural diagnosis and m to the test horizon size. As no nested loops or iterative optimization procedures are involved, the computational overhead of MDFH is negligible compared to that of model training.

3.6.9. Stage 9: Model Selectors

Based on the information obtained in the previous stages, different forecasting model selectors are applied to each demand series. The objective of this stage is to identify, for each forecasting horizon considered, the model exhibiting the best relative performance under different selection criteria. To this end, three complementary approaches are implemented: the RMSSE_h selector, AHSIV, and ERA.

RMSSE_h

The RMSSE_h selector, formally described in Algorithm A2, implements a monometric selection criterion based on the ordinal ranking of models according to their projected scaled error at forecast horizon h , denoted as RMSSE, previously adjusted using the MDFH procedure. The model with the lowest projected scaled error is selected as optimal, without applying additional normalization or combining multiple metrics, since RMSSE is scale-invariant to the magnitude of the series.

Algorithm A2 operationalizes this procedure by extracting the MDFH-adjusted RMSSE values for each candidate model, ranking them in ascending order, and selecting the model with the minimum projected error. This approach constitutes a simple, transparent, and fully reproducible baseline, serving as a benchmark against which more complex adaptive and multivariate selection mechanisms are contrasted.

From a computational perspective, the RMSSE_h selector exhibits time complexity $O(K \log K)$, where K denotes the number of candidate models. This complexity arises from the ordinal ranking (sorting) step, while the remaining operations are linear in K . Consequently, the computational overhead of Algorithm 2 is negligible relative to model training and forecast generation procedures.

AHSIV

The AHSIV algorithm, formally described in Algorithm A3, selects the optimal forecasting model by adapting its decision criterion to the statistical structure of demand. First, the series is characterized according to its demand frequency and overall variability. When demand is classified as regular and structurally stable, the algorithm adopts a multi-objective approach based on Pareto dominance over future-projected error metrics (RMSSE and MAE adjusted via MDFH), subsequently refining the selection using complementary performance indicators such as sMAPE and BIAS. Conversely, when demand exhibits high intermittency or elevated variability, AHSIV adopts a conservative strategy and directly selects the model minimizing the projected scaled error.

Algorithm A3 operationalizes this adaptive logic and concludes by generating an ordinal ranking and a normalized AHSIV score, enabling consistent comparison of the relative performance of all candidate models.

From a computational standpoint, AHSIV exhibits worst-case time complexity $O(K^2)$, where K denotes the number of candidate models. This complexity arises from the Pareto dominance evaluation step, which in its general form requires pairwise comparisons among models. All remaining operations, including metric extraction, median computation, ranking normalization, and score calculation, are linear or $O(K \log K)$, and therefore do not dominate the overall computational cost. Given that K is typically small relative to dataset size, the computational overhead of AHSIV remains negligible compared to model estimation procedures.

ERA

The ERA algorithm, formally described in Algorithm A4, implements a multivariate selector that identifies the model with the best overall performance by simultaneously considering multiple evaluation metrics. Rather than directly combining the numerical values of the metrics, ERA

transforms each metric into an ordinal ranking, enabling homogeneous comparison across models even when the metrics differ in scale or distribution.

The error metrics MAE and RMSE, previously adjusted to the forecasting horizon using MDFH, are treated as metrics to be minimized, whereas the coefficient of determination R^2 is treated as a metric to be maximized. Additional accuracy measures, such as MAPE, are also incorporated under a minimization criterion. The individual rankings are aggregated by summation, producing a total ranking that synthesizes each model's global performance balance. This aggregated ranking is subsequently normalized to obtain an equilibrium score F_{ERA} , bounded in the interval [0, 1], where higher values indicate better overall performance. Finally, models are ordered according to this score, and the model that maximizes F_{ERA} is selected as optimal.

From a computational perspective, Algorithm A4 exhibits time complexity $O(K \log K)$, where K denotes the number of candidate models. This complexity arises from the ordinal ranking operations applied to each metric and the final ranking of the aggregated score. Since the number of metrics is fixed and small, the overall computational burden remains negligible relative to model estimation and forecasting procedures.

3.6.10. Stage 10: GRA Measurement

At this stage, the performance of the selected models is evaluated using the Global Relative Accuracy (GRA) metric. In the previous step, the different model selectors identified, based on their respective evaluation metrics, those models exhibiting the best relative performance and that are therefore expected to generate greater coherence between forecasted and actual demand.

The selected models produce predictions for the future cycles considered in the analysis. These predictions are subsequently compared with the observed real demand values obtained in Step 2 of the methodological procedure, corresponding to the Backtesting stage. Based on this ex post comparison between predicted and observed demand volumes, the GRA metric is computed, enabling assessment of the aggregated alignment between forecasts and actual demand behavior from a strategic perspective.

GRA is systematically calculated for different forecasting horizons H , ranging from 1 to 12 cycles, as well as under different training–testing partition schemes, specifically 91:9, 80:20, and 70:30. This approach allows analysis of the stability and consistency of each selector's performance across short-, medium-, and long-term scenarios, as well as under varying levels of historical data availability. In this manner, GRA is employed as an additional comparative criterion to identify which model selector achieves the best overall performance in terms of volumetric coherence between forecasted and observed demand across the evaluated scenarios.

3.6.11. Stage 11: Results

This stage presents the empirical results obtained from the application of the proposed experimental framework. The results are aimed at comparatively evaluating the performance of the different forecasting model selectors considered, specifically the $RMSSE_h$ selector, the multivariate ERA approach, and the adaptive AHSIV selector, under different forecasting scenarios.

For each dataset, results are reported across forecasting horizons $H \in \{1, 2, \dots, 12\}$ and under training–testing partition schemes of 91:9, 80:20, and 70:30. First, the traditional predictive performance metrics obtained by the selected models are analyzed, establishing a quantitative benchmark for the behavior of each selection criterion.

Subsequently, the values of the GRA metric are presented, computed *ex post* for the models selected by each approach. GRA is employed as an aggregated indicator of volumetric coherence between forecasted and observed demand, enabling comparison of the selectors from a strategic perspective. The joint analysis of these results makes it possible to identify the selector that exhibits the most consistent and robust performance across different forecasting horizons and training–testing configurations.

3.7. Experimental Protocol

An experimental execution protocol was defined to systematically evaluate the proposed methodology under different data configurations and temporal partition schemes. Each execution is identified by an ID and corresponds to a specific combination of dataset (Walmart, M3, M4, and M5) and training–testing partition scheme (91:9, 80:20, and 70:30), yielding a total of 12 experimental configurations.

For each configuration, the entire methodological pipeline was executed without omitting any stage. Specifically, the following steps were applied sequentially: data preparation; fixed-origin temporal backtesting; training and evaluation of forecasting models; hyperparameter optimization; application of the Hierarchical Evaluation Function (HEF); computation of performance metrics and generation of multi-step forecasts; metric adjustment through MDFH; model selection using the RMSSE_h , AHSIV, and ERA selectors; and final evaluation using the GRA metric. The executed stages are indicated with an “X” in the protocol matrix.

This protocol ensures that all combinations of datasets and temporal partitions are evaluated under identical experimental conditions, allowing isolation of the effects of dataset characteristics, historical data availability, and forecasting horizon. In this way, a controlled, reproducible framework is established to compare the performance and robustness of model selectors across heterogeneous demand scenarios, as summarized in Table B1.

3.8. Hardware and Software

The computational implementation of the forecasting models was carried out using a comprehensive set of Python scientific computing and machine learning libraries. Statistical and time series models, such as ARIMA and SES, were implemented using the Statsmodels library (Seabold, Perktold, & others, 2010). Classical regression and machine learning models, including LR, LSR, RR, ENR, HR, PLR, KNN, SVR, DTR, RFR, and GBR, as well as Bayesian regressors, were developed using the Scikit-learn library (Pedregosa et al., 2011).

The XGBoost model was implemented using the XGBoost library (Chen & Guestrin, 2016), while CatBoost was implemented using its official programming interface (Prokhorenkova, Gusev, Vorobev, Dorogush, & Gulin, 2018).

Neural network–based models, including MLP, LSTM, GRU, BiLSTM, BRNN, and the Transformer model for time series forecasting (TRF), were implemented using TensorFlow and its high-level Keras interface (Abadi et al., 2016; Chollet, 2015). These architectures were configured in multi-step regression mode, enabling direct forecast generation across different prediction horizons.

Data preparation, manipulation, and analysis were conducted using the Pandas (Team, 2020), SciPy (Virtanen et al., 2020), and NumPy (Harris et al., 2020) libraries. Results visualization was performed using Matplotlib (Hunter, 2007) and Seaborn (Waskom, 2021). Hyperparameter optimization was addressed using search techniques aligned with the structural characteristics of each model, employing the Bayesian optimization framework Optuna (Akiba, Sano, Yanase, Ohta, & Koyama, 2019).

Full details of the experimental environment, along with optimizer configurations and the parameter ranges explored for each model, are presented in Appendix C.

4. Results

Across the different training–testing partition schemes considered (91:9, 80:20, and 70:30), the analysis of GRA by forecasting horizon is conducted consistently for the Walmart, M5, M4, and M3 datasets, using complementary representations based on heatmaps, boxplots, and nonparametric statistical tests. In all cases, the evaluation is structured by forecasting horizon $h = 1, \dots, 12$, enabling analysis of the evolution of the selectors’ relative performance in multi-step forecasting scenarios.

Across all three partition schemes, the median GRA heatmaps reveal a clear differentiation among the evaluated selection criteria. In particular, AHSIV and the RMSSE_h selector concentrate high and stable GRA values throughout the entire forecasting horizon considered, whereas the ERA selector consistently exhibits lower central values. This general structure is consistently reflected in the GRA boxplots by horizon, where AHSIV and RMSSE_h display high medians and moderate dispersion levels, in contrast to ERA, which shows greater relative variability and a higher presence of values in the lower tail of the distribution.

From an inferential perspective, Shapiro–Wilk normality tests systematically reject the normality assumption for the GRA distributions across different selectors and horizons, thereby justifying the use of nonparametric tests. Within this framework, global Kruskal–Wallis tests and Dunn post-hoc analyses with Bonferroni correction consistently indicate that the statistically significant differences observed are explained by the inferior performance of the ERA selector, with no significant differences detected between AHSIV and RMSSE_h .

Finally, the analysis of aggregated global GRA, final rankings by horizon, and the heatmaps of selection frequency for AHSIV and RMSSE_h show that the choice of the optimal model varies as a function of the forecasting horizon, with no single model being selected dominantly across all horizons analyzed. This behavior, common across the different partition schemes, highlights the dependence of relative performance on the forecasting horizon considered and provides the basis for the detailed analysis presented in the following subsections.

4.1. Training 91% and Testing 9%

Under the 91% training and 9% testing scheme, the median GRA heatmaps by forecasting horizon (Figures 2, 3, 4, and 5) indicate that AHSIV and the RMSSE_h selector maintain high and stable GRA values throughout the entire horizon considered, whereas ERA consistently exhibits lower values across all analyzed datasets.

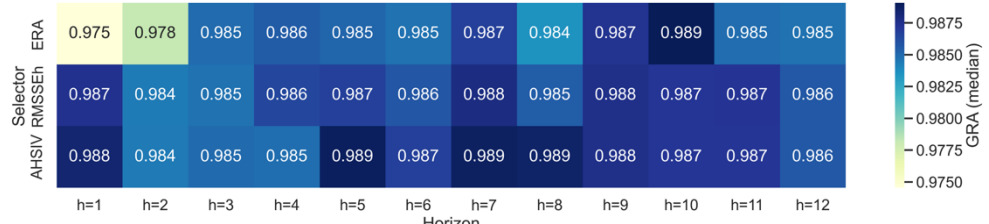


Figure 2. GRA heatmap (median) by selector and horizon, Walmart, training and testing 91:9.

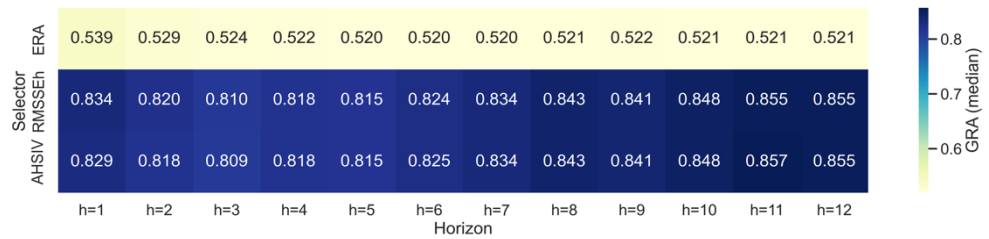


Figure 3. GRA heatmap (median) by selector and horizon, M5, training and testing 91:9.

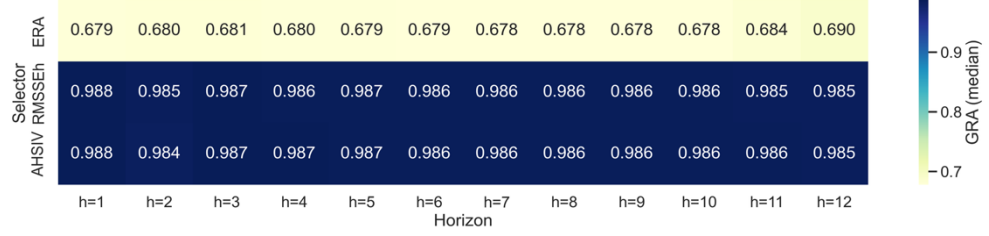


Figure 4. GRA heatmap (median) by selector and horizon, M4, training and testing 91:9.

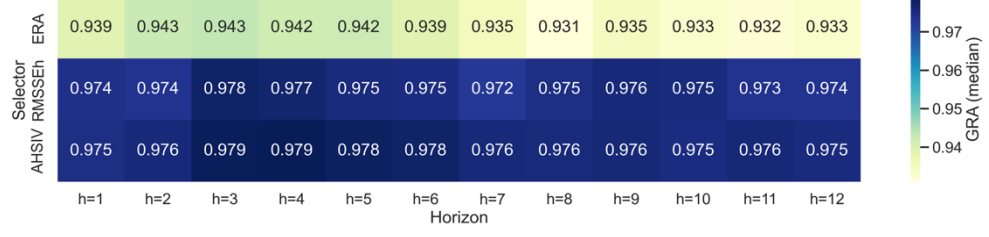


Figure 5. GRA heatmap (median) by selector and horizon, M3, training and testing 91:9.

This pattern is confirmed by the GRA boxplots by forecasting horizon (Figures 6, 7, 8, and 9), where AHSIV and the RMSSE_h selector concentrate their distributions at high GRA values with moderate dispersion, in contrast to ERA, which exhibits greater relative variability and a more pronounced lower tail.

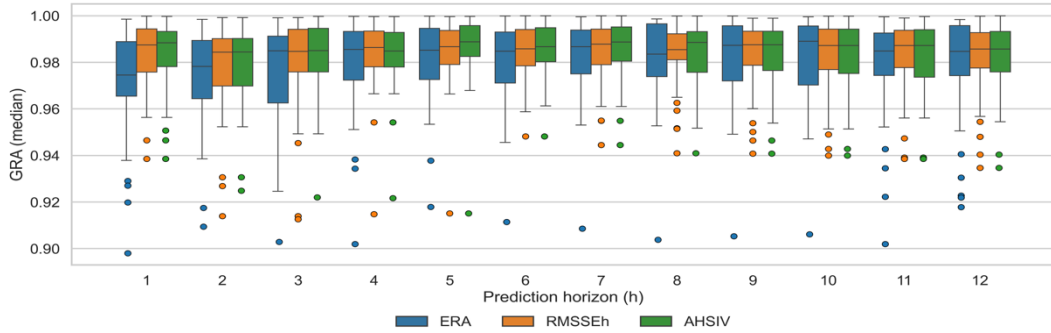


Figure 6. GRA distribution by horizon and selector, Walmart, training and testing 91:9.

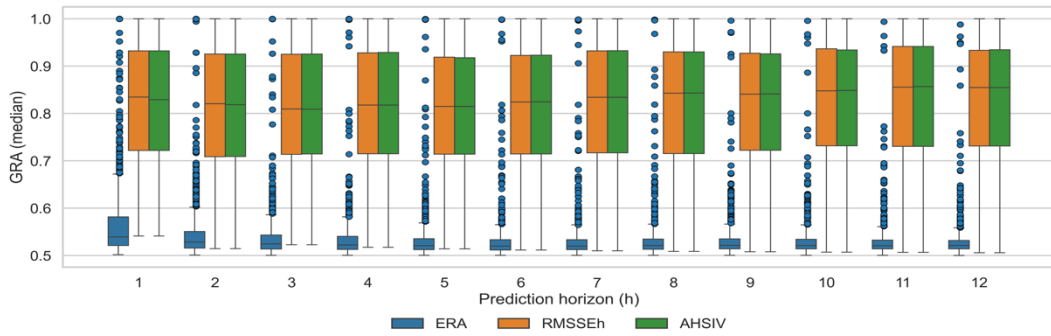


Figure 7. GRA distribution by horizon and selector, M5, training and testing 91:9.

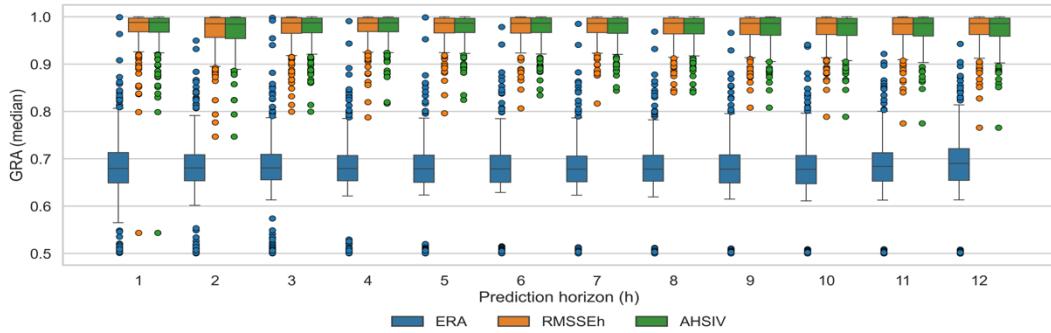


Figure 8. GRA distribution by horizon and selector, M4, training and testing 91:9.

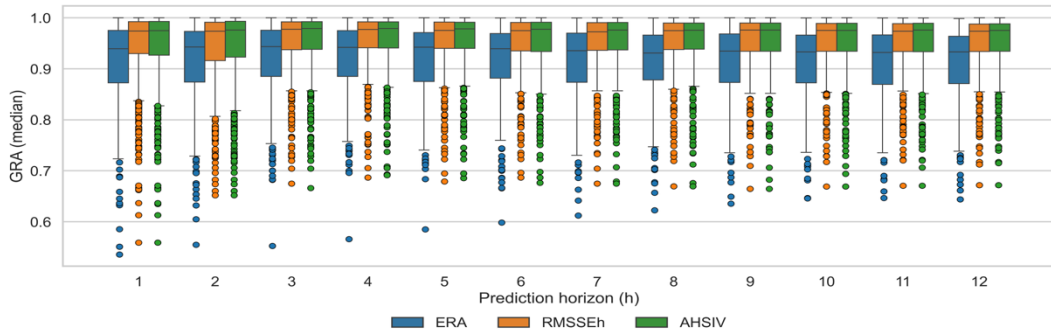


Figure 9. GRA distribution by horizon and selector, M3, training and testing 91:9.

From an inferential perspective, Kruskal-Wallis tests identify statistically significant differences among selectors for the M5, M4, and M3 datasets (Tables D7, D12, and D17), whereas for Walmart, such differences are restricted to the shortest forecasting horizon (Table

D2). Dunn's post-hoc analysis confirms that these differences are exclusively explained by the inferior performance of ERA, with no statistically significant differences detected between AHSIV and RMSSE_h (Tables D2, D7, D12, and D17).

The aggregated global GRA and the final ranking by horizon indicate that AHSIV attains first position with greater frequency across the considered horizons (Tables D3, D8, D13, and D18).

Finally, the heatmaps of selection frequency show that model choice under AHSIV and RMSSE_h varies substantially as a function of the forecasting horizon (Figures D2, D3, D5, D6, D8, D9, D11, and D12). In contrast, the ERA selector exhibits comparatively lower variability in model selection frequency across the considered horizons (Figures D1, D4, D7, and D10).

4.2. Training 80% and Testing 20%

Under the 80% training and 20% testing scheme, the median GRA heatmaps by forecasting horizon (Figures 10, 11, 12, and 13) reproduce the previously observed pattern, with high and stable GRA values for AHSIV and RMSSE_h , and systematically lower central values for ERA, particularly in the M5, M4, and M3 datasets.

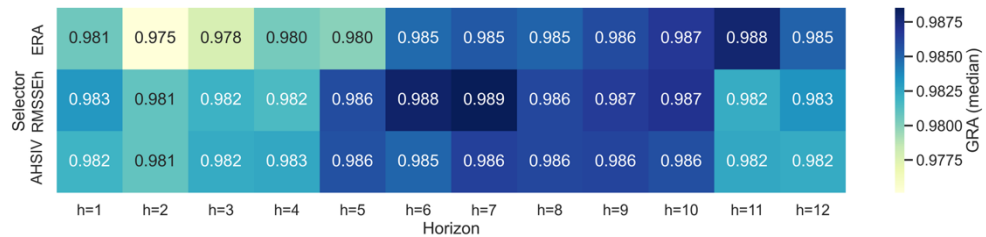


Figure 10. GRA heatmap (median) by selector and horizon, Walmart, training and testing 80:20.

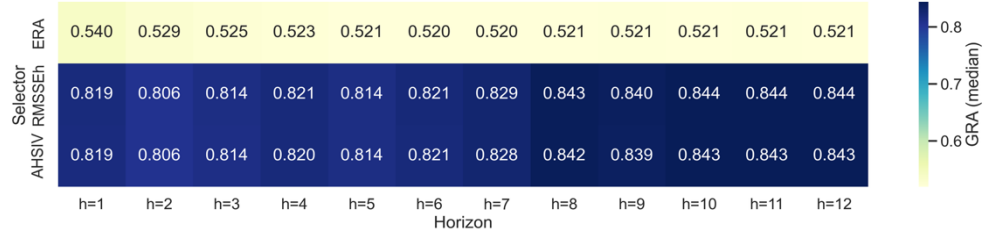


Figure 11. GRA heatmap (median) by selector and horizon, M5, training and testing 80:20.

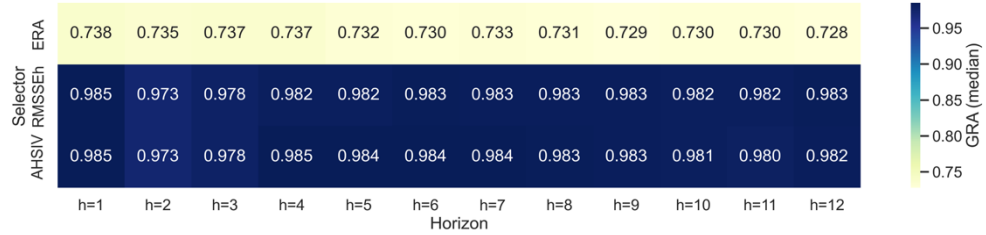


Figure 12. GRA heatmap (median) by selector and horizon, M4, training and testing 80:20.

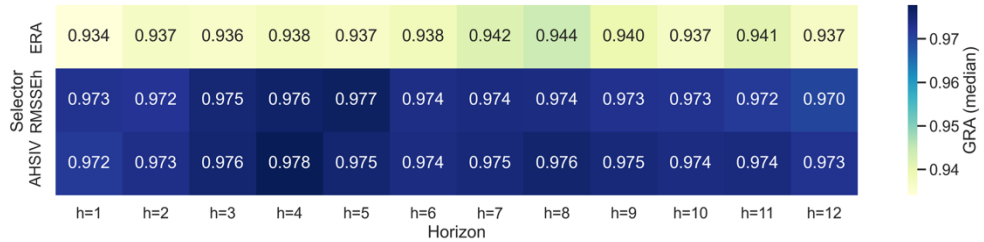


Figure 13. GRA heatmap (median) by selector and horizon, M3, training and testing 80:20.

The GRA boxplots by forecasting horizon (Figures 14, 15, 16, and 17) show that AHSIV and RMSSE_h exhibit distributions concentrated at high GRA values, whereas ERA displays greater relative variability and a more frequent presence of values in the lower tail.

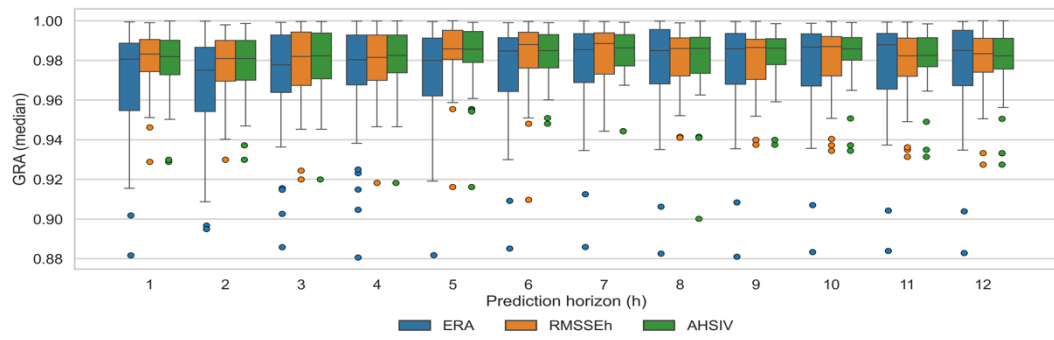


Figure 14. Distribution of GRA by Forecasting Horizon and Selector, Walmart, Training–Testing 80:20.

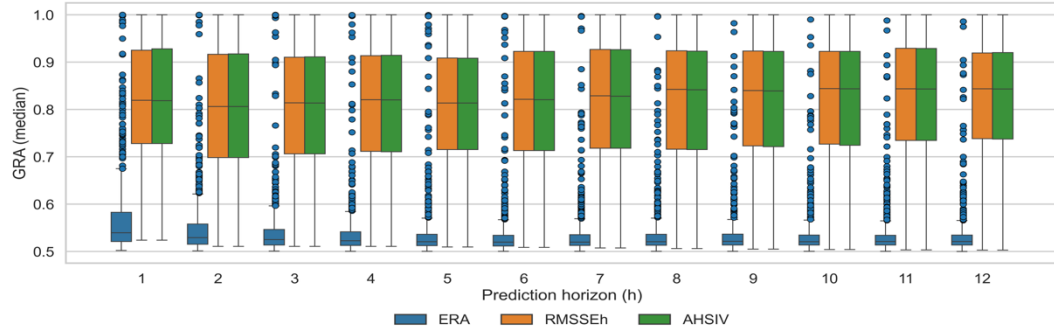


Figure 15. Distribution of GRA by Forecasting Horizon and Selector, M5, Training–Testing 80:20.

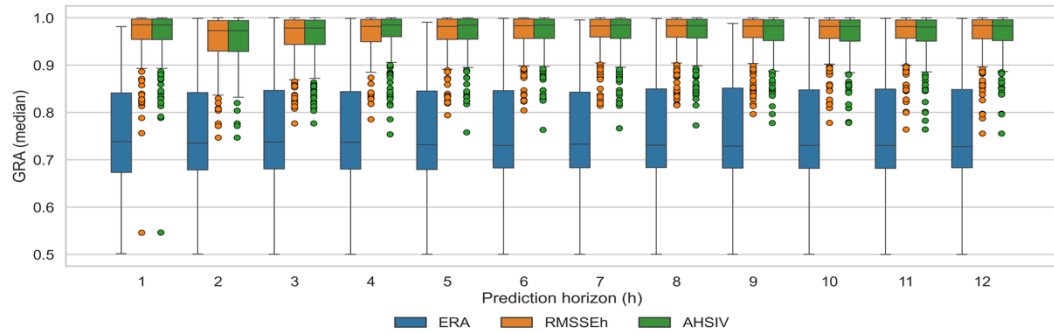


Figure 16. Distribution of GRA by Forecasting Horizon and Selector, M4, Training–Testing 80:20.

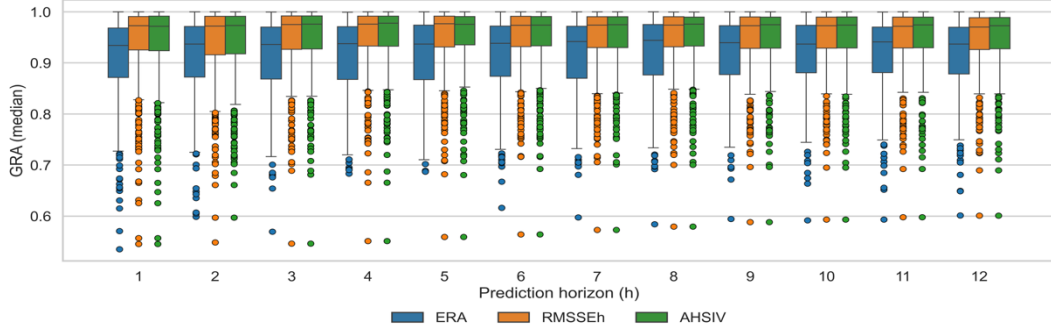


Figure 17. Distribution of GRA by Forecasting Horizon and Selector, M3, Training–Testing 80:20.

From an inferential perspective, no statistically significant differences among selectors are detected for the Walmart dataset (Table E2). In contrast, for the M5, M4, and M3 datasets, global Kruskal–Wallis tests indicate significant differences across all analyzed horizons (Tables E7, E12, and E17), which are exclusively explained by contrasts between ERA and the other two selectors. In no case are statistically significant differences observed between AHSIV and RMSSE_h.

Robust descriptive statistics, together with the aggregated global GRA and the final ranking by horizon, consistently place AHSIV in the leading positions, closely followed by RMSSE_h, while ERA systematically occupies the last position (Tables E3, E8, E13, and E18). Consistently, the heatmaps of selection frequency show that under AHSIV and RMSSE_h, model selection exhibits clear variability as a function of the forecasting horizon (Figures E2, E3, E5, E6, E8, E9, E11, and E12), whereas such variability is less pronounced for the ERA selector (Figures E1, E4, E7, and E10).

4.3. Training 70% and Testing 30%

Under the 70% training and 30% testing scheme, the median GRA heatmaps by forecasting horizon (Figures 18, 19, 20, and 21) confirm high and stable GRA values for AHSIV and RMSSE_h across all analyzed datasets, whereas ERA exhibits persistently lower central values.

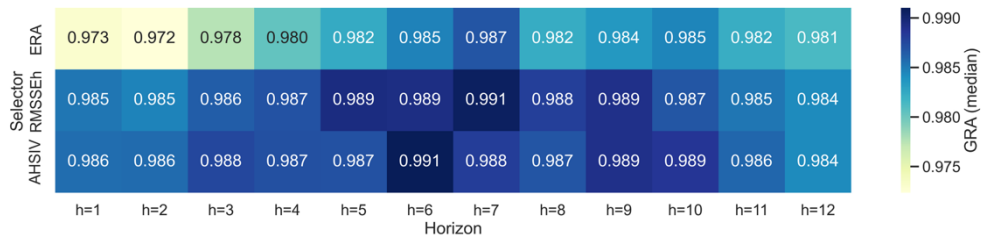


Figure 18. GRA heatmap (median) by selector and horizon, Walmart, training and testing 70:30.

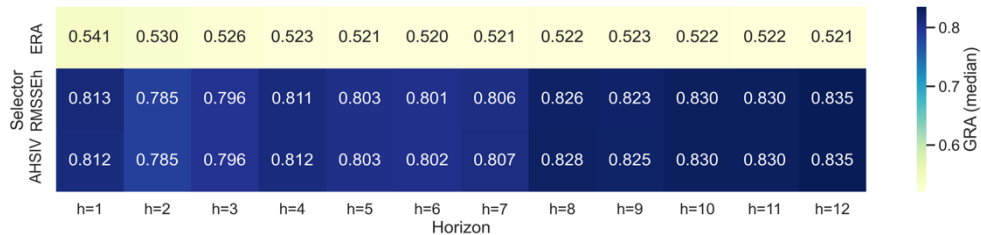


Figure 19. GRA heatmap (median) by selector and horizon, M5, training and testing 70:30.

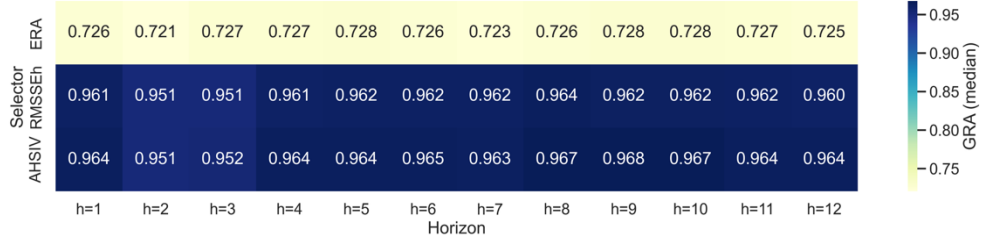


Figure 20. GRA heatmap (median) by selector and horizon, M4, training and testing 70:30.

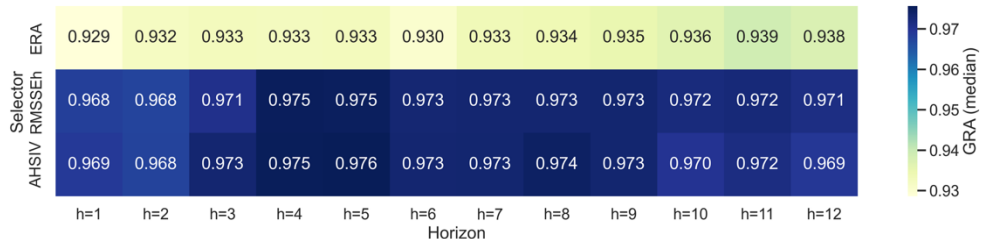


Figure 21. GRA heatmap (median) by selector and horizon, M3, training and testing 70:30.

The GRA boxplots by forecasting horizon (Figures 22, 23, 24, and 25) show that AHSIV and RMSSE_h maintain high medians and bounded dispersion, in contrast to ERA, which exhibits greater relative variability and a systematic presence of outliers in the lower tail.

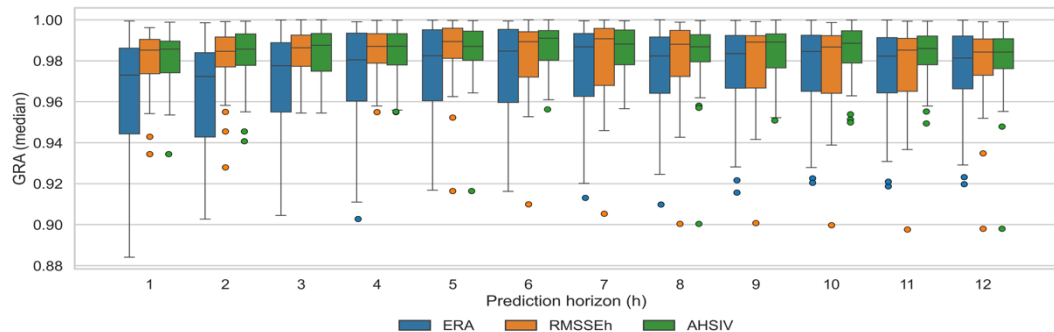


Figure 22. Distribution of GRA by Forecasting Horizon and Selector, Walmart, Training–Testing 70:30.

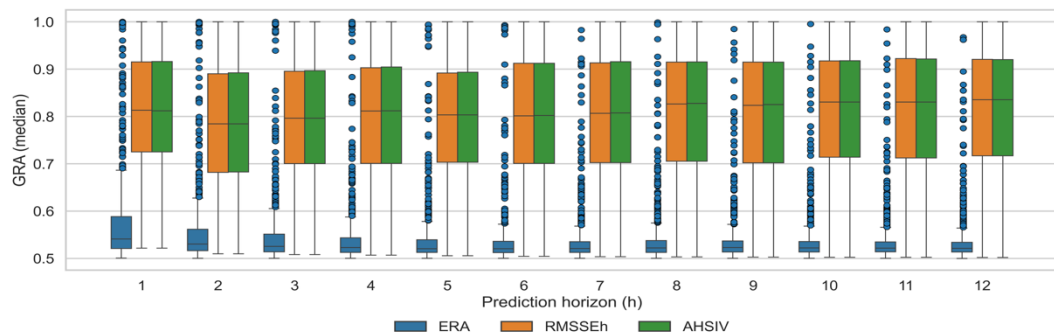


Figure 23. Distribution of GRA by Forecasting Horizon and Selector, M5, Training–Testing 70:30.

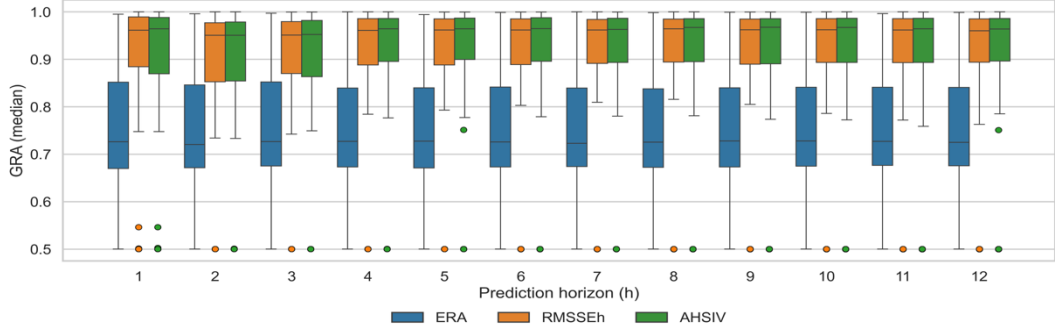


Figure 24. Distribution of GRA by Forecasting Horizon and Selector, M4, Training–Testing 70:30.

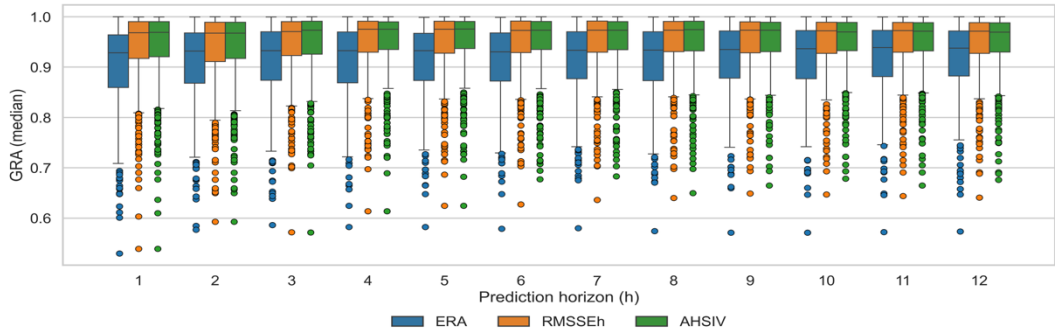


Figure 25. Distribution of GRA by Forecasting Horizon and Selector, M3, Training–Testing 70:30.

From an inferential perspective, Kruskal–Wallis tests identify statistically significant differences across all horizons for the M5, M4, and M3 datasets (Tables F7, F12, and F17), whereas for Walmart, such differences are concentrated in the shortest horizons (Table F2). Dunn’s post-hoc analysis confirms that these differences are exclusively attributable to the inferior performance of ERA, with no statistically significant differences detected between AHSIV and RMSSE_h (Tables F2, F7, F12, and F17).

The aggregated global GRA and the final ranking by horizon reinforce this pattern, consistently placing AHSIV in the leading positions, marginally alternating with RMSSE_h , while ERA systematically remains in the last position (Tables F3, F8, F13, and F18). Consistent with these findings, the heatmaps of selection frequency show that under AHSIV and RMSSE_h , model choice clearly depends on the forecasting horizon (Figures F2, F3, F5, F6, F8, F9, F11, and F12), whereas this dependence is less pronounced in the case of ERA (Figures F1, F4, F7, and F10).

The statistical results consistently reveal that model selection outcomes vary significantly across forecasting horizons. The Kruskal–Wallis tests reported across datasets and partition schemes indicate statistically significant differences among selectors for nearly all evaluated horizons, with extremely small p-values, confirming systematic divergence in ranking behavior as the forecast horizon extends. Post-hoc Dunn comparisons further demonstrate that these differences are not isolated but persist across multiple dataset configurations and training–testing splits. This empirical instability confirms that model selection cannot be treated as a static ranking problem evaluated at a single horizon. Instead, selector performance is inherently horizon-dependent and structurally sensitive. The observed ranking variability provides empirical justification for integrating horizon-aware metric projection via MDFH and regime-conditioned adaptive logic into AHSIV. By explicitly

accounting for forecast-horizon degradation and structural demand regimes, AHSIV addresses the instability phenomenon documented in the statistical tests and provides a coherent selection framework under multi-step evaluation contexts.

5. Discussion

The empirical evidence presented in this study confirms that the selection of forecasting models is structurally unstable across horizons and demand regimes. The significant differences observed among selectors, combined with the consistent non-normal distributions of evaluation metrics, reinforce the conclusion that multi-step forecasting environments require horizon-aware, structure-sensitive selection mechanisms. Within this context, AHSIV exposes competitive statistical performance while increasing the frequency of top-ranked selections per horizon. Its regime-conditioned design mitigates the adverse effects of intermittency and high variability, while MDFH ensures coherent metric comparison across extended planning horizons. These findings support the theoretical premise that model selection must incorporate both temporal degradation dynamics and structural demand characteristics to achieve consistent performance in heterogeneous business environments.

5.1. *Horizon dependence as a structural determinant of model selection*

Empirical evidence consistently shows that demand forecasting model performance is structurally dependent on the forecasting horizon. The analysis of GRA distributions, inferential tests, and selection-frequency heatmaps across all datasets and partition schemes shows that no single forecasting model dominates across all horizons, and that relative rankings vary systematically as horizon length increases. This finding is consistent with the established literature documenting horizon-induced error growth and ranking instability in multi-step forecasting contexts (Tashman, 2000; Hyndman & Athanasopoulos, 2021; Makridakis, Spiliotis, & Assimakopoulos, 2018; Makridakis, Spiliotis, & Assimakopoulos, 2022).

These results reinforce the notion that the forecasting horizon should not be interpreted merely as a technical parameter but as a structural determinant of predictive behavior (Chatfield, 2000). In heterogeneous multi-SKU environments, horizon-specific variability interacts with intermittency, scale, and structural regime, generating shifts in relative model performance that cannot be adequately captured by a single global selection rule. Consequently, selection mechanisms that ignore explicit horizon dependence risk producing structurally biased decisions when extended beyond the evaluation window.

5.2. *Statistical equivalence versus functional adaptability*

From an inferential standpoint, the non-parametric tests conducted under the 91:9, 80:20, and 70:30 schemes consistently indicate statistical equivalence between AHSIV and the RMSSE_h selector in terms of aggregated mean GRA, whereas ERA exhibits significantly inferior performance across most datasets and horizons. This pattern remains stable across partition schemes, suggesting that the relative competitiveness between AHSIV and RMSSE_h is robust to variations in the amount of historical information allocated to training and testing.

However, the horizon-specific analysis reveals a functional distinction. AHSIV more frequently selects the model that maximizes GRA at particular forecasting horizons. This increased frequency of optimal horizon-level selection reflects structural adaptability rather than superiority in global mean performance. While RMSSE_h provides a transparent and statistically competitive monometric baseline, AHSIV demonstrates greater sensitivity to horizon-induced performance variability.

Importantly, the consistency of this pattern across 91:9, 80:20, and 70:30 partitions suggests that the adaptive logic embedded in AHSIV does not depend critically on a specific train–test proportion. At the same time, the results under the 70:30 scheme indicate that longer test windows tend to increase inferential clarity when distinguishing ERA from the other selectors, likely due to greater variability exposure and enhanced statistical power. Nevertheless, the study does not include a formal interaction analysis between the selector and partition scheme. Consequently, while the evidence indicates robustness rather than instability across splits, a more systematic sensitivity analysis of selector performance under varying historical data availability constitutes a relevant extension for future research.

5.3. Methodological implications: the role of MDFH

A central methodological contribution of the study lies in the explicit incorporation of error degradation through the MDFH procedure. The forecasting literature consistently establishes that forecast error tends to increase with horizon due to innovation accumulation and structural uncertainty (Box, Jenkins, Reinsel, & Ljung, 2015; Hyndman & Athanasopoulos, 2021; Chatfield, 2000). At the same time, theoretical work emphasizes that error extrapolation is only valid under structural stability and may become unreliable in the presence of bias or explosive behavior (Clements & Hendry, 1998; Clements & Hendry, 2005; Armstrong, 2001).

By conditioning degradation on structural regime diagnostics derived exclusively from observed data, MDFH prevents optimistic comparisons based solely on short test horizons and ensures coherent model evaluation across future forecasting steps. The robustness of results across the three partition schemes suggests that MDFH remains stable across different levels of historical information, although the estimation of degradation parameters under very short test windows warrants further examination. Future work may therefore explore rolling-origin cross-validation or repeated-window resampling to assess the stability of degradation parameters and selection outcomes across alternative data availability scenarios.

Within this framework, AHSIV does not introduce ad hoc metrics. Instead, it reorganizes established accuracy and bias measures within a horizon-adjusted decision architecture that integrates scaled metrics, bias control, demand regime classification, and multiobjective Pareto dominance into a statistically coherent selection process.

5.4. Operational and strategic implications

From an applied perspective, interpreting GRA as a volumetric coherence metric between forecasted and realized demand establishes a direct connection between model selection and inventory planning decisions (Silver, Pyke, Peterson, & others, 1998; Mentzer & Moon, 2004; Nowotarski & Weron, 2015). High and stable GRA values reflect improved alignment between procurement volumes and

actual market behavior, thereby reducing the economic consequences of systematic over- or underestimation.

The evidence that AHSIV and RMSSE_h maintain stable performance across partition schemes reinforces the managerial relevance of both approaches under different data availability conditions. When the objective is methodological simplicity and strong aggregated performance, RMSSE_h represents a parsimonious and transparent alternative. Conversely, in environments characterized by structural heterogeneity and differentiated planning horizons, AHSIV provides additional functional robustness by adapting selection logic to regime and horizon, thereby enhancing coherence across operational time frames.

6. Conclusions

This study addressed the problem of selecting a demand forecasting model in business environments characterized by structural heterogeneity, forecasting-horizon dependence, and the absence of a universally dominant model. The empirical results confirm that predictive performance is inherently horizon-dependent and that relative model rankings vary systematically as projections extend into future periods.

The explicit incorporation of horizon-induced error degradation via MDFH ensures coherent multi-step comparisons and mitigates optimistic bias arising from short evaluation windows. Within this adjusted framework, AHSIV achieves statistical equivalence with the best monometric baseline in terms of aggregated GRA, while increasing the probability of selecting the best-performing model at specific forecasting horizons.

The robustness of these findings across the 91:9, 80:20, and 70:30 partition schemes indicates that the relative competitiveness between AHSIV and RMSSE_h is not driven by a particular allocation of historical data. However, further research may formally examine interaction effects between partition length, degradation estimation, and selection stability through repeated resampling or rolling-origin designs.

Overall, the results demonstrate that optimal demand forecasting model selection cannot be reduced to a single global ranking rule independent of horizon. Instead, adaptive, structurally informed selection mechanisms provide a principled, replicable approach to addressing horizon-induced variability in multi-SKU demand environments. Future research may extend this framework by incorporating cost-sensitive evaluation functions, probabilistic forecast metrics, and dynamic weighting schemes aligned with differentiated operational planning cycles.

CRediT authorship contribution statement

Adolfo González: Conceptualization, Methodology, Software, Writing – original draft, Investigation, Supervision, Writing – review & editing. **Victor Parada:** Writing – review & editing.

Declaration of competing interest

The authors declare that they have no known competing financial interests or personal relationships that could have appeared to influence the work reported in this paper.

Funding

This research received no external funding.

Data availability

The datasets analyzed in this study are publicly available from the following sources: Walmart dataset (Yasser, 2021), M3 (Makridakis & Hibon, The M3-Competition: results, conclusions and implications, 2000), M4 (Makridakis, Spiliotis, & Assimakopoulos, 2018), and M5 (Makridakis, Spiliotis, & Assimakopoulos, 2022).

Appendix A

Algorithm A1. Metric Degradation by Forecast Horizon (MDFH)

ALGORITHM MDFH(y_pred, metric_value, h_test, h_future, metric_type, y_test_true, y_test_pred, block_size, alpha_bounds)

INPUT:

y_pred → Vector used for structural regime diagnosis (evaluated trajectory)
metric_value → Metric value computed on test horizon
h_test → Test horizon
h_future → Future forecast horizon
metric_type → {RMSE, RMSSE, MAE}
y_test_true → True values on test horizon (optional)
y_test_pred → Predicted values on test horizon (optional)
block_size → Block size for empirical alpha estimation
alpha_bounds → Lower and upper bounds for alpha regularization

OUTPUT:

metric_final → Horizon-adjusted metric value

BEGIN

IF length(y_pred) < 2 THEN
 RETURN metric_value
END IF

IF metric_type ∉ {RMSE, RMSSE, MAE} THEN
 RETURN metric_value
END IF

1) Structural regime diagnosis

delta ← difference(y_pred)
delta_abs ← abs(delta)

mean_delta ← mean(delta_abs)
std_delta ← std(delta_abs)
cv_delta ← std_delta / mean_delta

delta2_abs_mean ← mean(abs(difference(delta)))

IF cv_delta < 0.2 AND delta2_abs_mean < 0.1 * mean_delta THEN
 regimen ← "estable"
ELSE IF cv_delta < 0.5 THEN
 regimen ← "sesgo"
ELSE
 regimen ← "explosion"
END IF

IF regimen ≠ "estable" THEN
 RETURN metric_value
END IF

```

# -----
# 2) Empirical estimation of alpha
# -----

alpha ← None

IF y_test_true and y_test_pred are available AND
length(y_test_true) = length(y_test_pred) AND
length(y_test_true) ≥ 2 * block_size THEN

    errors ← abs(y_test_true - y_test_pred)

    n_blocks ← floor(length(errors) / block_size)

    IF n_blocks ≥ 2 THEN

        block_mae ← median absolute error within each block
        block_h ← mean horizon index of each block

        IF first and last block values valid THEN
            alpha_raw ← log(block_mae_last / block_mae_first)
            / log(block_h_last / block_h_first)

            IF alpha_raw is finite THEN
                alpha ← clip(alpha_raw, alpha_bounds)
            END IF
        END IF

        END IF

    END IF

# -----
# 3) Fallback alpha
# -----

IF alpha is None THEN
    alpha ← 0.5
END IF

# -----
# 4) Final adjustment
# -----

factor ← (h_future / h_test)^alpha
metric_final ← metric_value * factor

RETURN metric_final

END

```

Algorithm A2. Selector RMSSE evaluated at forecast horizon h

```

ALGORITHM RMSSE_h(df, n_ciclos)
INPUT:
    df          → DataFrame with forecasting metrics per model
    n_ciclos   → Forecast horizon

OUTPUT:
    df          → DataFrame with Rank and F_RMSSE score

REQUIRE:
    RMSSE_F_n_ciclos ∈ df
    → Metric adjusted using MDFH

COMPUTE:
    F_RMSSE ← RMSSE_F_n_ciclos

ASSIGN:
    Rank ← ordinal ranking of F_RMSSE (ascending)

RETURN df

```

END ALGORITHM

Algorithm A3. Hybrid Selector for Intermittency and Variability (AHSIV)

```
ALGORITHM AHSIV (df, n_ciclos)
  INPUT:
    df          → DataFrame with forecasting metrics per model
    n_ciclos   → Forecast horizon
  OUTPUT:
    df          → DataFrame with Rank AHSIV and AHSIV score
  REQUIRE:
    RMSSE_F_n_ciclos, MAE_F_n_ciclos
    → Metrics adjusted using MDFH
    sMAPE, c, p, BIAS ∈ df
  INITIALIZE:
    p_star ← 0.5
    c_star ← 0.7
  COMPUTE:
    freq ← median(p)
    cv ← median(c)
  IF freq ≥ p_star AND cv < c_star THEN
    COMPUTE Pareto front minimizing:
    {RMSSE_F_n_ciclos, MAE_F_n_ciclos}
  ASSIGN:
    FPARETO_RMSSE_MAE
  NORMALIZE:
    FPARETO_n ← ranking normalization of FPARETO_RMSSE_MAE
  SELECT:
    candidatos ← two models with smallest FPARETO_n
  SORT candidatos BY:
    sMAPE (ascending)
  SELECT:
    elegido ← model minimizing |BIAS|
  ELSE
    SELECT:
      elegido ← model minimizing RMSSE_F_n_ciclos
  END IF
  INITIALIZE:
    Rank_AHSIV ← NaN for all models
  ASSIGN:
    Rank_AHSIV (elegido) ← 1
  ASSIGN:
    increasing Rank_AHSIV to remaining models
  COMPUTE:
    AHSIV ← (Rank_AHSIV - 1) / (N - 1)
  RETURN df
END ALGORITHM
```

Algorithm A4. Selector Equilibrium Ranking Aggregation (ERA)

```
ALGORITHM ERA(df, n_ciclos)
  INPUT:
    df          → DataFrame with forecasting metrics per model
    n_ciclos   → Forecast horizon
  OUTPUT:
    df          → DataFrame with F ERA score and Rank
  REQUIRE:
    MAE_F_n_ciclos, RMSE_F_n_ciclos ∈ df
    → Metrics adjusted using MDFH
```

```

MAPE, R2 ⊆ df

DEFINE:
  metricas_min ← {MAE_F_n_ciclos, RMSE_F_n_ciclos, MAPE}
  metricas_max ← {R2}

INITIALIZE:
  rank_cols ← ∅

FOR each metric m ∈ metricas_min DO
  IF m ∈ df THEN
    COMPUTE:
      rank_m ← ordinal rank of m (ascending)
      ADD rank_m to rank_cols
  END IF
END FOR

FOR each metric m ∈ metricas_max DO
  IF m ∈ df THEN
    COMPUTE:
      rank_m ← ordinal rank of m (descending)
      ADD rank_m to rank_cols
  END IF
END FOR

REQUIRE:
  rank_cols ≠ ∅

COMPUTE:
  ranking_total ← sum of all ranks in rank_cols

NORMALIZE:
  IF max(ranking_total) > min(ranking_total) THEN
    F ERA ← 1 - (ranking_total - min) / (max - min)
  ELSE
    F ERA ← 1
  END IF

ASSIGN:
  Rank ← ordinal ranking of F ERA (descending)

SORT:
  df by F ERA (descending)

RETURN df
END ALGORITHM

```

Table A1. Prediction Models.

Model	Cluster	Explanation
ARIMA	ES	Autoregressive Integrated Moving Average is a classical time series approach that captures linear relationships through autoregressive components, moving averages, and differencing to address trends. It is particularly effective for stationary data or for series that can be rendered stationary through appropriate transformations (Box, Jenkins, Reinsel, & Ljung, 2015).
KNN	ES	K-Nearest Neighbors is a nonparametric technique that estimates values based on the average of the k nearest neighbors in the feature space. It is characterized by its simplicity, interpretability, and its capacity to handle nonlinear data structures (Altman, 1992).
DTR	ES	Decision Tree Regression generates partitions through hierarchical decision rules, resulting in interpretable models, although they are prone to overfitting (Breiman, Friedman, Olshen, & Stone, 1984).
RFR	ES	Random Forest Regressor constructs an ensemble of multiple decision trees trained on random subsets of the data, thereby improving predictive accuracy and reducing overfitting (Breiman, Random forests, 2001).
PLR	ES	Polynomial Regression extends linear regression by incorporating polynomial terms, thereby enabling the modeling of nonlinear relationships in a straightforward manner (Montgomery, Peck, & Vining, 2021).
MLP	ES	Multilayer Perceptron is an artificial neural network with one or more hidden layers, capable of capturing complex nonlinear relationships and widely used in regression and classification tasks (Haykin, 1994).
LR	-	Linear Regression is a fundamental regression model that estimates the relationship between independent and dependent variables by minimizing the squared error (Montgomery, Peck, & Vining, 2021).

SVR	SCS	Support Vector Regression is an extension of support vector machines for regression tasks, designed to identify a function that lies within a specified tolerance margin from the observed values, employing kernel functions to capture complex relationships (Smola & Schölkopf, 2004).
LSR	SCS	Lasso Regression incorporates an L1 regularization penalty, thereby facilitating automatic variable selection by shrinking less relevant coefficients to zero (Tibshirani, 1996).
RR	SCS	Ridge Regression applies an L2 regularization penalty, which mitigates multicollinearity without eliminating variables (Hoerl & Kennard, 1970).
ENR	SCS	Elastic Net Regression combines L1 and L2 penalties, enabling the selection of relevant variables while controlling for collinearity (Zou & Hastie, 2005).
GBR	SCS	Gradient Boosting Regressor constructs decision trees sequentially, where each new tree corrects the errors of the preceding ones, achieving high predictive performance at the cost of increased calibration complexity (Friedman, 2001).
XGBoost	SCS	An optimized implementation of gradient boosting improves computational speed, regularization, and the handling of missing data, making it particularly effective for structured prediction problems (Chen & Guestrin, 2016).
HR	SCS	Huber Regressor is a robust regression technique that employs the Huber loss function, combining sensitivity to small squared errors with resistance to outliers (Huber P. J., 1992).
BR	SCS	Bayesian Ridge Regression introduces prior distributions over the regression coefficients, thereby incorporating uncertainty into the parameter estimates (MacKay, 1992).
SES	SCS	Simple Exponential Smoothing is applied to time series without trend or seasonality, assigning greater weight to recent observations through an exponential decay rule (Brown, 1959).
CatBoost	SCS	A boosting algorithm that efficiently handles categorical variables without explicit encoding and reduces overfitting through ordered boosting (Prokhorenkova, Gusev, Vorobev, Dorogush, & Gulin, 2018).
LSTM	SCS	Long Short-Term Memory is a recurrent architecture designed to capture long-term dependencies in sequential data, particularly useful in time series applications (Hochreiter, 1997). In the present study, a regression-oriented variant is implemented, consisting of two LSTM layers (with 128 and 64 units, respectively, and tanh activation), a dropout mechanism of 30%, an intermediate dense layer with 32 neurons (ReLU activation), and a linear output layer. The model is compiled using the Adam optimizer and employs mean squared error (MSE) as the loss function.
GRU	SCS	Gated Recurrent Unit is a recurrent architecture designed to model temporal dependencies through a simplified gating mechanism, reducing computational complexity compared to LSTM while maintaining an adequate capacity to represent sequential dynamics, which makes it particularly suitable for time series applications (Cho et al., 2014). In the present study, a regression-oriented variant is implemented, consisting of a single GRU layer with 64 units and tanh activation, followed by an intermediate dense layer with 64 neurons and ReLU activation. The output layer corresponds to a dense layer whose dimensionality is adjusted according to the prediction horizon under consideration, thereby enabling direct multi-step forecasting. The model is compiled using the Adam optimizer and employs mean squared error (MSE) as the loss function, ensuring consistency in predictive performance evaluation.
BiLSTM	SCS	Bidirectional Long Short-Term Memory Neural Network is a bidirectional recurrent architecture that extends the LSTM model by simultaneously processing the temporal sequence in both forward and backward directions, thereby enabling the capture of past and future dependencies within the observation window and improving the representation of complex temporal patterns (Schuster & Paliwal, 1997; Graves & Schmidhuber, 2005). In the present study, a multi-step regression-oriented variant is implemented, consisting of two stacked BiLSTM layers with 64 and 32 units, respectively. The first layer operates in full sequential mode, while the second condenses the temporal information into a final state representation. To mitigate the risk of overfitting, dropout regularization with a rate of 20% is applied after each recurrent layer. The resulting representation is subsequently processed through two intermediate dense layers with 64 and 32 neurons, respectively, both using ReLU activation, before applying a dense output layer with linear activation whose dimensionality is adjusted according to the prediction horizon under consideration, thereby enabling direct multi-step forecasting. The model is trained using the Adam optimizer and employs mean squared error (MSE) as the loss function, ensuring consistency in predictive performance evaluation.
BRNN	SCS	Bidirectional Simple Recurrent Neural Network is a bidirectional recurrent architecture based on simple recurrent units, which processes the input temporal sequence simultaneously in forward and backward directions, thereby capturing bidirectional temporal dependencies within the observation window, albeit with a simpler structure than LSTM or GRU variants (Schuster & Paliwal, 1997). In the present study, a multi-step regression-oriented variant is implemented,

consisting of a single bidirectional SimpleRNN layer with 64 units and tanh activation, which condenses the temporal information into a final representative state. The resulting representation is subsequently processed through an intermediate dense layer with 64 neurons and ReLU activation, before applying a dense output layer whose dimensionality is adjusted according to the prediction horizon under consideration, thereby enabling direct multi-step forecasting. The model is trained using the Adam optimizer and employs mean squared error (MSE) as the loss function, ensuring consistent evaluation of predictive performance.

TRF	SCS	Transformer Model for Time Series is an architecture based on autoregressive self-attention mechanisms that dispenses with explicit recurrence and enables the modeling of long-range temporal dependencies through multi-head attention, making it particularly suitable for capturing complex and non-local relationships in temporal sequences (Vaswani, 2017). In the present study, a multi-step regression-oriented variant is implemented, beginning with a dense projection of the input into a 64-dimensional representation space, followed by a Transformer block composed of a multi-head attention mechanism with two heads and an internal feed-forward network of 128 units. The block incorporates residual connections, layer normalization, and dropout regularization, allowing stable information propagation and robust learning of temporal dependencies. The resulting representation is subsequently transformed through flattening and two intermediate dense layers with 64 and 32 neurons, respectively, both using ReLU activation, before applying a dense output layer with linear activation whose dimensionality is adjusted according to the prediction horizon under consideration, thereby enabling direct multi-step forecasting. The model is trained using the Adam optimizer and employs mean squared error (MSE) as the loss function, ensuring consistency in predictive performance evaluation.
-----	-----	---

Appendix B

Table B1. Execution scheme of the experimental protocol.

ID	1	2	3	4	5	6	7	8	9	10
1	Walmart	X	91:09	X	X	X	X	X	X	X
2	Walmart	X	80:20	X	X	X	X	X	X	X
3	Walmart	X	70:30	X	X	X	X	X	X	X
4	M3	X	91:09	X	X	X	X	X	X	X
5	M3	X	80:20	X	X	X	X	X	X	X
6	M3	X	70:30	X	X	X	X	X	X	X
7	M4	X	91:09	X	X	X	X	X	X	X
8	M4	X	80:20	X	X	X	X	X	X	X
9	M4	X	70:30	X	X	X	X	X	X	X
10	M5	X	91:09	X	X	X	X	X	X	X
11	M5	X	80:20	X	X	X	X	X	X	X
12	M5	X	70:30	X	X	X	X	X	X	X

Appendix C

Experimental Environment, Optimizer Configurations, and Parameter Search Spaces

The computational experiments were conducted using Jupyter Notebooks within a Conda environment, employing Python version 3.12.7, on a macOS operating system (Darwin Kernel 24.6.0) running on a 64-bit ARM architecture (Apple M4), with 14 physical cores, 14 logical cores, and 32 GB of RAM. All executions were performed exclusively in CPU mode to ensure reproducibility of the results. Although the processor provides graphics computing capabilities, no GPU-specific acceleration frameworks, such as CUDA or the Metal backend for TensorFlow, were utilized.

Optimizer Configuration

Parameter and hyperparameter optimization was addressed through two distinct approaches. In the case of Optuna, each training and optimization cycle was conducted under a fixed budget of 21 trials, enabling efficient exploration of the search space through Bayesian techniques. In contrast, Grid

Search was implemented via exhaustive parameter sweeps, systematically evaluating all possible combinations within the predefined discrete search spaces.

Parameter Search Spaces

Table C1 presents the parameter search spaces considered for each model during the training and optimization processes. These ranges were defined based on the specialized literature and the adopted experimental design, with the objective of ensuring comparability of results across the different evaluated models.

Table C1. Parameter ranges explored for the models considered in this study.

Model	Parameters
ARIMA	p=0 between 5, d=0 between 3, q=0 between 5
KNN	n_neighbors between 1 and 35
DTR	max_depth between 1 and 32; min_samples_split = 2; min_samples_leaf = 1; random_state = 21
RFR	n_estimators between 1 and 100; random_state = 21
PLR	degree between 1 and 3; include_bias = False; interaction_only = True
MLP	hidden_layer_sizes = [layer 1: 16–32; layer 2: 0–32; layer 3: 0–32]; activation = 'relu'; solver = 'adam'; max_iter = 1000; early_stopping = True; n_iter_no_change = 10; random_state = 21
LR	Defaults
SVR	kernel = 'rbf'; C between 0.01 and 20; degree between 2 and 5; epsilon between 0.01 and 1; gamma = 'scale'.
LSR	alpha between 0.01 and 5; random_state = seed_value; max_iter = 8000.
RR	alpha between 0.1 and 10; max_iter = 8000
ENR	alpha between 0.01 and 0.02; l1_ratio between 1e-3 and 0.1
GBR	n_estimators between 10 and 2000; learning_rate between 0.1 and 0.3; random_state = seed_value
XGBoost	n_estimators between 10 and 2000; learning_rate between 0.1 and 0.3; max_depth between 3 and 5; enable_categorical = True; random_state = seed_value
HR	epsilon between 1 and 3; max_iter = 1000; alpha = 0.0001; tol = 1e-4
BR	max_iter between 50 and 1000; alpha_1 between 1e-6 and 1e-2; alpha_2 between 1e-6 and 1e-2
SES	smoothing_level between 0.01 and 0.9; optimized = False
CatBoost	iterations between 100 and 1000; depth between 3 and 10; learning_rate between 0.01 and 0.3; loss_function = 'Huber:delta=1.0'; train_dir = tmp_dir; verbose = False; random_seed = 21
LSTM	epochs between 1 and 80
GRU	epochs between 1 and 80
BiLSTM	epochs between 1 and 80
BRNN	epochs between 1 and 80
TRF	epochs between 1 and 80

Appendix D

Walmart

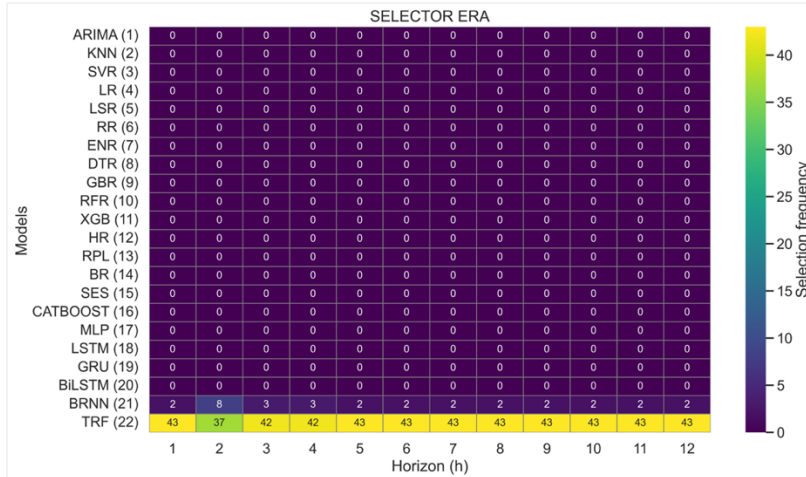


Figure D1. Model Selection Frequency by Forecast Horizon (ERA, Walmart 91:9).

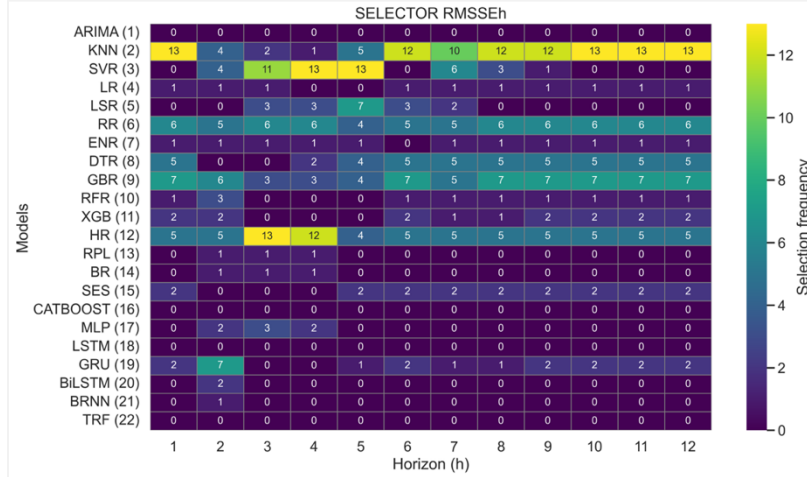


Figure D2. Model Selection Frequency by Forecast Horizon ($RMSSE_h$, Walmart 91:9).

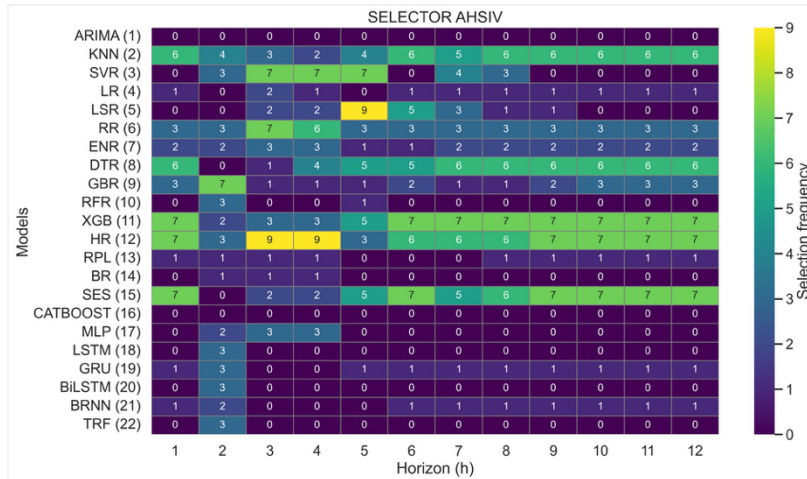


Figure D3. Model Selection Frequency by Forecast Horizon (AHSIV, Walmart 91:9).

Table D1. Normality (Shapiro–Wilk) - Walmart - Training 91% and Testing 9%

Horizon	ERA (result)	ERA (W, p)	RMSSEh (result)	RMSSEh (W, p)	AHSIV (result)	AHSIV (W, p)
h = 1	Not normal	0.8826, 2.85e-04	Not normal	0.8839, 3.09e-04	Not normal	0.8414, 2.22e-05
h = 2	Not normal	0.8944, 6.38e-04	Not normal	0.8567, 5.48e-05	Not normal	0.8808, 2.51e-04
h = 3	Not normal	0.8443, 2.63e-05	Not normal	0.7867, 1.23e-06	Not normal	0.8487, 3.39e-05
h = 4	Not normal	0.8393, 1.96e-05	Not normal	0.7691, 5.32e-07	Not normal	0.8213, 7.23e-06
h = 5	Not normal	0.8719, 1.41e-04	Not normal	0.7574, 3.11e-07	Not normal	0.7200, 6.18e-08
h = 6	Not normal	0.8447, 2.68e-05	Not normal	0.9292, 8.76e-03	Not normal	0.9092, 1.86e-03
h = 7	Not normal	0.8292, 1.12e-05	Not normal	0.8882, 4.15e-04	Not normal	0.8890, 4.38e-04
h = 8	Not normal	0.8204, 6.89e-06	Not normal	0.8666, 1.01e-04	Not normal	0.8821, 2.75e-04
h = 9	Not normal	0.8323, 1.32e-05	Not normal	0.8412, 2.20e-05	Not normal	0.8380, 1.82e-05
h = 10	Not normal	0.8347, 1.52e-05	Not normal	0.8487, 3.39e-05	Not normal	0.8468, 3.03e-05
h = 11	Not normal	0.8099, 3.96e-06	Not normal	0.8497, 3.60e-05	Not normal	0.8685, 1.14e-04
h = 12	Not normal	0.7762, 7.42e-07	Not normal	0.8703, 1.27e-04	Not normal	0.8796, 2.33e-04

Table D2. Kruskal–Wallis, Dunn - Walmart - Training 91% and Testing 9%

Horizon	Kruskal–Wallis			Test post-hoc de Dunn		
	Result	H	p-value	ERA vs RMSSEh	ERA vs AHSIV	RMSSEh vs AHSIV
h = 1	Significant differences	9.7202	7.7499e-03	Significant (p = 0.01639)	Significant (p = 0.02684)	Not significant (p = 1.00000)
h = 2	No significant differences were detected.	1.4056	4.9519e-01	Not significant (p = 1.00000)	Not significant (p = 0.81461)	Not significant (p = 1.00000)
h = 3	No significant differences were detected.	2.0028	3.6736e-01	Not significant (p = 0.82523)	Not significant (p = 0.55462)	Not significant (p = 1.00000)

h = 4	No significant differences were detected.	0.7604	6.8372e-01	Not significant (p = 1.00000)	Not significant (p = 1.00000)	Not significant (p = 1.00000)
h = 5	No significant differences were detected.	3.0621	2.1630e-01	Not significant (p = 0.99588)	Not significant (p = 0.24227)	Not significant (p = 1.00000)
h = 6	No significant differences were detected.	1.8352	3.9947e-01	Not significant (p = 1.00000)	Not significant (p = 0.53350)	Not significant (p = 1.00000)
h = 7	No significant differences were detected.	1.0685	5.8611e-01	Not significant (p = 1.00000)	Not significant (p = 0.90980)	Not significant (p = 1.00000)
h = 8	No significant differences were detected.	0.1964	9.0649e-01	Not significant (p = 1.00000)	Not significant (p = 1.00000)	Not significant (p = 1.00000)
h = 9	No significant differences were detected.	0.1083	9.4729e-01	Not significant (p = 1.00000)	Not significant (p = 1.00000)	Not significant (p = 1.00000)
h = 10	No significant differences were detected.	0.0328	9.8373e-01	Not significant (p = 1.00000)	Not significant (p = 1.00000)	Not significant (p = 1.00000)
h = 11	No significant differences were detected.	0.5495	7.5976e-01	Not significant (p = 1.00000)	Not significant (p = 1.00000)	Not significant (p = 1.00000)
h = 12	No significant differences were detected.	0.0555	9.7262e-01	Not significant (p = 1.00000)	Not significant (p = 1.00000)	Not significant (p = 1.00000)

Table D3. Global Synthesis of Descriptive Statistics by Forecast Horizon and Selector - Walmart - Training 91% and Testing 9%

Horizon	Selector	count	mean	median	std	min	max	IQR	MAD	Robust CV	GRA global	Final ranking
1	ERA	45	0.97196	0.97454	0.02272	0.89806	0.99858	0.02338	0.01375	0.02399	43.73840	3
1	RMSSEh	45	0.98335	0.98748	0.01489	0.93854	0.99982	0.01853	0.00826	0.01876	44.25089	1
1	AHSIV	45	0.98317	0.98837	0.01452	0.93854	0.99975	0.01513	0.00584	0.01531	44.24275	2
2	ERA	45	0.97367	0.97822	0.02108	0.90939	0.99848	0.02499	0.01162	0.02554	43.81535	3
2	RMSSEh	45	0.97761	0.98440	0.01926	0.91399	0.99920	0.02036	0.01015	0.02068	43.99259	2
2	AHSIV	45	0.97896	0.98447	0.01683	0.92491	0.99920	0.02044	0.01008	0.02077	44.05329	1
3	ERA	45	0.97675	0.98498	0.02041	0.90290	0.99914	0.02872	0.00950	0.02916	43.95368	3
3	RMSSEh	45	0.98060	0.98474	0.01976	0.91263	0.99922	0.01832	0.00932	0.01861	44.12721	2
3	AHSIV	45	0.98293	0.98502	0.01512	0.92200	0.99970	0.01875	0.00923	0.01904	44.23168	1
4	ERA	45	0.97880	0.98555	0.02023	0.90195	0.99977	0.02094	0.01006	0.02125	44.04619	3
4	RMSSEh	45	0.98386	0.98641	0.01447	0.91484	0.99968	0.01538	0.00815	0.01559	44.27352	1
4	AHSIV	45	0.98366	0.98487	0.01383	0.92168	0.99968	0.01487	0.00738	0.01510	44.26454	2
5	ERA	45	0.98066	0.98520	0.01731	0.91787	0.99980	0.02200	0.00995	0.02233	44.12948	3
5	RMSSEh	45	0.98474	0.98671	0.01407	0.91516	0.99962	0.01459	0.00729	0.01479	44.31337	2
5	AHSIV	45	0.98641	0.98885	0.01397	0.91516	0.99969	0.01326	0.00692	0.01341	44.38867	1
6	ERA	45	0.98072	0.98476	0.01710	0.91143	0.99987	0.02195	0.00891	0.02229	44.13229	3
6	RMSSEh	45	0.98460	0.98577	0.01165	0.94822	0.99995	0.01567	0.00837	0.01590	44.30701	2
6	AHSIV	45	0.98615	0.98672	0.01064	0.94822	0.99998	0.01462	0.00782	0.01482	44.37675	1
7	ERA	45	0.98134	0.98671	0.01764	0.90856	0.99955	0.01877	0.00985	0.01903	44.16049	3
7	RMSSEh	45	0.98466	0.98780	0.01284	0.94452	0.99994	0.01527	0.00745	0.01545	44.30969	2
7	AHSIV	45	0.98569	0.98878	0.01250	0.94452	0.99994	0.01471	0.00759	0.01488	44.35596	1
8	ERA	45	0.98066	0.98353	0.01865	0.90383	0.99862	0.02266	0.01244	0.02304	44.12992	3
8	RMSSEh	45	0.98304	0.98550	0.01375	0.94096	0.99986	0.01123	0.00680	0.01139	44.23664	2
8	AHSIV	45	0.98391	0.98858	0.01325	0.94096	0.99986	0.01747	0.00629	0.01767	44.27601	1
9	ERA	45	0.98133	0.98732	0.01854	0.90536	0.99988	0.02368	0.01073	0.02398	44.16004	3
9	RMSSEh	45	0.98272	0.98755	0.01471	0.94083	0.99894	0.01459	0.00727	0.01478	44.22255	2
9	AHSIV	45	0.98384	0.98755	0.01382	0.94083	0.99894	0.01679	0.00727	0.01700	44.27261	1
10	ERA	45	0.98130	0.98908	0.01889	0.90617	0.99956	0.02533	0.01008	0.02561	44.15840	3
10	RMSSEh	45	0.98263	0.98720	0.01568	0.93999	0.99984	0.01736	0.00710	0.01759	44.21826	2
10	AHSIV	45	0.98356	0.98720	0.01458	0.93999	0.99984	0.01902	0.00774	0.01927	44.26018	1
11	ERA	45	0.97869	0.98490	0.02127	0.90198	0.99959	0.01826	0.00843	0.01854	44.04111	3
11	RMSSEh	45	0.98187	0.98726	0.01613	0.93859	0.99906	0.01605	0.00716	0.01626	44.18406	2
11	AHSIV	45	0.98300	0.98720	0.01520	0.93859	0.99964	0.02045	0.00838	0.02071	44.23499	1
12	ERA	45	0.97916	0.98473	0.02204	0.91783	0.99843	0.02144	0.01069	0.02177	44.06233	3
12	RMSSEh	45	0.98153	0.98571	0.01673	0.93471	0.99985	0.01515	0.00768	0.01537	44.16867	2
12	AHSIV	45	0.98218	0.98571	0.01558	0.93471	0.99996	0.01737	0.00784	0.01763	44.19815	1

M5

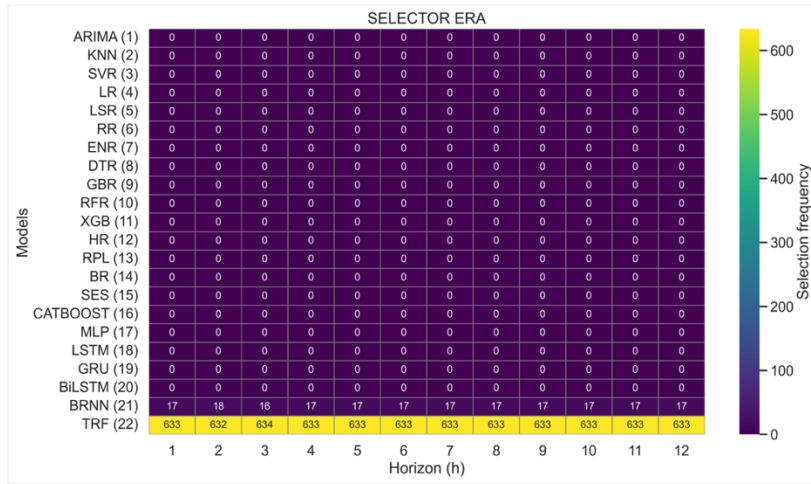


Figure D4. Model Selection Frequency by Forecast Horizon (ERA, M5, 91:9).

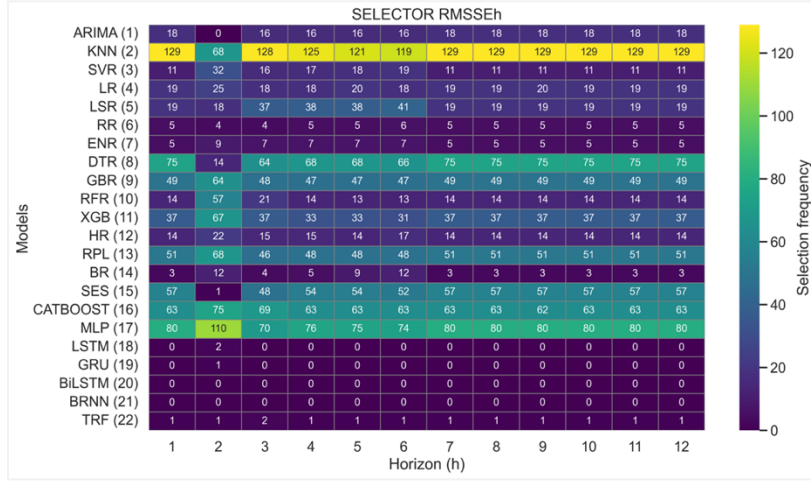


Figure D5. Model Selection Frequency by Forecast Horizon (RMSSE_h, M5, 91:9).

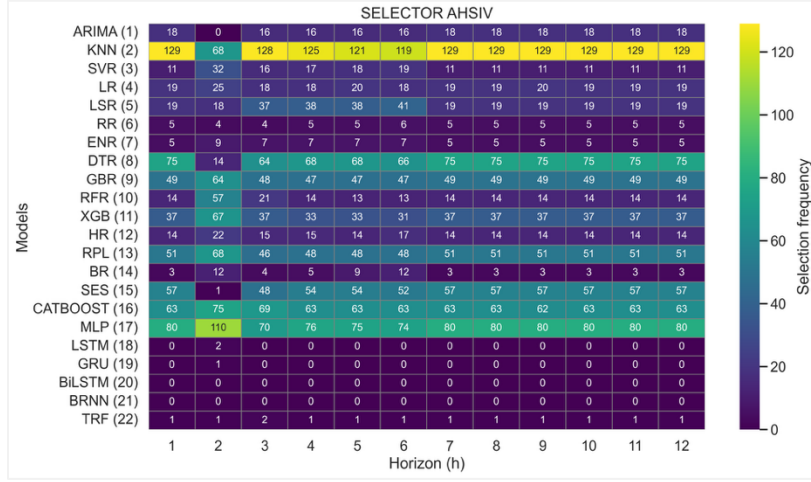


Figure D6. Model Selection Frequency by Forecast Horizon (AHSIV, M5, 91:9).

Table D6. Normality (Shapiro–Wilk) – M5 - Training 91% and Testing 9%

Horizon	ERA (result)	ERA (W, p)	RMSSEh (result)	RMSSEh (W, p)	AHSIV (result)	AHSIV (W, p)
1	0.0000000000000000	0.0000000000000000	0.0000000000000000	0.0000000000000000	0.0000000000000000	0.0000000000000000

h = 1	Not normal	0.6686, 1.09e-33	Not normal	0.9529, 1.49e-13	Not normal	0.9532, 1.66e-13
h = 2	Not normal	0.5616, 2.27e-37	Not normal	0.9573, 8.49e-13	Not normal	0.9570, 7.66e-13
h = 3	Not normal	0.4882, 1.71e-39	Not normal	0.9606, 3.43e-12	Not normal	0.9608, 3.66e-12
h = 4	Not normal	0.4520, 1.89e-40	Not normal	0.9600, 2.69e-12	Not normal	0.9601, 2.74e-12
h = 5	Not normal	0.4415, 1.02e-40	Not normal	0.9643, 1.79e-11	Not normal	0.9646, 2.02e-11
h = 6	Not normal	0.4408, 9.82e-41	Not normal	0.9582, 1.24e-12	Not normal	0.9585, 1.42e-12
h = 7	Not normal	0.4467, 1.39e-40	Not normal	0.9505, 5.95e-14	Not normal	0.9502, 5.31e-14
h = 8	Not normal	0.4539, 2.12e-40	Not normal	0.9443, 6.54e-15	Not normal	0.9443, 6.66e-15
h = 9	Not normal	0.4664, 4.47e-40	Not normal	0.9442, 6.43e-15	Not normal	0.9444, 6.87e-15
h = 10	Not normal	0.4594, 2.94e-40	Not normal	0.9348, 3.12e-16	Not normal	0.9349, 3.22e-16
h = 11	Not normal	0.4525, 1.95e-40	Not normal	0.9310, 9.95e-17	Not normal	0.9312, 1.04e-16
h = 12	Not normal	0.4368, 7.79e-41	Not normal	0.9306, 8.83e-17	Not normal	0.9305, 8.52e-17

Table D7. Kruskal–Wallis, Dunn – M5 - Training 91% and Testing 9%

Horizon	Kruskal–Wallis			Test post-hoc de Dunn		
	Result	H	p-value	ERA vs RMSSEh	ERA vs AHSIV	RMSSEh vs AHSIV
h = 1	Significant differences	1045.9900	7.3477e-228	Significant (p = 0.00000)	Significant (p = 0.00000)	Not significant (p = 1.00000)
h = 2	Significant differences	1107.7481	2.8546e-241	Significant (p = 0.00000)	Significant (p = 0.00000)	Not significant (p = 1.00000)
h = 3	Significant differences	1151.6245	8.4707e-251	Significant (p = 0.00000)	Significant (p = 0.00000)	Not significant (p = 1.00000)
h = 4	Significant differences	1162.0012	4.7277e-253	Significant (p = 0.00000)	Significant (p = 0.00000)	Not significant (p = 1.00000)
h = 5	Significant differences	1169.6075	1.0543e-254	Significant (p = 0.00000)	Significant (p = 0.00000)	Not significant (p = 1.00000)
h = 6	Significant differences	1180.7346	4.0434e-257	Significant (p = 0.00000)	Significant (p = 0.00000)	Not significant (p = 1.00000)
h = 7	Significant differences	1186.0602	2.8204e-258	Significant (p = 0.00000)	Significant (p = 0.00000)	Not significant (p = 1.00000)
h = 8	Significant differences	1170.0686	8.3720e-255	Significant (p = 0.00000)	Significant (p = 0.00000)	Not significant (p = 1.00000)
h = 9	Significant differences	1172.3570	2.6664e-255	Significant (p = 0.00000)	Significant (p = 0.00000)	Not significant (p = 1.00000)
h = 10	Significant differences	1174.0918	1.1200e-255	Significant (p = 0.00000)	Significant (p = 0.00000)	Not significant (p = 1.00000)
h = 11	Significant differences	1171.8615	3.4159e-255	Significant (p = 0.00000)	Significant (p = 0.00000)	Not significant (p = 1.00000)
h = 12	Significant differences	1168.1026	2.2374e-254	Significant (p = 0.00000)	Significant (p = 0.00000)	Not significant (p = 1.00000)

Table D8. Global Synthesis of Descriptive Statistics by Forecast Horizon and Selector – M5 - Training 91% and Testing 9%

Horizon	Selector	count	mean	median	std	min	max	IQR	MAD	Robust CV	GRA global	Final ranking
1	ERA	650	0.57120	0.53923	0.08885	0.50158	1.00000	0.06052	0.02347	0.11224	371.28289	3
1	RMSSEh	650	0.82314	0.83441	0.12382	0.54128	1.00000	0.21015	0.10253	0.25186	535.04198	1
1	AHSIV	650	0.82297	0.82907	0.12359	0.54128	1.00000	0.21015	0.10498	0.25348	534.92974	2
2	ERA	650	0.55060	0.52851	0.07248	0.50079	0.99998	0.03488	0.01522	0.06600	357.88972	3
2	RMSSEh	650	0.81239	0.82045	0.13002	0.51417	1.00000	0.21675	0.10797	0.26418	528.05331	2
2	AHSIV	650	0.81252	0.81841	0.13014	0.51417	1.00000	0.21626	0.10873	0.26424	528.13713	1
3	ERA	650	0.54276	0.52411	0.06738	0.50053	0.99990	0.02958	0.01290	0.05644	352.79466	3
3	RMSSEh	650	0.81233	0.80952	0.12773	0.52273	1.00000	0.21133	0.10457	0.26106	528.01368	2
3	AHSIV	650	0.81242	0.80901	0.12759	0.52273	1.00000	0.21099	0.10400	0.26080	528.07095	1
4	ERA	650	0.53948	0.52207	0.06548	0.50040	0.99983	0.02757	0.01183	0.05280	350.65995	3
4	RMSSEh	650	0.81548	0.81767	0.12669	0.51724	1.00000	0.21342	0.10587	0.26101	530.05981	2
4	AHSIV	650	0.81562	0.81767	0.12673	0.51724	1.00000	0.21385	0.10627	0.26154	530.15234	1
5	ERA	650	0.53668	0.52044	0.06230	0.50032	0.99976	0.02311	0.01057	0.04440	348.84447	3
5	RMSSEh	650	0.81206	0.81499	0.12607	0.51389	1.00000	0.20481	0.10238	0.25130	527.83963	1
5	AHSIV	650	0.81194	0.81499	0.12594	0.51389	1.00000	0.20365	0.10204	0.24988	527.76078	2
6	ERA	650	0.53472	0.51973	0.05847	0.50026	0.99865	0.02162	0.00982	0.04160	347.56706	3
6	RMSSEh	650	0.81455	0.82443	0.12760	0.51163	1.00000	0.20802	0.10486	0.25232	529.45718	1
6	AHSIV	650	0.81445	0.82457	0.12745	0.51163	1.00000	0.20879	0.10476	0.25321	529.39502	2
7	ERA	650	0.53443	0.51979	0.05640	0.50023	0.99861	0.02088	0.00921	0.04016	347.37696	3
7	RMSSEh	650	0.81807	0.83427	0.12987	0.51000	1.00000	0.21550	0.10371	0.25830	531.74481	2
7	AHSIV	650	0.81829	0.83427	0.13009	0.51000	1.00000	0.21561	0.10421	0.25844	531.88641	1
8	ERA	650	0.53515	0.52083	0.05597	0.50020	0.99815	0.02133	0.00924	0.04095	347.84610	3
8	RMSSEh	650	0.81825	0.84277	0.13206	0.50877	1.00000	0.21499	0.10538	0.25510	531.86054	2
8	AHSIV	650	0.81830	0.84312	0.13209	0.50877	1.00000	0.21489	0.10567	0.25487	531.89321	1
9	ERA	650	0.53402	0.52152	0.05061	0.50018	0.99637	0.02110	0.00922	0.04046	347.11246	3
9	RMSSEh	650	0.81852	0.84067	0.13135	0.50781	1.00000	0.20468	0.09498	0.24347	532.04119	1
9	AHSIV	650	0.81837	0.84097	0.13118	0.50781	1.00000	0.20368	0.09437	0.24220	531.94056	2
10	ERA	650	0.53320	0.52090	0.04906	0.50016	0.99571	0.02049	0.00856	0.03934	346.57834	3
10	RMSSEh	650	0.82385	0.84783	0.13238	0.50704	1.00000	0.20491	0.09698	0.24168	535.50395	1

10	AHSIV	650	0.82378	0.84840	0.13227	0.50704	1.00000	0.20230	0.09657	0.23845	535.45416	2
11	ERA	650	0.53300	0.52065	0.04952	0.50015	0.99396	0.01876	0.00832	0.03604	346.44755	3
11	RMSSEh	650	0.82632	0.85540	0.13300	0.50641	1.00000	0.21130	0.09607	0.24702	537.10993	1
11	AHSIV	650	0.82632	0.85688	0.13299	0.50641	1.00000	0.21130	0.09577	0.24659	537.10768	2
12	ERA	650	0.53225	0.52076	0.04914	0.50013	0.98813	0.01796	0.00800	0.03448	345.96139	3
12	RMSSEh	650	0.82603	0.85468	0.13250	0.50588	1.00000	0.20219	0.09303	0.23657	536.91792	2
12	AHSIV	650	0.82607	0.85468	0.13257	0.50588	1.00000	0.20346	0.09383	0.23805	536.94621	1

M4

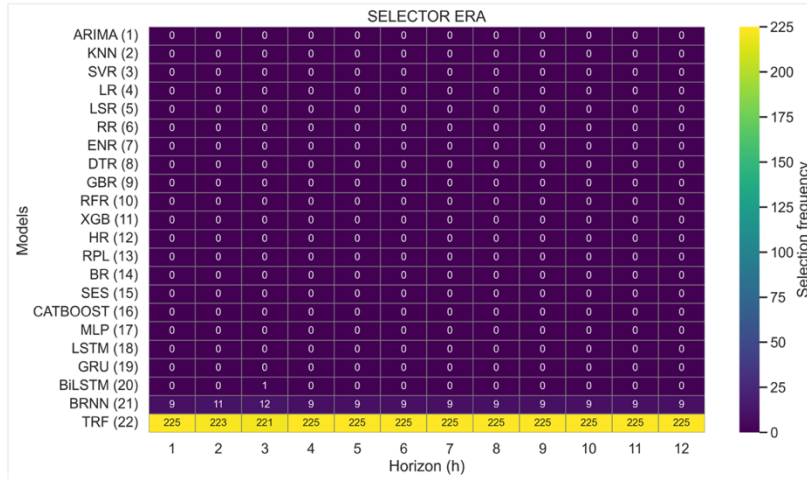


Figure D7. Model Selection Frequency by Forecast Horizon (ERA, M4 91:9).

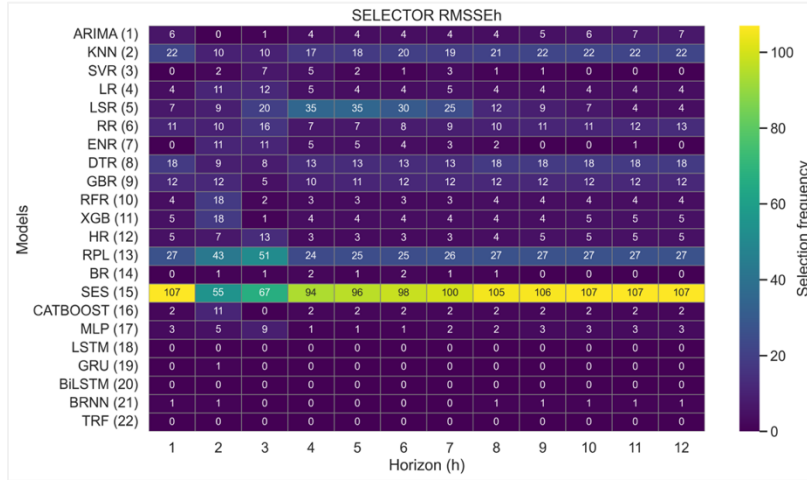


Figure D8. Model Selection Frequency by Forecast Horizon ($RMSSE_h$, M4 91:9).

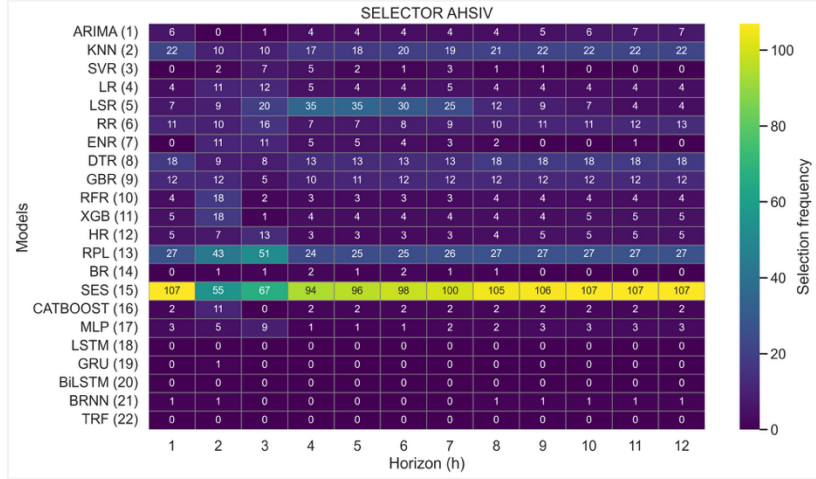


Figure D9. Model Selection Frequency by Forecast Horizon (AHSIV, M4 91:9).

Table D11. Normality (Shapiro–Wilk) – M4 - Training 91% and Testing 9%

Horizon	ERA (result)	ERA (W, p)	RMSSEh (result)	RMSSEh (W, p)	AHSIV (result)	AHSIV (W, p)
h = 1	Not normal	0.9230, 1.13e-09	Not normal	0.5641, 7.63e-24	Not normal	0.5786, 1.68e-23
h = 2	Not normal	0.9100, 1.14e-10	Not normal	0.7450, 1.01e-18	Not normal	0.7644, 5.04e-18
h = 3	Not normal	0.9001, 2.31e-11	Not normal	0.7371, 5.36e-19	Not normal	0.7478, 1.27e-18
h = 4	Not normal	0.8918, 6.56e-12	Not normal	0.7262, 2.31e-19	Not normal	0.7445, 9.68e-19
h = 5	Not normal	0.8836, 2.00e-12	Not normal	0.7453, 1.03e-18	Not normal	0.7538, 2.06e-18
h = 6	Not normal	0.8827, 1.76e-12	Not normal	0.7611, 3.82e-18	Not normal	0.7688, 7.34e-18
h = 7	Not normal	0.8815, 1.49e-12	Not normal	0.7761, 1.39e-17	Not normal	0.7763, 1.42e-17
h = 8	Not normal	0.8811, 1.41e-12	Not normal	0.7705, 8.56e-18	Not normal	0.7748, 1.25e-17
h = 9	Not normal	0.8814, 1.45e-12	Not normal	0.7683, 7.06e-18	Not normal	0.7815, 2.26e-17
h = 10	Not normal	0.8812, 1.42e-12	Not normal	0.7645, 5.10e-18	Not normal	0.7838, 2.79e-17
h = 11	Not normal	0.8813, 1.45e-12	Not normal	0.7559, 2.46e-18	Not normal	0.7815, 2.26e-17
h = 12	Not normal	0.8820, 1.59e-12	Not normal	0.7542, 2.14e-18	Not normal	0.7801, 2.01e-17

Table D12. Kruskal–Wallis, Dunn – M4 - Training 91% and Testing 9%

Horizon	Kruskal–Wallis			Test post-hoc de Dunn		
	Result	H	p-value	ERA vs RMSSEh	ERA vs AHSIV	RMSSEh vs AHSIV
h = 1	Significant differences	451.6491	8.4265e-99	Significant (p = 0.00000)	Significant (p = 0.00000)	Not significant (p = 1.00000)
h = 2	Significant differences	461.9302	4.9333e-101	Significant (p = 0.00000)	Significant (p = 0.00000)	Not significant (p = 1.00000)
h = 3	Significant differences	452.7383	4.8879e-99	Significant (p = 0.00000)	Significant (p = 0.00000)	Not significant (p = 1.00000)
h = 4	Significant differences	461.3888	6.4669e-101	Significant (p = 0.00000)	Significant (p = 0.00000)	Not significant (p = 1.00000)
h = 5	Significant differences	460.0752	1.2472e-100	Significant (p = 0.00000)	Significant (p = 0.00000)	Not significant (p = 1.00000)
h = 6	Significant differences	463.5475	2.1976e-101	Significant (p = 0.00000)	Significant (p = 0.00000)	Not significant (p = 1.00000)
h = 7	Significant differences	462.9811	2.9169e-101	Significant (p = 0.00000)	Significant (p = 0.00000)	Not significant (p = 1.00000)
h = 8	Significant differences	464.5837	1.3090e-101	Significant (p = 0.00000)	Significant (p = 0.00000)	Not significant (p = 1.00000)
h = 9	Significant differences	464.5116	1.3570e-101	Significant (p = 0.00000)	Significant (p = 0.00000)	Not significant (p = 1.00000)
h = 10	Significant differences	465.4128	8.6474e-102	Significant (p = 0.00000)	Significant (p = 0.00000)	Not significant (p = 1.00000)
h = 11	Significant differences	465.7851	7.1789e-102	Significant (p = 0.00000)	Significant (p = 0.00000)	Not significant (p = 1.00000)
h = 12	Significant differences	464.7724	1.1911e-101	Significant (p = 0.00000)	Significant (p = 0.00000)	Not significant (p = 1.00000)

Table D13. Global Synthesis of Descriptive Statistics by Forecast Horizon and Selector – M4 - Training 91% and Testing 9%

Horizon	Selector	count	mean	median	std	min	max	IQR	MAD	Robust CV	GRA global	Final ranking
1	ERA	234	0.67459	0.67925	0.09105	0.50097	0.99906	0.06399	0.03168	0.09420	157.85378	3
1	RMSSEh	234	0.97392	0.98788	0.04324	0.54348	1.00000	0.02901	0.01202	0.02936	227.89824	1

1	AHSIV	234	0.97284	0.98795	0.04493	0.54348	1.00000	0.02985	0.01190	0.03022	227.64395	2
2	ERA	234	0.67293	0.68046	0.09155	0.50049	0.94973	0.05529	0.02783	0.08125	157.46481	3
2	RMSSEh	234	0.96867	0.98507	0.04174	0.74668	1.00000	0.04172	0.01493	0.04235	226.66850	2
2	AHSIV	234	0.96869	0.98417	0.04050	0.74668	1.00000	0.04403	0.01583	0.04474	226.67250	1
3	ERA	234	0.67313	0.68054	0.09565	0.50039	0.99785	0.05366	0.02713	0.07886	157.51275	3
3	RMSSEh	234	0.97204	0.98700	0.03763	0.79967	1.00000	0.03268	0.01299	0.03311	227.45794	2
3	AHSIV	234	0.97354	0.98721	0.03458	0.79967	1.00000	0.03065	0.01279	0.03105	227.80908	1
4	ERA	234	0.66861	0.67954	0.09127	0.50033	0.99098	0.05316	0.02703	0.07823	156.45361	3
4	RMSSEh	234	0.97644	0.98628	0.03095	0.78755	1.00000	0.02899	0.01270	0.02939	228.48701	1
4	AHSIV	234	0.97579	0.98709	0.03131	0.81695	1.00000	0.02954	0.01259	0.02992	228.33594	2
5	ERA	234	0.66774	0.67902	0.09145	0.50030	0.99866	0.05763	0.02887	0.08488	156.24999	3
5	RMSSEh	234	0.97650	0.98659	0.02982	0.79646	1.00000	0.03139	0.01315	0.03181	228.50180	1
5	AHSIV	234	0.97571	0.98651	0.03047	0.82458	1.00000	0.03038	0.01332	0.03079	228.31525	2
6	ERA	234	0.66721	0.67865	0.09103	0.50025	0.97859	0.05732	0.02889	0.08446	156.12773	3
6	RMSSEh	234	0.97575	0.98590	0.03034	0.80676	1.00000	0.03224	0.01386	0.03270	228.32519	1
6	AHSIV	234	0.97511	0.98643	0.03089	0.83432	1.00000	0.03073	0.01352	0.03115	228.17593	2
7	ERA	234	0.66704	0.67832	0.09121	0.50020	0.98509	0.05453	0.02744	0.08040	156.08638	3
7	RMSSEh	234	0.97615	0.98619	0.02899	0.81670	1.00000	0.03071	0.01347	0.03114	228.42003	1
7	AHSIV	234	0.97505	0.98626	0.03040	0.84400	1.00000	0.03232	0.01356	0.03277	228.16246	2
8	ERA	234	0.66674	0.67830	0.09075	0.50018	0.96870	0.05444	0.02839	0.08026	156.01760	3
8	RMSSEh	234	0.97574	0.98634	0.02996	0.84041	1.00000	0.03348	0.01366	0.03394	228.32377	1
8	AHSIV	234	0.97469	0.98643	0.03118	0.84041	1.00000	0.03301	0.01357	0.03347	228.07858	2
9	ERA	234	0.66666	0.67810	0.09084	0.50015	0.96607	0.05909	0.02996	0.08713	155.99846	3
9	RMSSEh	234	0.97453	0.98605	0.03176	0.80807	1.00000	0.03460	0.01395	0.03509	228.04049	1
9	AHSIV	234	0.97346	0.98619	0.03283	0.80807	1.00000	0.03714	0.01381	0.03766	227.78975	2
10	ERA	234	0.66606	0.67758	0.09039	0.50014	0.94133	0.05968	0.03013	0.08808	155.85757	3
10	RMSSEh	234	0.97439	0.98578	0.03206	0.78891	1.00000	0.03498	0.01422	0.03548	228.00683	1
10	AHSIV	234	0.97301	0.98589	0.03304	0.78891	1.00000	0.03632	0.01411	0.03684	227.68447	2
11	ERA	234	0.67128	0.68387	0.09248	0.50013	0.92188	0.05994	0.02918	0.08765	157.07899	3
11	RMSSEh	234	0.97383	0.98538	0.03325	0.77485	1.00000	0.03545	0.01462	0.03598	227.87664	1
11	AHSIV	234	0.97249	0.98583	0.03388	0.77485	1.00000	0.03813	0.01417	0.03868	227.56243	2
12	ERA	234	0.67607	0.68992	0.09493	0.50012	0.94266	0.06697	0.03267	0.09707	158.20074	3
12	RMSSEh	234	0.97336	0.98539	0.03382	0.76578	1.00000	0.03462	0.01461	0.03514	227.76659	1
12	AHSIV	234	0.97187	0.98545	0.03457	0.76578	1.00000	0.03801	0.01455	0.03857	227.41775	2

M3

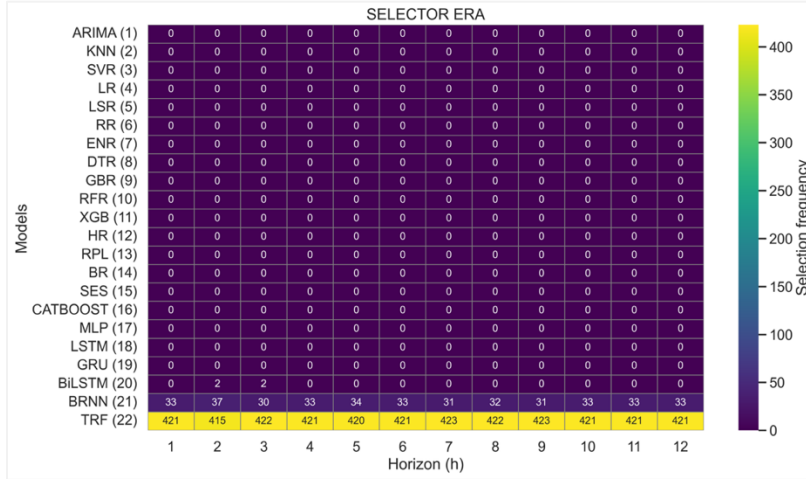


Figure D10. Model Selection Frequency by Forecast Horizon (ERA, M3, 91:9).

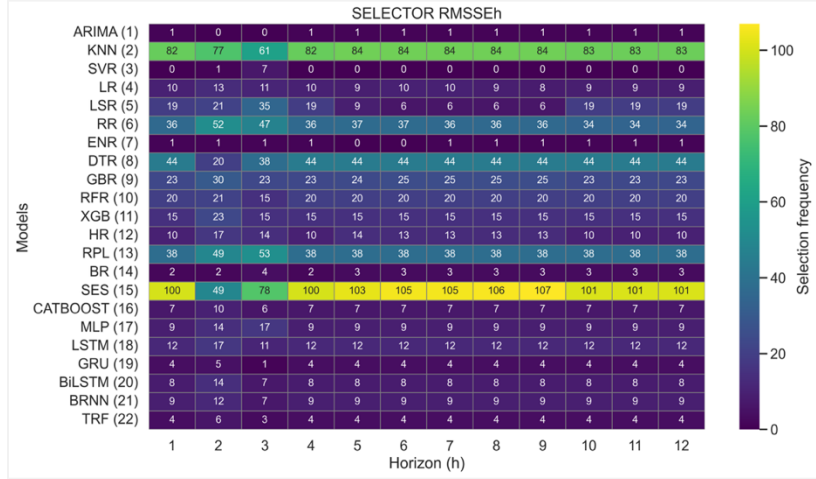


Figure D11. Model Selection Frequency by Forecast Horizon (RMSSE_h, M3, 91:9).

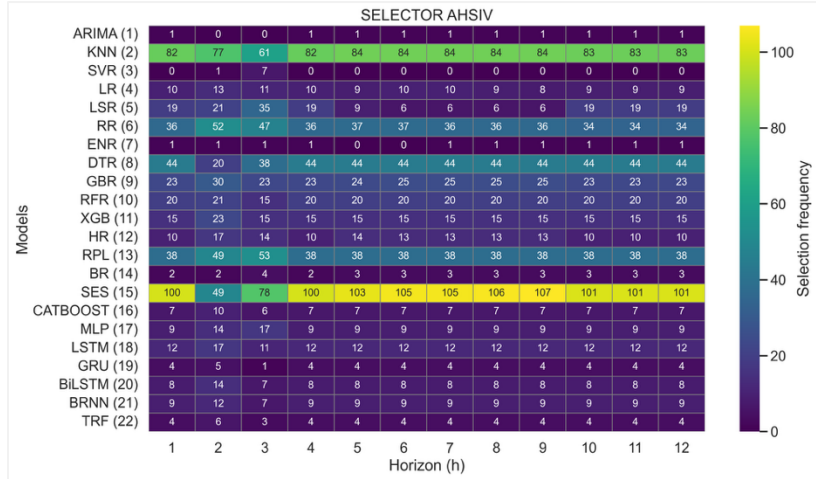


Figure D12. Model Selection Frequency by Forecast Horizon (AHSIV, M3, 91:9).

Table D16. Normality (Shapiro–Wilk) – M3 - Training 91% and Testing 9%

Horizon	ERA (result)	ERA (W, p)	RMSSEh (result)	RMSSEh (W, p)	AHSIV (result)	AHSIV (W, p)
h = 1	Not normal	0.8541, 4.08e-20	Not normal	0.7308, 1.92e-26	Not normal	0.7330, 2.36e-26
h = 2	Not normal	0.8604, 1.07e-19	Not normal	0.7672, 7.33e-25	Not normal	0.7579, 2.78e-25
h = 3	Not normal	0.8666, 2.88e-19	Not normal	0.7538, 1.83e-25	Not normal	0.7425, 5.89e-26
h = 4	Not normal	0.8825, 4.26e-18	Not normal	0.7528, 1.66e-25	Not normal	0.7373, 3.57e-26
h = 5	Not normal	0.8871, 9.83e-18	Not normal	0.7559, 2.27e-25	Not normal	0.7451, 7.66e-26
h = 6	Not normal	0.8773, 1.72e-18	Not normal	0.7610, 3.82e-25	Not normal	0.7514, 1.44e-25
h = 7	Not normal	0.8901, 1.71e-17	Not normal	0.7717, 1.19e-24	Not normal	0.7609, 3.81e-25
h = 8	Not normal	0.8982, 7.96e-17	Not normal	0.7524, 1.58e-25	Not normal	0.7425, 5.91e-26
h = 9	Not normal	0.8980, 7.70e-17	Not normal	0.7577, 2.74e-25	Not normal	0.7429, 6.17e-26
h = 10	Not normal	0.8974, 6.87e-17	Not normal	0.7583, 2.91e-25	Not normal	0.7505, 1.31e-25
h = 11	Not normal	0.9020, 1.70e-16	Not normal	0.7634, 4.92e-25	Not normal	0.7507, 1.34e-25
h = 12	Not normal	0.8977, 7.21e-17	Not normal	0.7662, 6.63e-25	Not normal	0.7553, 2.14e-25

Table D17. Kruskal–Wallis, Dunn – M3 - Training 91% and Testing 9%

Horizon	Kruskal–Wallis			Test post-hoc de Dunn		
	Result	H	p-value	ERA vs RMSSEh	ERA vs AHSIV	RMSSEh vs AHSIV
h = 1	Significant differences	91.6994	1.2238e-20	Significant (p = 0.00000)	Significant (p = 0.00000)	Not significant (p = 1.00000)
h = 2	Significant differences	80.7135	2.9737e-18	Significant (p = 0.00000)	Significant (p = 0.00000)	Not significant (p = 1.00000)
h = 3	Significant differences	110.2212	1.1635e-24	Significant (p = 0.00000)	Significant (p = 0.00000)	Not significant (p = 1.00000)
h = 4	Significant differences	124.2661	1.0374e-27	Significant (p = 0.00000)	Significant (p = 0.00000)	Not significant (p = 1.00000)

h = 5	Significant differences	139.0597	6.3617e-31	Significant (p = 0.00000)	Significant (p = 0.00000)	Significant (p = 0.00000)	Not significant (p = 1.00000)
h = 6	Significant differences	130.8492	3.8589e-29	Significant (p = 0.00000)	Significant (p = 0.00000)	Significant (p = 0.00000)	Not significant (p = 1.00000)
h = 7	Significant differences	130.4558	4.6976e-29	Significant (p = 0.00000)	Significant (p = 0.00000)	Significant (p = 0.00000)	Not significant (p = 1.00000)
h = 8	Significant differences	160.7607	1.2339e-35	Significant (p = 0.00000)	Significant (p = 0.00000)	Significant (p = 0.00000)	Not significant (p = 1.00000)
h = 9	Significant differences	154.8608	2.3573e-34	Significant (p = 0.00000)	Significant (p = 0.00000)	Significant (p = 0.00000)	Not significant (p = 1.00000)
h = 10	Significant differences	158.4025	4.0117e-35	Significant (p = 0.00000)	Significant (p = 0.00000)	Significant (p = 0.00000)	Not significant (p = 1.00000)
h = 11	Significant differences	158.5712	3.6872e-35	Significant (p = 0.00000)	Significant (p = 0.00000)	Significant (p = 0.00000)	Not significant (p = 1.00000)
h = 12	Significant differences	158.4432	3.9310e-35	Significant (p = 0.00000)	Significant (p = 0.00000)	Significant (p = 0.00000)	Not significant (p = 1.00000)

Table D18. Global Synthesis of Descriptive Statistics by Forecast Horizon and Selector – M3 - Training 91% and Testing 9%

Horizon	Selector	count	mean	median	std	min	max	IQR	MAD	Robust CV	GRA global	Final ranking
1	ERA	454	0.91164	0.93926	0.08374	0.53612	0.99996	0.10271	0.04283	0.10935	413.88513	3
1	RMSSEh	454	0.94348	0.97417	0.07447	0.55908	0.99999	0.06277	0.02124	0.06443	428.33787	1
1	AHSIV	454	0.94274	0.97474	0.07565	0.55908	0.99999	0.06616	0.02117	0.06787	428.00329	2
2	ERA	454	0.91320	0.94268	0.08078	0.55512	0.99982	0.09942	0.04132	0.10546	414.59134	3
2	RMSSEh	454	0.94116	0.97361	0.07273	0.65220	0.99996	0.07529	0.02265	0.07733	427.28854	2
2	AHSIV	454	0.94201	0.97588	0.07365	0.65220	0.99996	0.07011	0.02076	0.07184	427.67290	1
3	ERA	454	0.91980	0.94345	0.07284	0.55264	0.99994	0.09064	0.03984	0.09608	417.59012	3
3	RMSSEh	454	0.95281	0.97753	0.05843	0.67514	0.99990	0.05467	0.01873	0.05593	432.57758	1
3	AHSIV	454	0.95235	0.97881	0.06058	0.66627	0.99988	0.05438	0.01741	0.05556	432.36586	2
4	ERA	454	0.92106	0.94183	0.06922	0.56616	0.99994	0.08995	0.03998	0.09551	418.15951	3
4	RMSSEh	454	0.95531	0.97694	0.05497	0.68663	0.99992	0.05090	0.01885	0.05210	433.71216	1
4	AHSIV	454	0.95516	0.97910	0.05671	0.69138	0.99981	0.05140	0.01689	0.05250	433.64474	2
5	ERA	454	0.91830	0.94215	0.06931	0.58512	0.99982	0.09582	0.03704	0.10170	416.90927	3
5	RMSSEh	454	0.95469	0.97536	0.05494	0.67930	0.99992	0.05162	0.01956	0.05293	433.42993	1
5	AHSIV	454	0.95468	0.97805	0.05605	0.68554	0.99992	0.05132	0.01715	0.05247	433.42342	2
6	ERA	454	0.91572	0.93913	0.07288	0.59852	0.99974	0.08755	0.03735	0.09322	415.73824	3
6	RMSSEh	454	0.95243	0.97491	0.05694	0.68696	0.99984	0.05551	0.01992	0.05693	432.40534	1
6	AHSIV	454	0.95243	0.97755	0.05816	0.67633	0.99984	0.05729	0.01811	0.05861	432.40355	2
7	ERA	454	0.91462	0.93527	0.07192	0.61228	0.99965	0.09611	0.04110	0.10276	415.23865	3
7	RMSSEh	454	0.95212	0.97238	0.05555	0.67509	0.99992	0.05402	0.02202	0.05555	432.26462	1
7	AHSIV	454	0.95199	0.97586	0.05766	0.67509	0.99992	0.05400	0.01924	0.05534	432.20432	2
8	ERA	454	0.91357	0.93101	0.06978	0.62246	0.99945	0.08772	0.04101	0.09422	414.76031	3
8	RMSSEh	454	0.95368	0.97475	0.05491	0.66945	1.00000	0.05202	0.01887	0.05337	432.96985	1
8	AHSIV	454	0.95310	0.97567	0.05717	0.66945	1.00000	0.05105	0.01822	0.05232	432.70726	2
9	ERA	454	0.91304	0.93468	0.07071	0.63549	0.99996	0.09502	0.04124	0.10166	414.52126	3
9	RMSSEh	454	0.95246	0.97576	0.05638	0.66477	0.99980	0.05513	0.01872	0.05649	432.41520	1
9	AHSIV	454	0.95231	0.97600	0.05823	0.66477	0.99997	0.05533	0.01784	0.05669	432.34998	2
10	ERA	454	0.91177	0.93304	0.07091	0.64579	0.99947	0.09334	0.04053	0.10003	413.94264	3
10	RMSSEh	454	0.95195	0.97535	0.05605	0.66931	0.99991	0.05455	0.01825	0.05593	432.18574	1
10	AHSIV	454	0.95147	0.97504	0.05797	0.66931	0.99991	0.05506	0.01881	0.05647	431.96917	2
11	ERA	454	0.91186	0.93193	0.07001	0.64669	0.99974	0.09679	0.04033	0.10386	413.98528	3
11	RMSSEh	454	0.95162	0.97347	0.05588	0.67095	0.99950	0.05465	0.01862	0.05614	432.03703	1
11	AHSIV	454	0.95159	0.97597	0.05764	0.67095	0.99950	0.05572	0.01794	0.05709	432.02054	2
12	ERA	454	0.91142	0.93309	0.06975	0.64421	0.99859	0.09303	0.03850	0.09970	413.78516	3
12	RMSSEh	454	0.95046	0.97359	0.05676	0.67174	0.99991	0.05369	0.01909	0.05515	431.50799	1
12	AHSIV	454	0.95034	0.97533	0.05850	0.67174	0.99988	0.05379	0.01860	0.05515	431.45423	2

Appendix E

Walmart

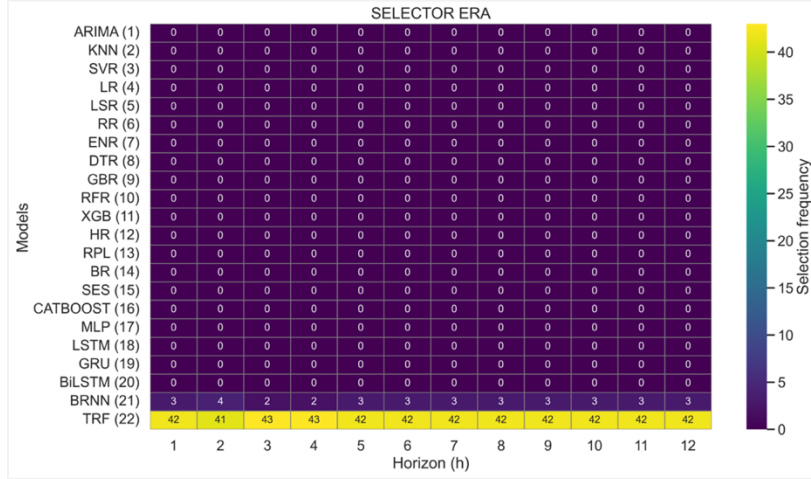


Figure E1. Model Selection Frequency by Forecast Horizon (ERA, Walmart 80:20).

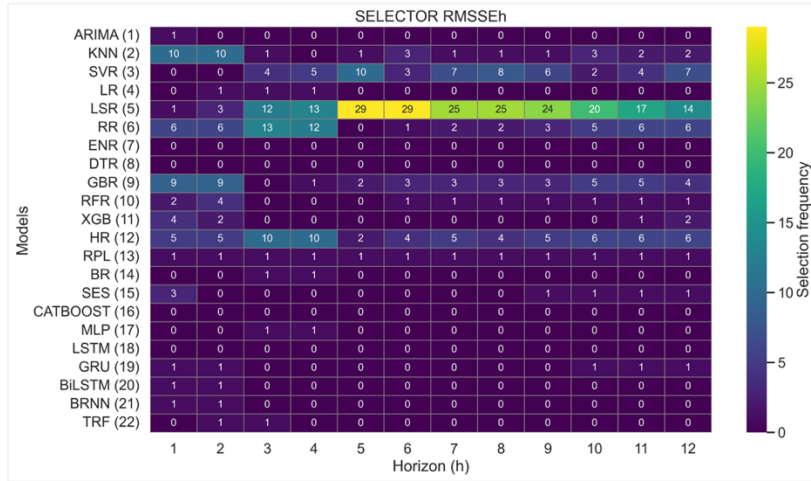


Figure E2. Model Selection Frequency by Forecast Horizon (RMSSE_h, Walmart 80:20).

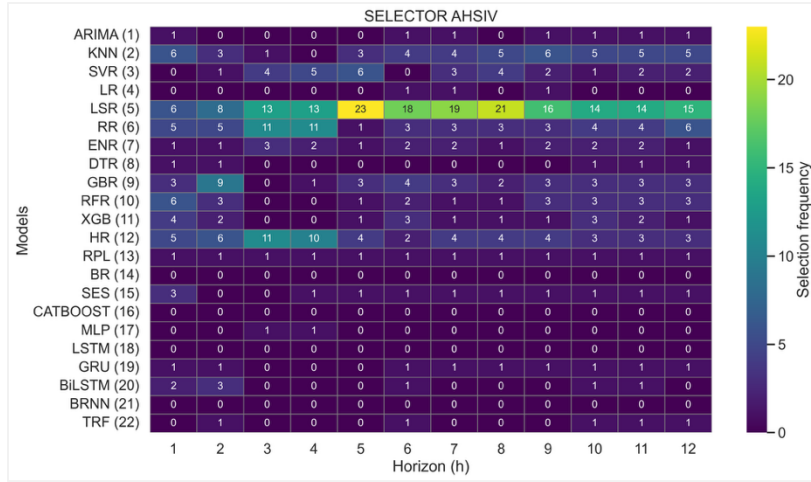


Figure E3. Model Selection Frequency by Forecast Horizon (AHSIV, Walmart 80:20).

Table E1. Normality (Shapiro–Wilk) - Walmart - Training 80% and Testing 20%

Horizon	ERA (result)	ERA (W, p)	RMSSEh (result)	RMSSEh (W, p)	AHSIV (result)	AHSIV (W, p)
h = 1	Not normal	0.8554, 5.07e-05	Not normal	0.8928, 5.70e-04	Not normal	0.9074, 1.62e-03

h = 2	Not normal	0.8934, 5.94e-04	Not normal	0.9159, 3.07e-03	Not normal	0.9077, 1.66e-03
h = 3	Not normal	0.8386, 1.89e-05	Not normal	0.8875, 3.96e-04	Not normal	0.8892, 4.45e-04
h = 4	Not normal	0.8247, 8.68e-06	Not normal	0.9045, 1.32e-03	Not normal	0.8931, 5.82e-04
h = 5	Not normal	0.8502, 3.71e-05	Not normal	0.8144, 5.00e-06	Not normal	0.8162, 5.51e-06
h = 6	Not normal	0.8184, 6.18e-06	Not normal	0.7958, 1.93e-06	Not normal	0.9156, 3.01e-03
h = 7	Not normal	0.8118, 4.37e-06	Not normal	0.8800, 2.40e-04	Not normal	0.8872, 3.88e-04
h = 8	Not normal	0.7941, 1.77e-06	Not normal	0.8940, 6.20e-04	Not normal	0.7771, 7.73e-07
h = 9	Not normal	0.7898, 1.43e-06	Not normal	0.8227, 7.78e-06	Not normal	0.8374, 1.76e-05
h = 10	Not normal	0.7797, 8.74e-07	Not normal	0.8333, 1.40e-05	Not normal	0.8425, 2.36e-05
h = 11	Not normal	0.7785, 8.25e-07	Not normal	0.8466, 3.00e-05	Not normal	0.8344, 1.49e-05
h = 12	Not normal	0.7660, 4.59e-07	Not normal	0.8658, 9.58e-05	Not normal	0.8185, 6.23e-06

Table E2. Kruskal–Wallis, Dunn - Training 80% and Testing 20%

Horizon	Kruskal–Wallis			Test post-hoc de Dunn		
	Result	H	p-value	ERA vs RMSSEh	ERA vs AHSIV	RMSSEh vs AHSIV
h = 1	No significant differences were detected.	3.1293	2.0916e-01	Not significant (p = 0.27871)	Not significant (p = 0.56135)	Not significant (p = 1.00000)
h = 2	No significant differences were detected.	3.2820	1.9379e-01	Not significant (p = 0.45728)	Not significant (p = 0.28027)	Not significant (p = 1.00000)
h = 3	No significant differences were detected.	0.8820	6.4338e-01	Not significant (p = 1.00000)	Not significant (p = 1.00000)	Not significant (p = 1.00000)
h = 4	No significant differences were detected.	0.8577	6.5127e-01	Not significant (p = 1.00000)	Not significant (p = 1.00000)	Not significant (p = 1.00000)
h = 5	No significant differences were detected.	5.2950	7.0826e-02	Not significant (p = 0.09810)	Not significant (p = 0.21105)	Not significant (p = 1.00000)
h = 6	No significant differences were detected.	2.4909	2.8781e-01	Not significant (p = 0.41809)	Not significant (p = 0.66956)	Not significant (p = 1.00000)
h = 7	No significant differences were detected.	0.5144	7.7320e-01	Not significant (p = 1.00000)	Not significant (p = 1.00000)	Not significant (p = 1.00000)
h = 8	No significant differences were detected.	0.2136	8.9873e-01	Not significant (p = 1.00000)	Not significant (p = 1.00000)	Not significant (p = 1.00000)
h = 9	No significant differences were detected.	0.0422	9.7912e-01	Not significant (p = 1.00000)	Not significant (p = 1.00000)	Not significant (p = 1.00000)
h = 10	No significant differences were detected.	0.1489	9.2827e-01	Not significant (p = 1.00000)	Not significant (p = 1.00000)	Not significant (p = 1.00000)
h = 11	No significant differences were detected.	0.2211	8.9535e-01	Not significant (p = 1.00000)	Not significant (p = 1.00000)	Not significant (p = 1.00000)
h = 12	No significant differences were detected.	0.7908	6.7340e-01	Not significant (p = 1.00000)	Not significant (p = 1.00000)	Not significant (p = 1.00000)

Table E3. Global Synthesis of Descriptive Statistics by Forecast Horizon and Selector - Walmart - Training 80% and Testing 20%

Horizon	Selector	count	mean	median	std	min	max	IQR	MAD	Robust CV	GRA global	Final ranking
1	ERA	45	0.96787	0.98060	0.02901	0.88166	0.99944	0.03404	0.01252	0.03471	43.55411	3
1	RMSSEh	45	0.97960	0.98315	0.01577	0.92885	0.99897	0.01627	0.00885	0.01654	44.08180	1
1	AHSIV	45	0.97843	0.98191	0.01681	0.92885	0.99990	0.01745	0.00903	0.01777	44.02937	2
2	ERA	45	0.96789	0.97513	0.02660	0.89494	0.99982	0.03236	0.01442	0.03319	43.55505	3
2	RMSSEh	45	0.97750	0.98093	0.01561	0.92995	0.99797	0.02051	0.01043	0.02091	43.98746	2
2	AHSIV	45	0.97828	0.98093	0.01622	0.92995	0.99866	0.01997	0.01053	0.02035	44.02256	1
3	ERA	45	0.97211	0.97775	0.02753	0.88580	0.99917	0.02897	0.01477	0.02963	43.74474	3
3	RMSSEh	45	0.97797	0.98203	0.01943	0.92005	0.99962	0.02690	0.01324	0.02739	44.00860	2
3	AHSIV	45	0.97995	0.98234	0.01697	0.92005	0.99962	0.02315	0.01164	0.02357	44.09772	1
4	ERA	45	0.97252	0.98037	0.02759	0.88067	0.99975	0.02507	0.01266	0.02558	43.76361	3
4	RMSSEh	45	0.97912	0.98152	0.01729	0.91824	0.99984	0.02284	0.01155	0.02327	44.06027	2
4	AHSIV	45	0.98004	0.98250	0.01644	0.91824	0.99984	0.01903	0.00914	0.01937	44.10200	1
5	ERA	45	0.97251	0.97994	0.02550	0.88181	0.99960	0.02914	0.01251	0.02974	43.76283	3
5	RMSSEh	45	0.98319	0.98589	0.01572	0.91618	0.99999	0.01471	0.00776	0.01492	44.24356	1
5	AHSIV	45	0.98267	0.98569	0.01568	0.91618	0.99923	0.01560	0.00863	0.01583	44.22035	2
6	ERA	45	0.97482	0.98476	0.02503	0.88515	0.99896	0.02713	0.01114	0.02755	43.86686	3
6	RMSSEh	45	0.98280	0.98803	0.01682	0.90967	0.99964	0.01813	0.00732	0.01835	44.22597	2
6	AHSIV	45	0.98364	0.98496	0.01231	0.94811	0.99899	0.01678	0.00859	0.01703	44.26401	1
7	ERA	45	0.97668	0.98542	0.02426	0.88593	0.99987	0.02461	0.01109	0.02497	43.95049	3
7	RMSSEh	45	0.98259	0.98852	0.01435	0.94431	0.99961	0.02083	0.00681	0.02107	44.21653	2
7	AHSIV	45	0.98349	0.98637	0.01271	0.94431	0.99920	0.01580	0.00771	0.01601	44.25687	1
8	ERA	45	0.97712	0.98498	0.02512	0.88258	0.99983	0.02741	0.01202	0.02782	43.97034	3
8	RMSSEh	45	0.98071	0.98607	0.01454	0.94104	0.99891	0.01913	0.00743	0.01940	44.13205	2
8	AHSIV	45	0.98077	0.98607	0.01826	0.90018	0.99980	0.01813	0.00780	0.01838	44.13465	1
9	ERA	45	0.97721	0.98595	0.02479	0.88104	0.99959	0.02555	0.00975	0.02591	43.97456	3
9	RMSSEh	45	0.98135	0.98657	0.01476	0.93746	0.99970	0.02025	0.00499	0.02053	44.16081	2
9	AHSIV	45	0.98235	0.98617	0.01358	0.93746	0.99856	0.01308	0.00580	0.01326	44.20584	1
10	ERA	45	0.97728	0.98673	0.02424	0.88341	0.99874	0.02637	0.00936	0.02673	43.97769	3
10	RMSSEh	45	0.98125	0.98699	0.01649	0.93447	0.99963	0.01985	0.00587	0.02012	44.15641	2
10	AHSIV	45	0.98246	0.98580	0.01482	0.93447	0.99906	0.01145	0.00578	0.01162	44.21081	1

11	ERA	45	0.97739	0.98786	0.02452	0.88394	0.99933	0.02806	0.00926	0.02840	43.98265	3
11	RMSSEh	45	0.97979	0.98226	0.01658	0.93140	0.99927	0.01929	0.00923	0.01964	44.09059	2
11	AHSIV	45	0.98146	0.98246	0.01493	0.93140	0.99839	0.01464	0.00903	0.01490	44.16582	1
12	ERA	45	0.97780	0.98504	0.02461	0.88292	0.99959	0.02787	0.01085	0.02829	44.00089	3
12	RMSSEh	45	0.97982	0.98337	0.01570	0.92751	0.99997	0.01706	0.00889	0.01735	44.09193	1
12	AHSIV	45	0.97954	0.98235	0.01678	0.92751	0.99997	0.01552	0.00879	0.01580	44.07921	2

MS

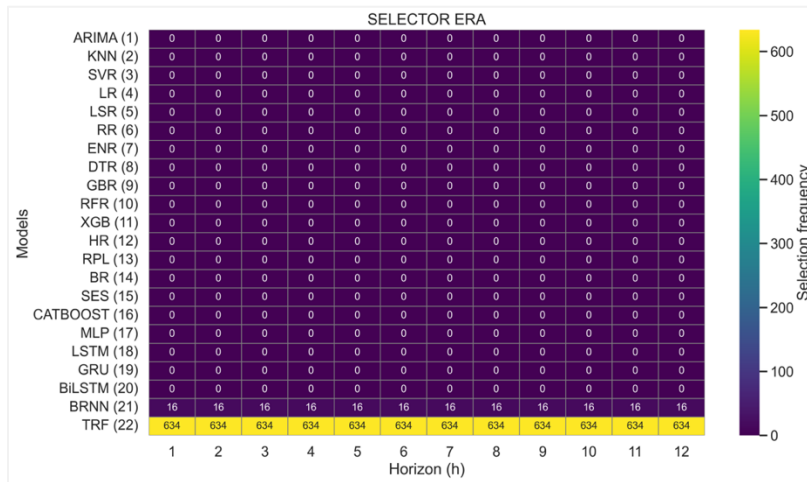


Figure E4. Model Selection Frequency by Forecast Horizon (ERA, M5, 80:20).

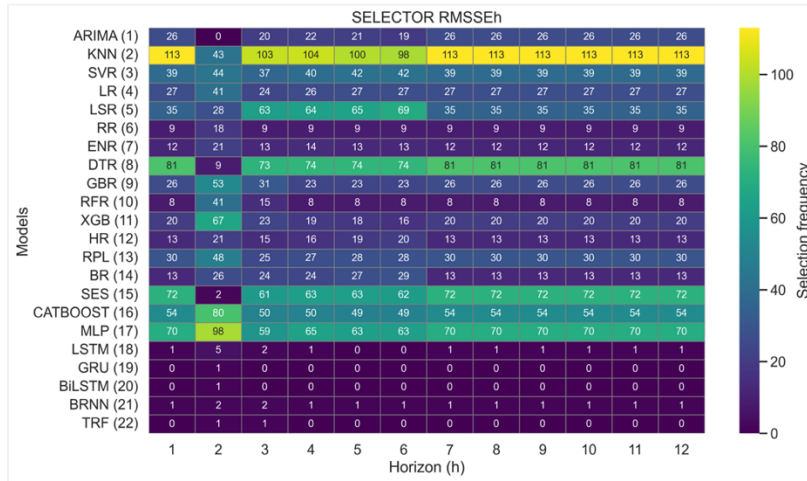


Figure E5. Model Selection Frequency by Forecast Horizon (RMSSEh, M5, 80:20).

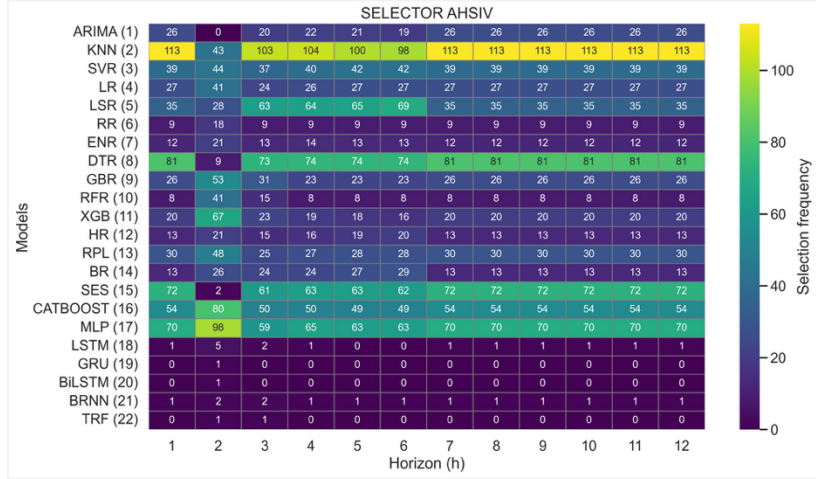


Figure E6. Model Selection Frequency by Forecast Horizon (AHSIV, M5, 80:20).

Table E6. Normality (Shapiro–Wilk) – M5 - Training 80% and Testing 20%

Horizon	ERA (result)	ERA (W, p)	RMSSEh (result)	RMSSEh (W, p)	AHSIV (result)	AHSIV (W, p)
h = 1	Not normal	0.6644, 7.55e-34	Not normal	0.9592, 1.84e-12	Not normal	0.9584, 1.36e-12
h = 2	Not normal	0.5872, 1.47e-36	Not normal	0.9601, 2.70e-12	Not normal	0.9595, 2.09e-12
h = 3	Not normal	0.4976, 3.10e-39	Not normal	0.9657, 3.39e-11	Not normal	0.9655, 3.06e-11
h = 4	Not normal	0.4697, 5.47e-40	Not normal	0.9629, 9.41e-12	Not normal	0.9629, 9.32e-12
h = 5	Not normal	0.4540, 2.12e-40	Not normal	0.9663, 4.65e-11	Not normal	0.9664, 4.89e-11
h = 6	Not normal	0.4518, 1.86e-40	Not normal	0.9589, 1.66e-12	Not normal	0.9590, 1.72e-12
h = 7	Not normal	0.4651, 4.14e-40	Not normal	0.9535, 1.89e-13	Not normal	0.9543, 2.53e-13
h = 8	Not normal	0.5000, 3.62e-39	Not normal	0.9457, 1.09e-14	Not normal	0.9465, 1.42e-14
h = 9	Not normal	0.5051, 5.00e-39	Not normal	0.9454, 9.70e-15	Not normal	0.9461, 1.23e-14
h = 10	Not normal	0.4965, 2.89e-39	Not normal	0.9421, 3.19e-15	Not normal	0.9425, 3.64e-15
h = 11	Not normal	0.4921, 2.19e-39	Not normal	0.9431, 4.40e-15	Not normal	0.9437, 5.33e-15
h = 12	Not normal	0.4755, 7.79e-40	Not normal	0.9436, 5.24e-15	Not normal	0.9440, 5.97e-15

Table E7. Kruskal–Wallis, Dunn – M5 - Training 80% and Testing 20%

Horizon	Kruskal–Wallis			Test post-hoc de Dunn		
	Result	H	p-value	ERA vs RMSSEh	ERA vs AHSIV	RMSSEh vs AHSIV
h = 1	Significant differences	1015.1245	3.7026e-221	Significant (p = 0.00000)	Significant (p = 0.00000)	Not significant (p = 1.00000)
h = 2	Significant differences	1054.7836	9.0499e-230	Significant (p = 0.00000)	Significant (p = 0.00000)	Not significant (p = 1.00000)
h = 3	Significant differences	1099.2184	2.0312e-239	Significant (p = 0.00000)	Significant (p = 0.00000)	Not significant (p = 1.00000)
h = 4	Significant differences	1110.9379	5.7930e-242	Significant (p = 0.00000)	Significant (p = 0.00000)	Not significant (p = 1.00000)
h = 5	Significant differences	1106.8596	4.4513e-241	Significant (p = 0.00000)	Significant (p = 0.00000)	Not significant (p = 1.00000)
h = 6	Significant differences	1122.3816	1.8964e-244	Significant (p = 0.00000)	Significant (p = 0.00000)	Not significant (p = 1.00000)
h = 7	Significant differences	1143.6752	4.5091e-249	Significant (p = 0.00000)	Significant (p = 0.00000)	Not significant (p = 1.00000)
h = 8	Significant differences	1131.9647	1.5739e-246	Significant (p = 0.00000)	Significant (p = 0.00000)	Not significant (p = 1.00000)
h = 9	Significant differences	1130.8085	2.8058e-246	Significant (p = 0.00000)	Significant (p = 0.00000)	Not significant (p = 1.00000)
h = 10	Significant differences	1128.4847	8.9674e-246	Significant (p = 0.00000)	Significant (p = 0.00000)	Not significant (p = 1.00000)
h = 11	Significant differences	1124.1201	7.9511e-245	Significant (p = 0.00000)	Significant (p = 0.00000)	Not significant (p = 1.00000)
h = 12	Significant differences	1117.0817	2.6840e-243	Significant (p = 0.00000)	Significant (p = 0.00000)	Not significant (p = 1.00000)

Table E8. Global Synthesis of Descriptive Statistics by Forecast Horizon and Selector – M5 - Training 80% and Testing 20%

Horizon	Selector	count	mean	median	std	min	max	IQR	MAD	Robust CV	GRA global	Final ranking
1	ERA	650	0.57342	0.53959	0.09277	0.50196	0.99994	0.06152	0.02380	0.11401	372.72002	3
1	RMSSEh	650	0.81993	0.81923	0.12274	0.52373	1.00000	0.19711	0.09931	0.24060	532.95373	2

1	AHSIV	650	0.82002	0.81858	0.12307	0.52373	1.00000	0.20004	0.10020	0.24438	533.01057	1
2	ERA	650	0.55389	0.52923	0.07601	0.50101	0.99988	0.04282	0.01641	0.08091	360.02900	3
2	RMSSEh	650	0.80278	0.80616	0.13201	0.51059	1.00000	0.21823	0.10930	0.27070	521.80383	2
2	AHSIV	650	0.80331	0.80616	0.13225	0.51059	1.00000	0.21912	0.10967	0.27181	522.15309	1
3	ERA	650	0.54590	0.52511	0.07347	0.50070	0.99985	0.03319	0.01373	0.06320	354.83399	3
3	RMSSEh	650	0.80412	0.81406	0.12849	0.51064	1.00000	0.20400	0.10324	0.25060	522.67805	1
3	AHSIV	650	0.80404	0.81351	0.12862	0.51064	1.00000	0.20461	0.10377	0.25152	522.62748	2
4	ERA	650	0.54262	0.52263	0.07119	0.50053	0.99951	0.02879	0.01250	0.05509	352.70174	3
4	RMSSEh	650	0.80860	0.82061	0.12828	0.51064	1.00000	0.20224	0.09962	0.24645	525.59143	1
4	AHSIV	650	0.80839	0.82023	0.12830	0.51064	1.00000	0.20367	0.10105	0.24831	525.45056	2
5	ERA	650	0.54048	0.52065	0.07075	0.50042	0.99941	0.02359	0.01082	0.04531	351.31439	3
5	RMSSEh	650	0.80417	0.81376	0.12682	0.50943	1.00000	0.19326	0.09724	0.23749	522.71228	1
5	AHSIV	650	0.80399	0.81376	0.12679	0.50943	1.00000	0.19294	0.09710	0.23710	522.59675	2
6	ERA	650	0.53803	0.51972	0.06581	0.50035	0.99805	0.02244	0.01030	0.04319	349.71793	3
6	RMSSEh	650	0.80738	0.82148	0.13095	0.50844	1.00000	0.20962	0.10372	0.25517	524.79671	1
6	AHSIV	650	0.80731	0.82050	0.13104	0.50844	1.00000	0.20962	0.10392	0.25547	524.75197	2
7	ERA	650	0.53696	0.51971	0.06091	0.50030	0.99751	0.02273	0.00969	0.04373	349.02455	3
7	RMSSEh	650	0.81455	0.82866	0.12950	0.50725	1.00000	0.20857	0.10263	0.25169	529.45828	1
7	AHSIV	650	0.81415	0.82808	0.12934	0.50725	1.00000	0.20827	0.10250	0.25151	529.19507	2
8	ERA	650	0.53788	0.52072	0.05893	0.50027	0.99714	0.02316	0.00958	0.04449	349.62119	3
8	RMSSEh	650	0.81533	0.84251	0.13101	0.50601	1.00000	0.20770	0.09676	0.24653	529.96613	1
8	AHSIV	650	0.81477	0.84162	0.13079	0.50601	1.00000	0.20792	0.09758	0.24705	529.59968	2
9	ERA	650	0.53710	0.52120	0.05575	0.50024	0.98226	0.02318	0.00942	0.04448	349.11663	3
9	RMSSEh	650	0.81665	0.84011	0.13038	0.50480	1.00000	0.20022	0.09612	0.23833	530.82099	1
9	AHSIV	650	0.81618	0.83893	0.13032	0.50480	1.00000	0.20154	0.09679	0.24023	530.51520	2
10	ERA	650	0.53628	0.52076	0.05446	0.50021	0.98993	0.02120	0.00903	0.04070	348.58348	3
10	RMSSEh	650	0.81921	0.84404	0.13002	0.50391	1.00000	0.19622	0.08883	0.23247	532.48908	1
10	AHSIV	650	0.81875	0.84346	0.12996	0.50391	1.00000	0.19836	0.08907	0.23517	532.19066	2
11	ERA	650	0.53578	0.52104	0.05393	0.50019	0.98793	0.02037	0.00891	0.03910	348.25849	3
11	RMSSEh	650	0.81959	0.84364	0.13067	0.50329	1.00000	0.19434	0.09360	0.23037	532.73502	1
11	AHSIV	650	0.81922	0.84335	0.13069	0.50329	1.00000	0.19435	0.09366	0.23045	532.49142	2
12	ERA	650	0.53514	0.52095	0.05384	0.50018	0.98602	0.02088	0.00842	0.04007	347.83804	3
12	RMSSEh	650	0.81831	0.84350	0.13062	0.50285	1.00000	0.18090	0.08870	0.21446	531.89988	1
12	AHSIV	650	0.81791	0.84311	0.13062	0.50285	1.00000	0.18276	0.08928	0.21677	531.64405	2

M4

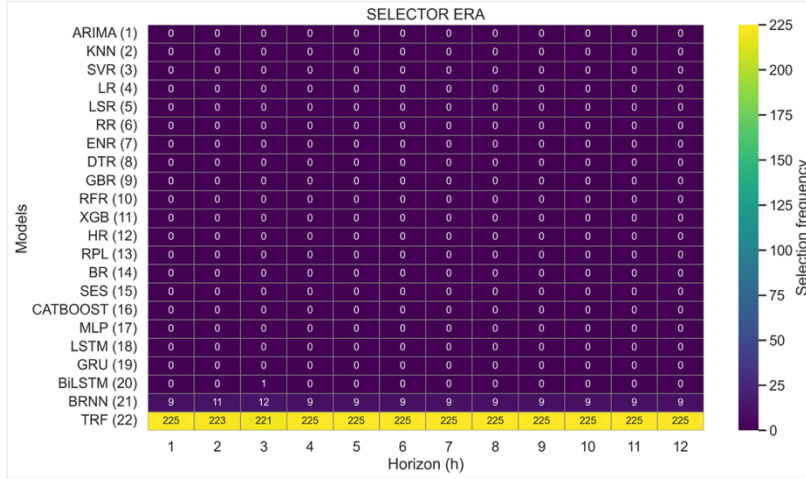


Figure E7. Model Selection Frequency by Forecast Horizon (ERA, M4 80:20).

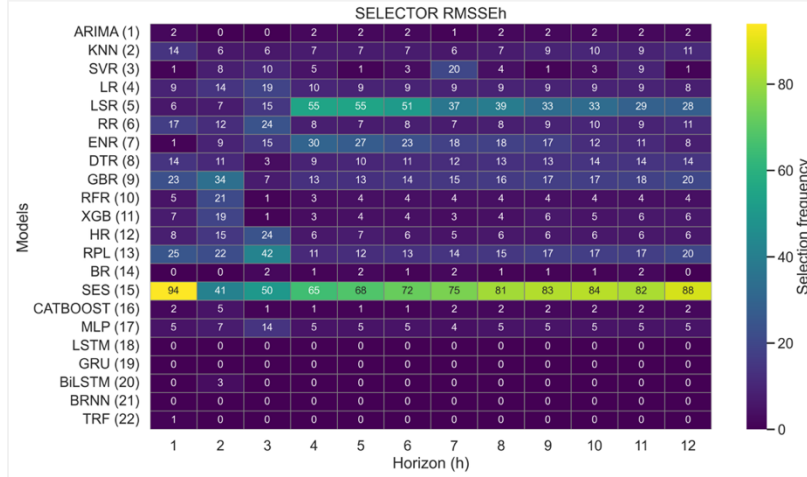


Figure E8. Model Selection Frequency by Forecast Horizon (RMSSE_h, M4 80:20).

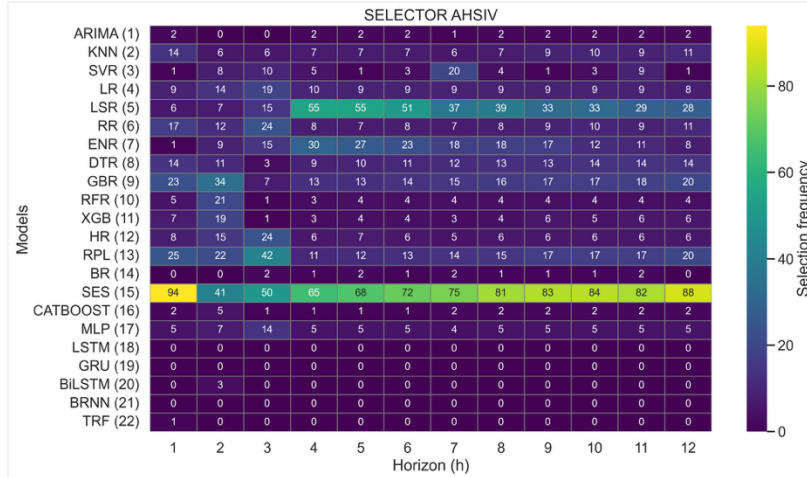


Figure E9. Model Selection Frequency by Forecast Horizon (AHSIV, M4 80:20).

Table E11. Normality (Shapiro–Wilk) - M4- Training 80% and Testing 20%

Horizon	ERA (result)	ERA (W, p)	RMSSEh (result)	RMSSEh (W, p)	AHSIV (result)	AHSIV (W, p)
h = 1	Not normal	0.9404, 3.60e-08	Not normal	0.6508, 1.21e-21	Not normal	0.6565, 1.73e-21
h = 2	Not normal	0.9399, 3.28e-08	Not normal	0.8252, 1.63e-15	Not normal	0.8358, 5.14e-15
h = 3	Not normal	0.9358, 1.37e-08	Not normal	0.7962, 8.85e-17	Not normal	0.7837, 2.77e-17
h = 4	Not normal	0.9350, 1.15e-08	Not normal	0.7671, 6.34e-18	Not normal	0.7222, 1.70e-19
h = 5	Not normal	0.9335, 8.61e-09	Not normal	0.7590, 3.19e-18	Not normal	0.7454, 1.04e-18
h = 6	Not normal	0.9337, 8.93e-09	Not normal	0.7651, 5.36e-18	Not normal	0.7578, 2.89e-18
h = 7	Not normal	0.9325, 7.00e-09	Not normal	0.7654, 5.48e-18	Not normal	0.7629, 4.45e-18
h = 8	Not normal	0.9322, 6.58e-09	Not normal	0.7601, 3.51e-18	Not normal	0.7637, 4.74e-18
h = 9	Not normal	0.9312, 5.38e-09	Not normal	0.7526, 1.87e-18	Not normal	0.7653, 5.43e-18
h = 10	Not normal	0.9335, 8.53e-09	Not normal	0.7565, 2.59e-18	Not normal	0.7672, 6.44e-18
h = 11	Not normal	0.9331, 7.86e-09	Not normal	0.7524, 1.84e-18	Not normal	0.7677, 6.72e-18
h = 12	Not normal	0.9336, 8.78e-09	Not normal	0.7522, 1.82e-18	Not normal	0.7775, 1.59e-17

Table E12. Kruskal–Wallis, Dunn - M4 - Training 80% and Testing 20%

Horizon	Kruskal–Wallis			Test post-hoc de Dunn		
	Result	H	p-value	ERA vs RMSSEh	ERA vs AHSIV	RMSSEh vs AHSIV
h = 1	Significant differences	404.4086	1.5268e-88	Significant (p = 0.00000)	Significant (p = 0.00000)	Not significant (p = 1.00000)
h = 2	Significant differences	351.0797	5.8078e-77	Significant (p = 0.00000)	Significant (p = 0.00000)	Not significant (p = 1.00000)
h = 3	Significant differences	372.9967	1.0111e-81	Significant (p = 0.00000)	Significant (p = 0.00000)	Not significant (p = 1.00000)

h = 4	Significant differences	390.4033	1.6788e-85	Significant (p = 0.00000)	Significant (p = 0.00000)	Not significant (p = 1.00000)
h = 5	Significant differences	386.3333	1.2847e-84	Significant (p = 0.00000)	Significant (p = 0.00000)	Not significant (p = 1.00000)
h = 6	Significant differences	379.5619	3.7946e-83	Significant (p = 0.00000)	Significant (p = 0.00000)	Not significant (p = 1.00000)
h = 7	Significant differences	385.8235	1.6577e-84	Significant (p = 0.00000)	Significant (p = 0.00000)	Not significant (p = 1.00000)
h = 8	Significant differences	386.3520	1.2727e-84	Significant (p = 0.00000)	Significant (p = 0.00000)	Not significant (p = 1.00000)
h = 9	Significant differences	386.5368	1.1604e-84	Significant (p = 0.00000)	Significant (p = 0.00000)	Not significant (p = 1.00000)
h = 10	Significant differences	376.4892	1.7636e-82	Significant (p = 0.00000)	Significant (p = 0.00000)	Not significant (p = 1.00000)
h = 11	Significant differences	377.1455	1.2703e-82	Significant (p = 0.00000)	Significant (p = 0.00000)	Not significant (p = 1.00000)
h = 12	Significant differences	376.3043	1.9345e-82	Significant (p = 0.00000)	Significant (p = 0.00000)	Not significant (p = 1.00000)

Table E13. Global Synthesis of Descriptive Statistics by Forecast Horizon and Selector - M4 - Training 80% and Testing 20%

Horizon	Selector	count	mean	median	std	min	max	IQR	MAD	Robust CV	GRA global	Final ranking
1	ERA	234	0.73442	0.73823	0.13562	0.50154	0.98137	0.16809	0.08787	0.22769	171.85435	3
1	RMSSEh	234	0.96567	0.98525	0.05283	0.54607	1.00000	0.04311	0.01439	0.04375	225.96601	2
1	AHSIV	234	0.96618	0.98482	0.05083	0.54634	1.00000	0.04337	0.01515	0.04404	226.08695	1
2	ERA	234	0.73693	0.73513	0.14055	0.50073	0.99885	0.16352	0.08099	0.22244	172.44058	3
2	RMSSEh	234	0.95382	0.97300	0.05224	0.74678	1.00000	0.06458	0.02613	0.06637	223.19339	2
2	AHSIV	234	0.95478	0.97300	0.05016	0.74678	1.00000	0.06544	0.02681	0.06726	223.41945	1
3	ERA	234	0.73898	0.73748	0.14038	0.50053	0.99990	0.16615	0.07882	0.22530	172.92127	3
3	RMSSEh	234	0.96015	0.97810	0.04757	0.77677	1.00000	0.05179	0.02175	0.05295	224.67584	2
3	AHSIV	234	0.96062	0.97805	0.04795	0.77677	1.00000	0.05129	0.02178	0.05244	224.78572	1
4	ERA	234	0.73825	0.73720	0.14035	0.50040	0.99869	0.16383	0.07596	0.22224	172.75139	3
4	RMSSEh	234	0.96659	0.98182	0.04128	0.78554	1.00000	0.04721	0.01770	0.04809	226.18117	2
4	AHSIV	234	0.96843	0.98487	0.04262	0.75403	1.00000	0.03706	0.01513	0.03763	226.61242	1
5	ERA	234	0.73847	0.73204	0.14165	0.50034	0.99064	0.16608	0.07375	0.22687	172.80279	3
5	RMSSEh	234	0.96763	0.98180	0.04088	0.79433	1.00000	0.04267	0.01806	0.04346	226.42547	2
5	AHSIV	234	0.96911	0.98437	0.04033	0.75787	1.00000	0.04255	0.01563	0.04323	226.77089	1
6	ERA	234	0.73824	0.73035	0.14193	0.50029	0.99864	0.16331	0.07025	0.22360	172.74747	3
6	RMSSEh	234	0.96737	0.98325	0.04136	0.80448	1.00000	0.04099	0.01675	0.04169	226.36419	2
6	AHSIV	234	0.96862	0.98428	0.04021	0.76328	1.00000	0.04065	0.01572	0.04130	226.65709	1
7	ERA	234	0.73767	0.73276	0.14117	0.50023	0.99545	0.15950	0.07219	0.21767	172.61389	3
7	RMSSEh	234	0.96687	0.98252	0.04181	0.81428	1.00000	0.03734	0.01717	0.03800	226.24769	2
7	AHSIV	234	0.96804	0.98444	0.04077	0.76651	1.00000	0.04098	0.01556	0.04163	226.52139	1
8	ERA	234	0.73708	0.73092	0.14055	0.50021	0.99821	0.16645	0.06765	0.22773	172.47681	3
8	RMSSEh	234	0.96656	0.98294	0.04240	0.81535	1.00000	0.03781	0.01663	0.03847	226.17600	2
8	AHSIV	234	0.96759	0.98345	0.04100	0.77300	1.00000	0.03929	0.01655	0.03995	226.41706	1
9	ERA	234	0.73714	0.72876	0.14068	0.50019	0.98796	0.16908	0.06919	0.23201	172.49014	3
9	RMSSEh	234	0.96643	0.98250	0.04316	0.79685	1.00000	0.03828	0.01650	0.03896	226.14437	2
9	AHSIV	234	0.96668	0.98267	0.04212	0.77795	1.00000	0.04411	0.01722	0.04489	226.20257	1
10	ERA	234	0.73705	0.73048	0.14159	0.50017	0.99957	0.16560	0.07207	0.22670	172.46877	3
10	RMSSEh	234	0.96576	0.98208	0.04374	0.77807	1.00000	0.03932	0.01692	0.04004	225.98689	2
10	AHSIV	234	0.96594	0.98133	0.04270	0.77807	1.00000	0.04482	0.01854	0.04567	226.02899	1
11	ERA	234	0.73652	0.73040	0.14129	0.50015	0.99873	0.16738	0.07450	0.22916	172.34562	3
11	RMSSEh	234	0.96546	0.98160	0.04454	0.76423	1.00000	0.03881	0.01766	0.03953	225.91785	1
11	AHSIV	234	0.96513	0.98006	0.04364	0.76423	1.00000	0.04505	0.01990	0.04596	225.84114	2
12	ERA	234	0.73658	0.72793	0.14151	0.50014	0.99884	0.16555	0.07249	0.22743	172.35955	3
12	RMSSEh	234	0.96516	0.98339	0.04502	0.75540	1.00000	0.04020	0.01661	0.04088	225.84746	2
12	AHSIV	234	0.96579	0.98225	0.04228	0.75540	1.00000	0.04414	0.01775	0.04494	225.99452	1

M3

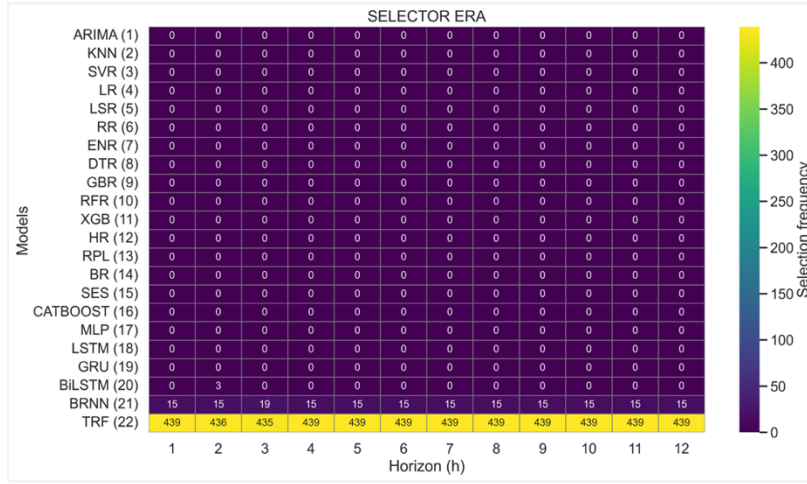


Figure E10. Model Selection Frequency by Forecast Horizon (ERA, M3, 80:20).

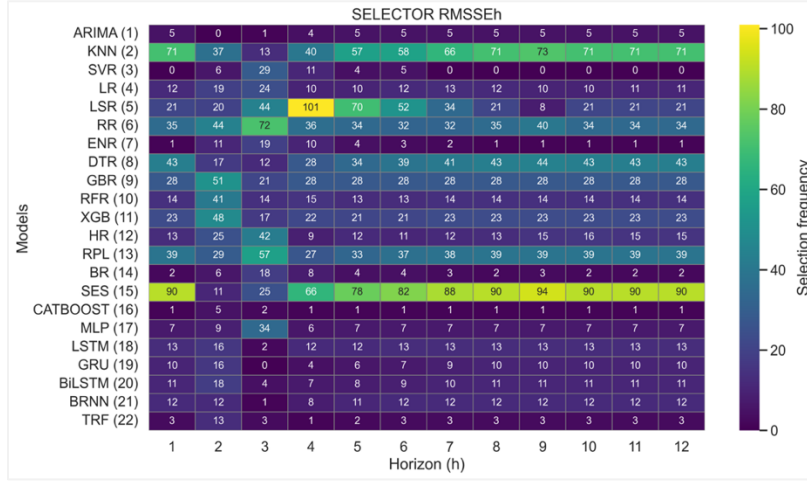


Figure E11. Model Selection Frequency by Forecast Horizon (RMSSE_h, M3, 80:20).

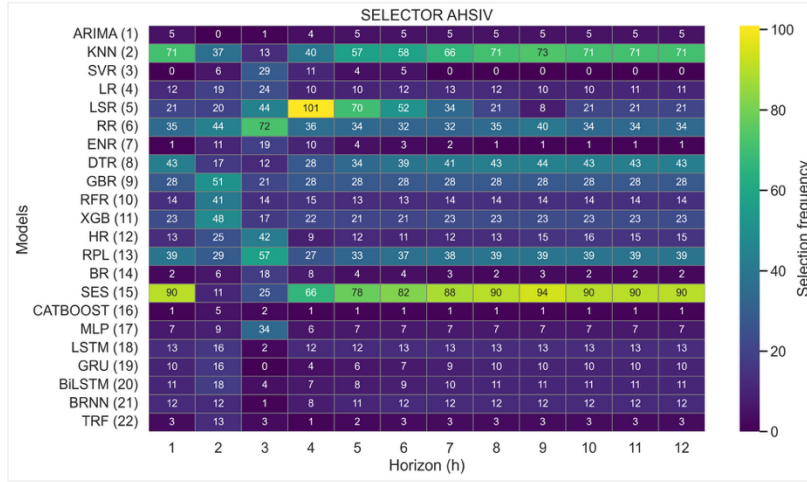


Figure E12. Model Selection Frequency by Forecast Horizon (AHSIV, M3, 80:20).

Table E16. Normality (Shapiro–Wilk) – M3- Training 80% and Testing 20%

Horizon	ERA (result)	ERA (W, p)	RMSSEh (result)	RMSSEh (W, p)	AHSIV (result)	AHSIV (W, p)
---------	--------------	------------	-----------------	---------------	----------------	--------------

h = 1	Not normal	0.8578, 7.22e-20	Not normal	0.7361, 3.16e-26	Not normal	0.7464, 8.72e-26
h = 2	Not normal	0.8640, 1.90e-19	Not normal	0.7602, 3.53e-25	Not normal	0.7692, 9.06e-25
h = 3	Not normal	0.8847, 6.26e-18	Not normal	0.7542, 1.90e-25	Not normal	0.7582, 2.86e-25
h = 4	Not normal	0.8958, 5.00e-17	Not normal	0.7386, 4.03e-26	Not normal	0.7389, 4.15e-26
h = 5	Not normal	0.8977, 7.25e-17	Not normal	0.7474, 9.61e-26	Not normal	0.7462, 8.54e-26
h = 6	Not normal	0.8900, 1.67e-17	Not normal	0.7582, 2.88e-25	Not normal	0.7543, 1.92e-25
h = 7	Not normal	0.8837, 5.29e-18	Not normal	0.7570, 2.53e-25	Not normal	0.7567, 2.46e-25
h = 8	Not normal	0.8824, 4.16e-18	Not normal	0.7560, 2.28e-25	Not normal	0.7547, 2.00e-25
h = 9	Not normal	0.8877, 1.09e-17	Not normal	0.7566, 2.44e-25	Not normal	0.7583, 2.89e-25
h = 10	Not normal	0.8917, 2.29e-17	Not normal	0.7611, 3.88e-25	Not normal	0.7622, 4.33e-25
h = 11	Not normal	0.8797, 2.60e-18	Not normal	0.7662, 6.63e-25	Not normal	0.7675, 7.57e-25
h = 12	Not normal	0.8860, 7.97e-18	Not normal	0.7775, 2.25e-24	Not normal	0.7738, 1.49e-24

Table E17. Kruskal–Wallis, Dunn – M3 - Training 80% and Testing 20%

Horizon	Kruskal–Wallis			Test post-hoc de Dunn		
	Result	H	p-value	ERA vs RMSSEh	ERA vs AHSIV	RMSSEh vs AHSIV
h = 1	Significant differences	108.6694	2.5277e-24	Significant (p = 0.00000)	Significant (p = 0.00000)	Not significant (p = 1.00000)
h = 2	Significant differences	84.3715	4.7748e-19	Significant (p = 0.00000)	Significant (p = 0.00000)	Not significant (p = 1.00000)
h = 3	Significant differences	116.1870	5.8926e-26	Significant (p = 0.00000)	Significant (p = 0.00000)	Not significant (p = 1.00000)
h = 4	Significant differences	131.0235	3.5368e-29	Significant (p = 0.00000)	Significant (p = 0.00000)	Not significant (p = 1.00000)
h = 5	Significant differences	122.3355	2.7238e-27	Significant (p = 0.00000)	Significant (p = 0.00000)	Not significant (p = 1.00000)
h = 6	Significant differences	116.4846	5.0779e-26	Significant (p = 0.00000)	Significant (p = 0.00000)	Not significant (p = 1.00000)
h = 7	Significant differences	112.6184	3.5094e-25	Significant (p = 0.00000)	Significant (p = 0.00000)	Not significant (p = 1.00000)
h = 8	Significant differences	106.4727	7.5814e-24	Significant (p = 0.00000)	Significant (p = 0.00000)	Not significant (p = 1.00000)
h = 9	Significant differences	106.4274	7.7550e-24	Significant (p = 0.00000)	Significant (p = 0.00000)	Not significant (p = 1.00000)
h = 10	Significant differences	103.3803	3.5583e-23	Significant (p = 0.00000)	Significant (p = 0.00000)	Not significant (p = 1.00000)
h = 11	Significant differences	110.7711	8.8381e-25	Significant (p = 0.00000)	Significant (p = 0.00000)	Not significant (p = 1.00000)
h = 12	Significant differences	101.8100	7.8027e-23	Significant (p = 0.00000)	Significant (p = 0.00000)	Not significant (p = 1.00000)

Table E18. Global Synthesis of Descriptive Statistics by Forecast Horizon and Selector – M3 - Training 80% and Testing 20%

Horizon	Selector	count	mean	median	std	min	max	IQR	MAD	Robust CV	GRA global	Final ranking
1	ERA	454	0.90795	0.93406	0.08276	0.53537	0.99996	0.09683	0.04220	0.10367	412.21048	3
1	RMSSEh	454	0.94209	0.97279	0.07464	0.54549	0.99992	0.06533	0.02300	0.06715	427.70987	2
1	AHSIV	454	0.94219	0.97156	0.07307	0.54549	0.99996	0.06778	0.02387	0.06976	427.75570	1
2	ERA	454	0.91094	0.93705	0.08075	0.59881	0.99986	0.09938	0.04118	0.10606	413.56840	3
2	RMSSEh	454	0.94079	0.97216	0.07344	0.54872	0.99998	0.07555	0.02226	0.07771	427.11682	1
2	AHSIV	454	0.94055	0.97341	0.07283	0.59717	0.99998	0.07375	0.02194	0.07577	427.01034	2
3	ERA	454	0.91364	0.93630	0.07388	0.56942	0.99971	0.10183	0.04276	0.10876	414.79302	3
3	RMSSEh	454	0.94783	0.97521	0.06481	0.54621	0.99994	0.06557	0.02074	0.06723	430.31421	1
3	AHSIV	454	0.94775	0.97572	0.06445	0.54621	0.99994	0.06471	0.02057	0.06632	430.27788	2
4	ERA	454	0.91523	0.93755	0.07116	0.68333	0.99919	0.10326	0.04241	0.11014	415.51504	3
4	RMSSEh	454	0.95098	0.97607	0.06180	0.55121	0.99992	0.05856	0.01899	0.06000	431.74626	2
4	AHSIV	454	0.95139	0.97778	0.06166	0.55121	0.99984	0.05914	0.01776	0.06048	431.93283	1
5	ERA	454	0.91523	0.93671	0.07132	0.68718	0.99998	0.10650	0.04254	0.11369	415.51636	3
5	RMSSEh	454	0.95078	0.97680	0.06149	0.55935	0.99994	0.06026	0.01851	0.06169	431.65462	1
5	AHSIV	454	0.95040	0.97541	0.06141	0.55935	1.00000	0.05519	0.01911	0.05658	431.48154	2
6	ERA	454	0.91453	0.93848	0.07274	0.61634	0.99986	0.09840	0.04114	0.10485	415.19568	3
6	RMSSEh	454	0.94878	0.97356	0.06305	0.56424	0.99996	0.05939	0.02213	0.06100	430.74420	2
6	AHSIV	454	0.94936	0.97386	0.06235	0.56424	0.99996	0.05761	0.02155	0.05915	431.00763	1
7	ERA	454	0.91620	0.94188	0.07242	0.59749	0.99982	0.10181	0.03854	0.10809	415.95652	3
7	RMSSEh	454	0.94916	0.97407	0.06221	0.57319	0.99996	0.06045	0.02047	0.06206	430.91650	2
7	AHSIV	454	0.95106	0.97487	0.05917	0.57319	0.99996	0.06049	0.02003	0.06205	431.78341	1
8	ERA	454	0.91756	0.94428	0.07187	0.58433	0.99991	0.09878	0.03754	0.10461	416.57043	3
8	RMSSEh	454	0.94988	0.97399	0.06072	0.57947	0.99974	0.05894	0.02036	0.06051	431.24560	2
8	AHSIV	454	0.95149	0.97579	0.05831	0.57947	0.99974	0.05657	0.01930	0.05798	431.97629	1
9	ERA	454	0.91782	0.93961	0.07062	0.59459	0.99989	0.09580	0.03936	0.10196	416.68846	3
9	RMSSEh	454	0.94933	0.97291	0.06084	0.58840	0.99988	0.06142	0.02091	0.06313	430.99616	2
9	AHSIV	454	0.95133	0.97486	0.05847	0.58840	0.99982	0.06080	0.02010	0.06237	431.90239	1
10	ERA	454	0.91762	0.93706	0.07008	0.59182	0.99978	0.09272	0.04044	0.09895	416.59887	3
10	RMSSEh	454	0.94889	0.97267	0.06080	0.59347	0.99996	0.06096	0.02068	0.06268	430.79475	2

10	AHSIV	454	0.95070	0.97399	0.05846	0.59347	0.99996	0.06080	0.01963	0.06242	431.61960	1
11	ERA	454	0.91798	0.94093	0.06940	0.59314	0.99964	0.08887	0.03560	0.09444	416.76455	3
11	RMSSEh	454	0.94872	0.97157	0.06013	0.59789	0.99991	0.06057	0.02156	0.06234	430.71668	2
11	AHSIV	454	0.95052	0.97431	0.05805	0.59789	0.99996	0.05999	0.02012	0.06158	431.53677	1
12	ERA	454	0.91642	0.93691	0.07029	0.60130	0.99997	0.09143	0.03872	0.09759	416.05246	3
12	RMSSEh	454	0.94668	0.97004	0.06109	0.60084	0.99994	0.06243	0.02312	0.06436	429.79105	2
12	AHSIV	454	0.94903	0.97278	0.05881	0.60084	0.99994	0.06133	0.02105	0.06304	430.85738	1

Appendix F

Walmart

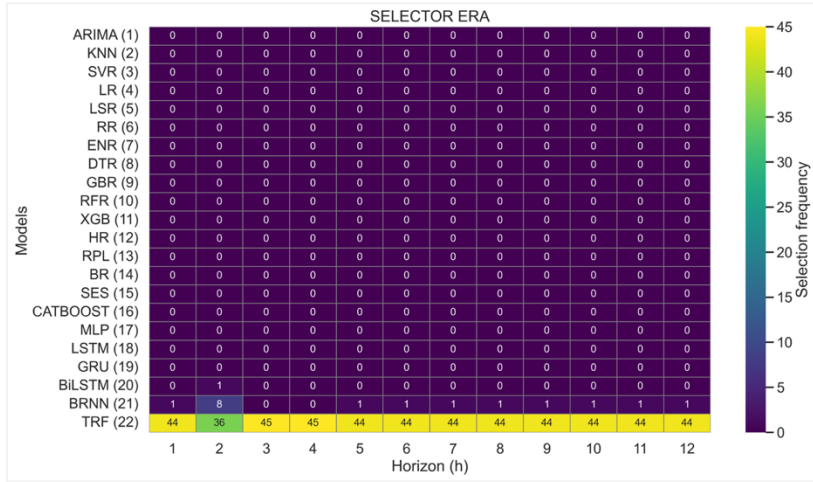


Figure F1. Model Selection Frequency by Forecast Horizon (ERA, Walmart 70:30).

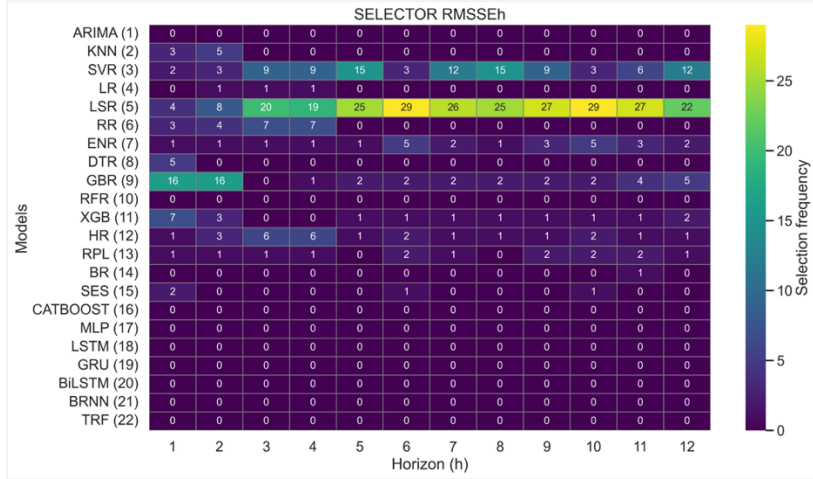


Figure F2. Model Selection Frequency by Forecast Horizon (RMSSE_h, Walmart, 70:30).

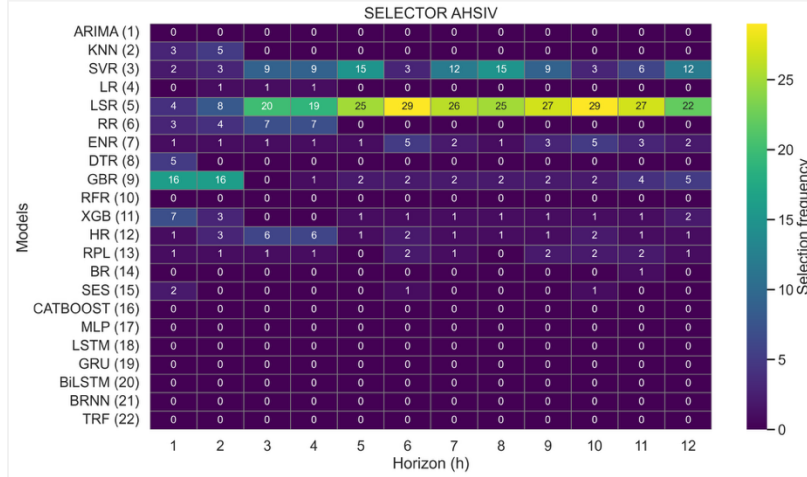


Figure F3. Model Selection Frequency by Forecast Horizon (AHSIV, Walmart 70:30).

Table F1. Normality (Shapiro–Wilk) - Walmart - Training 70% and Testing 30%

Horizon	ERA (result)	ERA (W, p)	RMSSEh (result)	RMSSEh (W, p)	AHSIV (result)	AHSIV (W, p)
h = 1	Not normal	0.8898, 4.62e-04	Not normal	0.8678, 1.09e-04	Not normal	0.8983, 8.42e-04
h = 2	Not normal	0.9194, 4.04e-03	Not normal	0.8825, 2.83e-04	Not normal	0.8948, 6.53e-04
h = 3	Not normal	0.8937, 6.09e-04	Not normal	0.9285, 8.28e-03	Not normal	0.8741, 1.63e-04
h = 4	Not normal	0.8667, 1.02e-04	Not normal	0.9327, 1.17e-02	Not normal	0.9045, 1.31e-03
h = 5	Not normal	0.8795, 2.31e-04	Not normal	0.7706, 5.69e-07	Not normal	0.7890, 1.38e-06
h = 6	Not normal	0.8602, 6.78e-05	Not normal	0.8126, 4.56e-06	Not normal	0.8881, 4.12e-04
h = 7	Not normal	0.8483, 3.31e-05	Not normal	0.7911, 1.53e-06	Not normal	0.8856, 3.48e-04
h = 8	Not normal	0.8672, 1.05e-04	Not normal	0.7955, 1.89e-06	Not normal	0.7321, 1.03e-07
h = 9	Not normal	0.8615, 7.34e-05	Not normal	0.8031, 2.79e-06	Not normal	0.8472, 3.10e-05
h = 10	Not normal	0.8653, 9.28e-05	Not normal	0.8286, 1.08e-05	Not normal	0.8506, 3.80e-05
h = 11	Not normal	0.8900, 4.68e-04	Not normal	0.8354, 1.58e-05	Not normal	0.9154, 2.96e-03
h = 12	Not normal	0.8776, 2.04e-04	Not normal	0.8102, 4.01e-06	Not normal	0.7589, 3.32e-07

Table F2. Kruskal–Wallis, Dunn - Walmart - Training 70% and Testing 30%

Horizon	Kruskal–Wallis			Test post-hoc de Dunn		
	Result	H	p-value	ERA vs RMSSEh	ERA vs AHSIV	RMSSEh vs AHSIV
h = 1	Significant differences	8.0570	1.7801e-02	Significant (p = 0.04520)	Significant (p = 0.03890)	Not significant (p = 1.00000)
h = 2	Significant differences	14.9776	5.5932e-04	Significant (p = 0.00503)	Significant (p = 0.00126)	Not significant (p = 1.00000)
h = 3	Significant differences	6.9661	3.0713e-02	Not significant (p = 0.09390)	Significant (p = 0.04939)	Not significant (p = 1.00000)
h = 4	No significant differences were detected.	4.1045	1.2844e-01	Not significant (p = 0.24510)	Not significant (p = 0.23125)	Not significant (p = 1.00000)
h = 5	No significant differences were detected.	5.1773	7.5123e-02	Not significant (p = 0.09170)	Not significant (p = 0.27093)	Not significant (p = 1.00000)
h = 6	No significant differences were detected.	5.6567	5.9111e-02	Not significant (p = 0.46545)	Not significant (p = 0.05451)	Not significant (p = 1.00000)
h = 7	No significant differences were detected.	4.2775	1.1780e-01	Not significant (p = 0.21043)	Not significant (p = 0.22990)	Not significant (p = 1.00000)
h = 8	No significant differences were detected.	2.4286	2.9692e-01	Not significant (p = 0.62315)	Not significant (p = 0.46311)	Not significant (p = 1.00000)
h = 9	No significant differences were detected.	1.8110	4.0434e-01	Not significant (p = 1.00000)	Not significant (p = 0.53611)	Not significant (p = 1.00000)
h = 10	No significant differences were detected.	4.0108	1.3461e-01	Not significant (p = 1.00000)	Not significant (p = 0.21548)	Not significant (p = 0.29070)
h = 11	No significant differences were detected.	1.7045	4.2645e-01	Not significant (p = 1.00000)	Not significant (p = 0.60155)	Not significant (p = 1.00000)
h = 12	No significant differences were detected.	0.7218	6.9705e-01	Not significant (p = 1.00000)	Not significant (p = 1.00000)	Not significant (p = 1.00000)

Table F3. Global Synthesis of Descriptive Statistics by Forecast Horizon and Selector - Walmart - Training 70% and Testing 30%

Horizon	Selector	count	mean	median	std	min	max	IQR	MAD	Robust CV	GRA global	Final ranking
1	ERA	45	0.96425	0.97300	0.02992	0.88416	0.99945	0.04187	0.01761	0.04303	43.39133	3
1	RMSSEh	45	0.98021	0.98523	0.01429	0.93445	0.99614	0.01677	0.00739	0.01702	44.10967	2
1	AHSIV	45	0.98062	0.98565	0.01359	0.93445	0.99882	0.01545	0.00720	0.01568	44.12768	1
2	ERA	45	0.96451	0.97234	0.02618	0.90268	0.99852	0.04125	0.01780	0.04242	43.40303	3
2	RMSSEh	45	0.98127	0.98461	0.01480	0.92799	0.99916	0.01461	0.00719	0.01484	44.15729	2
2	AHSIV	45	0.98212	0.98571	0.01477	0.94077	0.99931	0.01542	0.00789	0.01564	44.19532	1
3	ERA	45	0.96952	0.97756	0.02635	0.90453	0.99990	0.03386	0.01811	0.03463	43.62824	3
3	RMSSEh	45	0.98330	0.98637	0.01217	0.95446	0.99999	0.01529	0.00773	0.01551	44.24834	1
3	AHSIV	45	0.98281	0.98763	0.01440	0.95446	0.99999	0.01840	0.00759	0.01863	44.22636	2
4	ERA	45	0.97251	0.98039	0.02562	0.90280	0.99902	0.03317	0.01415	0.03383	43.76313	3
4	RMSSEh	45	0.98441	0.98701	0.01112	0.95498	0.99972	0.01440	0.00778	0.01459	44.29850	1
4	AHSIV	45	0.98362	0.98710	0.01291	0.95498	0.99982	0.01520	0.00782	0.01540	44.26284	2
5	ERA	45	0.97371	0.98248	0.02448	0.91685	0.99980	0.03458	0.01566	0.03519	43.81688	3
5	RMSSEh	45	0.98542	0.98943	0.01530	0.91645	0.99966	0.01471	0.00721	0.01486	44.34406	1
5	AHSIV	45	0.98460	0.98705	0.01454	0.91645	0.99962	0.01415	0.00717	0.01434	44.30695	2
6	ERA	45	0.97468	0.98473	0.02426	0.91628	0.99945	0.03569	0.01297	0.03625	43.86061	3
6	RMSSEh	45	0.98294	0.98933	0.01692	0.90991	0.99997	0.02213	0.00847	0.02237	44.23227	2
6	AHSIV	45	0.98712	0.99103	0.01135	0.95634	0.99997	0.01455	0.00677	0.01468	44.42048	1
7	ERA	45	0.97497	0.98682	0.02363	0.91311	0.99946	0.03066	0.00882	0.03107	43.87349	3
7	RMSSEh	45	0.98270	0.99070	0.01851	0.90535	0.99986	0.02780	0.00653	0.02806	44.22157	2
7	AHSIV	45	0.98538	0.98817	0.01194	0.95656	0.99949	0.01703	0.00714	0.01723	44.34189	1
8	ERA	45	0.97480	0.98230	0.02293	0.90986	0.99997	0.02744	0.01285	0.02793	43.86596	3
8	RMSSEh	45	0.98107	0.98804	0.01893	0.90039	0.99880	0.02250	0.00859	0.02278	44.14828	2
8	AHSIV	45	0.98304	0.98679	0.01685	0.90039	0.99965	0.01328	0.00657	0.01346	44.23663	1
9	ERA	45	0.97574	0.98352	0.02222	0.91568	0.99966	0.02574	0.01203	0.02617	43.90810	3
9	RMSSEh	45	0.98003	0.98909	0.01927	0.90080	0.99909	0.02553	0.00763	0.02581	44.10126	2
9	AHSIV	45	0.98409	0.98909	0.01305	0.95088	0.99992	0.01659	0.00523	0.01677	44.28402	1
10	ERA	45	0.97584	0.98458	0.02207	0.92045	0.99984	0.02739	0.01182	0.02782	43.91268	3
10	RMSSEh	45	0.97841	0.98676	0.01968	0.89977	0.99862	0.02813	0.00906	0.02851	44.02828	2
10	AHSIV	45	0.98557	0.98855	0.01265	0.94993	0.99990	0.01578	0.00637	0.01596	44.35085	1
11	ERA	45	0.97540	0.98222	0.02195	0.91876	0.99985	0.02698	0.01323	0.02747	43.89317	3
11	RMSSEh	45	0.97822	0.98525	0.02010	0.89766	0.99933	0.02585	0.00963	0.02624	44.01969	2
11	AHSIV	45	0.98352	0.98595	0.01235	0.94947	0.99933	0.01409	0.00793	0.01429	44.25823	1
12	ERA	45	0.97592	0.98133	0.02102	0.91979	0.99978	0.02574	0.01228	0.02623	43.91634	3
12	RMSSEh	45	0.97910	0.98426	0.01917	0.89805	0.99904	0.01773	0.00842	0.01802	44.05959	2
12	AHSIV	45	0.98094	0.98426	0.01746	0.89805	0.99908	0.01451	0.00799	0.01475	44.14223	1

M5

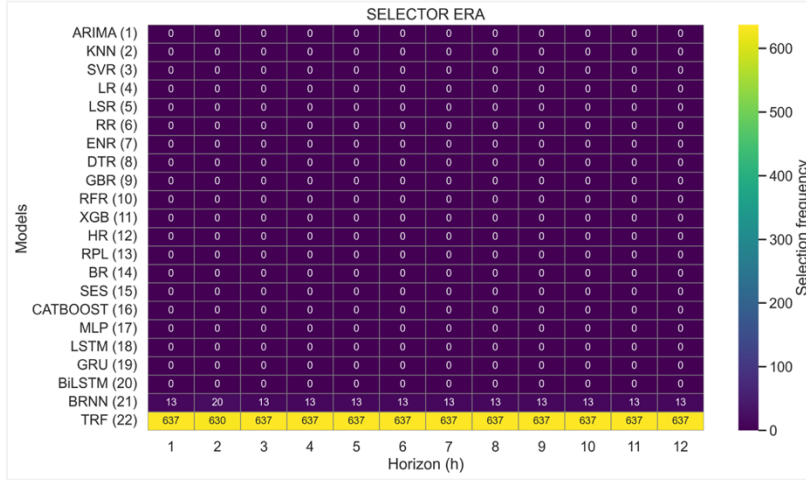


Figure F4. Model Selection Frequency by Forecast Horizon (ERA, M5, 70:30).

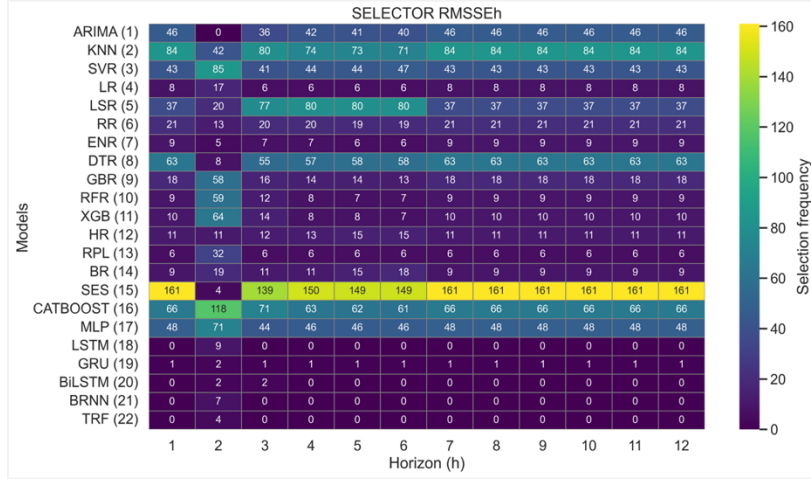


Figure F5. Model Selection Frequency by Forecast Horizon (RMSSE_h, M5, 70:30).

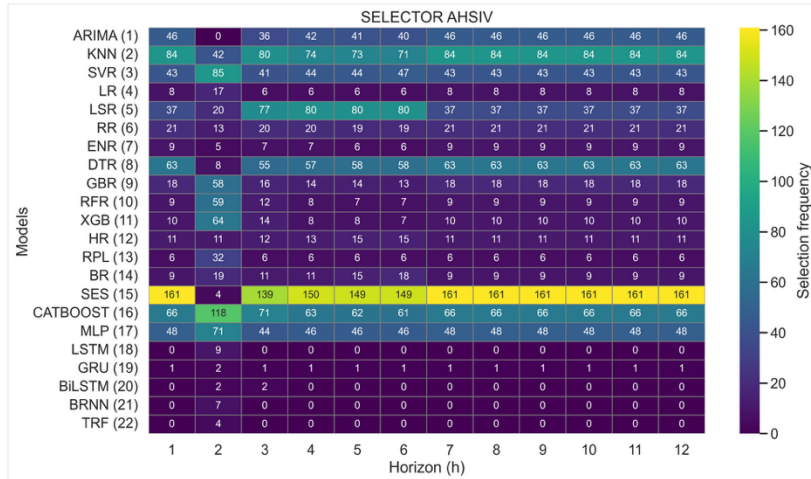


Figure F6. Model Selection Frequency by Forecast Horizon (AHSIV, M5, 70:30).

Table F6. Normality (Shapiro–Wilk) – M5 - Training 70% and Testing 30%

Horizon	ERA (result)	ERA (W, p)	RMSSEh (result)	RMSSEh (W, p)	AHSIV (result)	AHSIV (W, p)
h = 1	Not normal	0.6708, 1.33e-33	Not normal	0.9688, 1.54e-10	Not normal	0.9687, 1.51e-10
h = 2	Not normal	0.5715, 4.64e-37	Not normal	0.9687, 1.45e-10	Not normal	0.9687, 1.48e-10
h = 3	Not normal	0.5300, 2.58e-38	Not normal	0.9728, 1.23e-09	Not normal	0.9723, 9.53e-10
h = 4	Not normal	0.5031, 4.41e-39	Not normal	0.9689, 1.62e-10	Not normal	0.9680, 1.04e-10
h = 5	Not normal	0.4855, 1.45e-39	Not normal	0.9717, 7.07e-10	Not normal	0.9707, 4.03e-10
h = 6	Not normal	0.4847, 1.38e-39	Not normal	0.9645, 2.00e-11	Not normal	0.9637, 1.36e-11
h = 7	Not normal	0.5102, 1.96e-39	Not normal	0.9612, 4.35e-12	Not normal	0.9599, 2.57e-12
h = 8	Not normal	0.5082, 6.11e-39	Not normal	0.9537, 2.06e-13	Not normal	0.9528, 1.42e-13
h = 9	Not normal	0.5092, 6.51e-39	Not normal	0.9541, 2.34e-13	Not normal	0.9537, 2.05e-13
h = 10	Not normal	0.5001, 3.63e-39	Not normal	0.9486, 2.99e-14	Not normal	0.9481, 2.52e-14
h = 11	Not normal	0.5056, 5.16e-39	Not normal	0.9478, 2.22e-14	Not normal	0.9475, 2.00e-14
h = 12	Not normal	0.4919, 2.15e-39	Not normal	0.9449, 8.11e-15	Not normal	0.9442, 6.39e-15

Table F7. Kruskal–Wallis, Dunn – M5 - Training 70% and Testing 30%

Horizon	Kruskal–Wallis			Test post-hoc de Dunn		
	Result	H	p-value	ERA vs RMSSEh	ERA vs AHSIV	RMSSEh vs AHSIV
h = 1	Significant differences	962.4211	1.0302e-209	Significant (p = 0.00000)	Significant (p = 0.00000)	Not significant (p = 1.00000)
h = 2	Significant differences	945.2556	5.4999e-206	Significant (p = 0.00000)	Significant (p = 0.00000)	Not significant (p = 1.00000)
h = 3	Significant differences	1052.7492	2.5028e-229	Significant (p = 0.00000)	Significant (p = 0.00000)	Not significant (p = 1.00000)
h = 4	Significant differences	1070.8851	2.8858e-233	Significant (p = 0.00000)	Significant (p = 0.00000)	Not significant (p = 1.00000)

h = 5	Significant differences	1072.6496	1.1943e-233	Significant (p = 0.00000)	Significant (p = 0.00000)	Not significant (p = 1.00000)
h = 6	Significant differences	1089.4294	2.7128e-237	Significant (p = 0.00000)	Significant (p = 0.00000)	Not significant (p = 1.00000)
h = 7	Significant differences	1100.7450	9.4682e-240	Significant (p = 0.00000)	Significant (p = 0.00000)	Not significant (p = 1.00000)
h = 8	Significant differences	1081.0136	1.8234e-235	Significant (p = 0.00000)	Significant (p = 0.00000)	Not significant (p = 1.00000)
h = 9	Significant differences	1089.6423	2.4388e-237	Significant (p = 0.00000)	Significant (p = 0.00000)	Not significant (p = 1.00000)
h = 10	Significant differences	1090.5930	1.5162e-237	Significant (p = 0.00000)	Significant (p = 0.00000)	Not significant (p = 1.00000)
h = 11	Significant differences	1088.4406	4.4475e-237	Significant (p = 0.00000)	Significant (p = 0.00000)	Not significant (p = 1.00000)
h = 12	Significant differences	1085.2960	2.1428e-236	Significant (p = 0.00000)	Significant (p = 0.00000)	Not significant (p = 1.00000)

Table F8. Global Synthesis of Descriptive Statistics by Forecast Horizon and Selector – M5 - Training 70% and Testing 30%

Horizon	Selector	count	mean	median	std	min	max	IQR	MAD	Robust CV	GRA global	Final ranking
1	ERA	650	0.57763	0.54097	0.09798	0.50069	0.99998	0.06724	0.02509	0.12429	375.46017	3
1	RMSSEh	650	0.81236	0.81330	0.11990	0.52174	1.00000	0.19013	0.09471	0.23378	528.03378	1
1	AHSIV	650	0.81220	0.81190	0.12005	0.52174	1.00000	0.19107	0.09443	0.23534	527.93178	2
2	ERA	650	0.55975	0.53048	0.08867	0.50035	0.99994	0.04531	0.01751	0.08541	363.83910	3
2	RMSSEh	650	0.78311	0.78450	0.13277	0.50968	1.00000	0.20838	0.10428	0.26562	509.01912	2
2	AHSIV	650	0.78353	0.78450	0.13266	0.50968	1.00000	0.20972	0.10428	0.26732	509.29207	1
3	ERA	650	0.54891	0.52556	0.07615	0.50023	0.99993	0.03742	0.01399	0.07120	356.78836	3
3	RMSSEh	650	0.79291	0.79629	0.12503	0.50794	1.00000	0.19539	0.09845	0.24538	515.39208	2
3	AHSIV	650	0.79348	0.79629	0.12544	0.50794	1.00000	0.19661	0.09907	0.24690	515.76205	1
4	ERA	650	0.54496	0.52277	0.07307	0.50018	0.99993	0.03064	0.01261	0.05861	354.22598	3
4	RMSSEh	650	0.79749	0.81134	0.12649	0.50685	1.00000	0.20213	0.09947	0.24913	518.36699	2
4	AHSIV	650	0.79789	0.81187	0.12681	0.50685	1.00000	0.20388	0.10056	0.25112	518.62747	1
5	ERA	650	0.54228	0.52059	0.07128	0.50014	0.99439	0.02705	0.01108	0.05196	352.48020	3
5	RMSSEh	650	0.79354	0.80321	0.12538	0.50549	1.00000	0.18849	0.09208	0.23468	515.79909	2
5	AHSIV	650	0.79399	0.80321	0.12572	0.50549	1.00000	0.19033	0.09386	0.23697	516.09293	1
6	ERA	650	0.53989	0.52033	0.06664	0.50012	0.99320	0.02421	0.01075	0.04652	350.92984	3
6	RMSSEh	650	0.79720	0.80099	0.13088	0.50450	1.00000	0.21145	0.10696	0.26398	518.18223	2
6	AHSIV	650	0.79772	0.80189	0.13120	0.50450	1.00000	0.21175	0.10731	0.26406	518.51981	1
7	ERA	650	0.53885	0.52075	0.06088	0.50010	0.98251	0.02270	0.01016	0.04359	350.24936	3
7	RMSSEh	650	0.80117	0.80647	0.13011	0.50365	1.00000	0.21071	0.10449	0.26128	520.75770	2
7	AHSIV	650	0.80166	0.80745	0.13043	0.50365	1.00000	0.21317	0.10663	0.26400	521.08213	1
8	ERA	650	0.54005	0.52198	0.06293	0.50009	0.99881	0.02503	0.01050	0.04795	351.03086	3
8	RMSSEh	650	0.80399	0.82641	0.13317	0.50296	1.00000	0.20941	0.10275	0.25339	522.59552	2
8	AHSIV	650	0.80445	0.82751	0.13343	0.50296	1.00000	0.20976	0.10286	0.25349	522.89237	1
9	ERA	650	0.53871	0.52278	0.05864	0.50008	0.98460	0.02349	0.01070	0.04493	350.15949	3
9	RMSSEh	650	0.80320	0.82346	0.13104	0.50256	1.00000	0.21279	0.09910	0.25841	522.08078	2
9	AHSIV	650	0.80363	0.82507	0.13140	0.50256	1.00000	0.21319	0.09972	0.25839	522.35698	1
10	ERA	650	0.53803	0.52207	0.05796	0.50007	0.99533	0.02205	0.00998	0.04224	349.72270	3
10	RMSSEh	650	0.80812	0.83047	0.13208	0.50244	1.00000	0.20342	0.10043	0.24495	525.27960	2
10	AHSIV	650	0.80841	0.83047	0.13223	0.50244	1.00000	0.20357	0.10062	0.24513	525.46806	1
11	ERA	650	0.53774	0.52150	0.05729	0.50006	0.98377	0.02104	0.00991	0.04035	349.53377	3
11	RMSSEh	650	0.80994	0.83044	0.13378	0.50220	1.00000	0.20992	0.10112	0.25279	526.45824	2
11	AHSIV	650	0.81010	0.83044	0.13376	0.50220	1.00000	0.20924	0.10094	0.25196	526.56215	1
12	ERA	650	0.53694	0.52142	0.05684	0.50006	0.96751	0.02039	0.00929	0.03910	349.01031	3
12	RMSSEh	650	0.81066	0.83521	0.13382	0.50199	1.00000	0.20367	0.09632	0.24386	526.93012	2
12	AHSIV	650	0.81080	0.83543	0.13374	0.50199	1.00000	0.20349	0.09584	0.24358	527.02080	1

M4

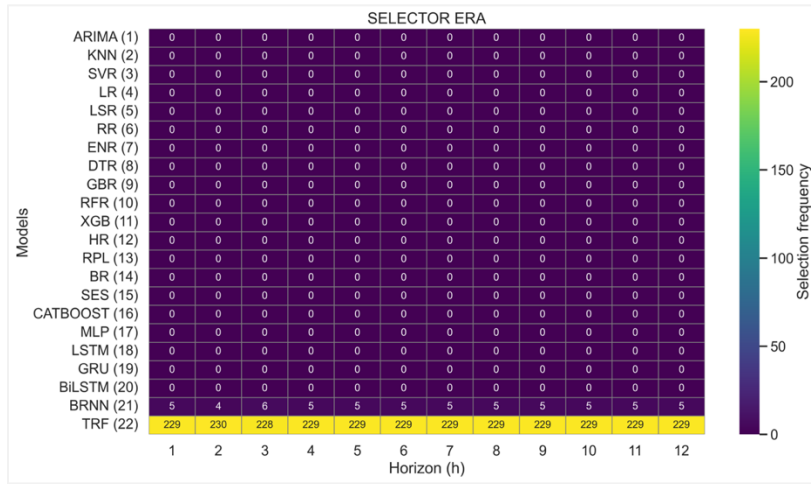


Figure F7. Model Selection Frequency by Forecast Horizon (ERA, M4 70:30).

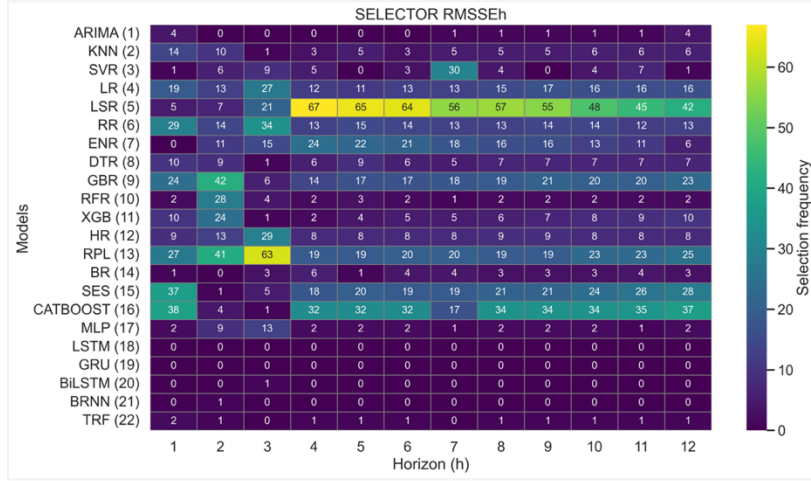


Figure F8. Model Selection Frequency by Forecast Horizon (RMSSE_h, M4 70:30).

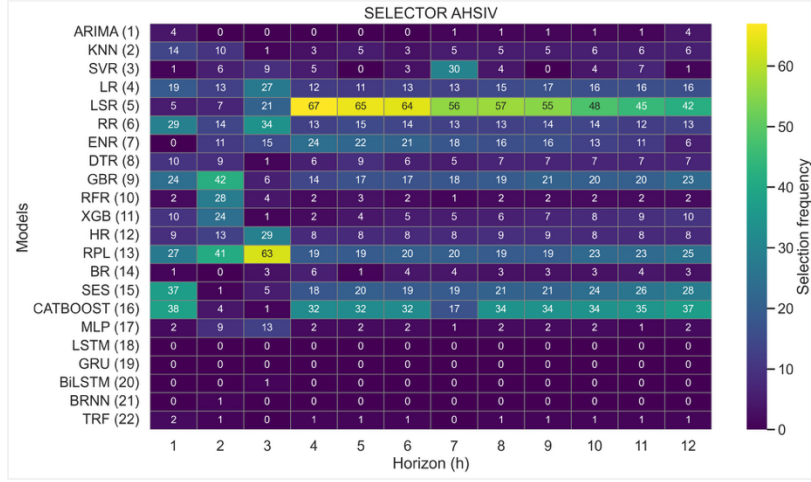


Figure F9. Model Selection Frequency by Forecast Horizon (AHSIV, M4 70:30).

Table F11. Normality (Shapiro–Wilk) - M4- Training 70% and Testing 30%

Horizon	ERA (result)	ERA (W, p)	RMSSEh (result)	RMSSEh (W, p)	AHSIV (result)	AHSIV (W, p)
h = 1	Not normal	0.9361, 1.45e-08	Not normal	0.6391, 5.77e-22	Not normal	0.6411, 6.56e-22
h = 2	Not normal	0.9334, 8.35e-09	Not normal	0.6710, 4.49e-21	Not normal	0.6734, 5.28e-21
h = 3	Not normal	0.9348, 1.11e-08	Not normal	0.6531, 1.40e-21	Not normal	0.6567, 1.76e-21
h = 4	Not normal	0.9334, 8.43e-09	Not normal	0.6281, 2.94e-22	Not normal	0.6208, 1.90e-22
h = 5	Not normal	0.9331, 7.84e-09	Not normal	0.6248, 2.41e-22	Not normal	0.6159, 1.42e-22
h = 6	Not normal	0.9329, 7.50e-09	Not normal	0.6176, 1.57e-22	Not normal	0.6141, 1.28e-22
h = 7	Not normal	0.9341, 9.56e-09	Not normal	0.6173, 1.54e-22	Not normal	0.6150, 1.34e-22
h = 8	Not normal	0.9350, 1.16e-08	Not normal	0.6169, 1.51e-22	Not normal	0.6126, 1.17e-22
h = 9	Not normal	0.9348, 1.11e-08	Not normal	0.6209, 1.90e-22	Not normal	0.6170, 1.51e-22
h = 10	Not normal	0.9348, 1.10e-08	Not normal	0.6193, 1.73e-22	Not normal	0.6173, 1.54e-22
h = 11	Not normal	0.9333, 8.21e-09	Not normal	0.6195, 1.75e-22	Not normal	0.6207, 1.89e-22
h = 12	Not normal	0.9333, 8.22e-09	Not normal	0.6214, 1.97e-22	Not normal	0.6192, 1.73e-22

Table F12. Kruskal–Wallis, Dunn - M4 - Training 70% and Testing 30%

Horizon	Kruskal–Wallis			Test post-hoc de Dunn		
	Result	H	p-value	ERA vs RMSSEh	ERA vs AHSIV	RMSSEh vs AHSIV
h = 1	Significant differences	130.1449	5.4878e-29	Significant (p = 0.00000)	Significant (p = 1.00000)	Not significant
h = 2	Significant differences	122.9497	2.0036e-27	Significant (p = 0.00000)	Significant (p = 0.00000)	Not significant
h = 3	Significant differences	120.4065	7.1458e-27	Significant (p = 0.00000)	Significant (p = 0.00000)	Not significant
h = 4	Significant differences	134.1824	7.2891e-30	Significant (p = 0.00000)	Significant (p = 0.00000)	Not significant
h = 5	Significant differences	138.4463	8.6451e-31	Significant (p = 0.00000)	Significant (p = 0.00000)	Not significant
h = 6	Significant differences	142.5827	1.0928e-31	Significant (p = 0.00000)	Significant (p = 0.00000)	Not significant
h = 7	Significant differences	139.5267	5.0369e-31	Significant (p = 0.00000)	Significant (p = 0.00000)	Not significant
h = 8	Significant differences	136.5556	2.2250e-30	Significant (p = 0.00000)	Significant (p = 0.00000)	Not significant
h = 9	Significant differences	139.6794	4.6666e-31	Significant (p = 0.00000)	Significant (p = 0.00000)	Not significant
h = 10	Significant differences	141.5723	1.8112e-31	Significant (p = 0.00000)	Significant (p = 0.00000)	Not significant
h = 11	Significant differences	145.9819	1.9973e-32	Significant (p = 0.00000)	Significant (p = 0.00000)	Not significant
h = 12	Significant differences	146.4420	1.5868e-32	Significant (p = 0.00000)	Significant (p = 0.00000)	Not significant

Table F13. Global Synthesis of Descriptive Statistics by Forecast Horizon and Selector - M4 - Training 70% and Testing 30%

Horizon	Selector	count	mean	median	std	min	max	IQR	MAD	Robust CV	GRA global	Final ranking
1	ERA	234	0.73697	0.72639	0.14657	0.50007	0.99515	0.18204	0.08692	0.25061	172.45034	3
1	RMSSEh	234	0.87494	0.96139	0.18037	0.50002	1.00000	0.10495	0.03281	0.10916	204.73657	1
1	AHSIV	234	0.87464	0.96411	0.18077	0.50002	1.00000	0.11856	0.03031	0.12298	204.66547	2
2	ERA	234	0.73299	0.72065	0.14237	0.50003	0.99594	0.17461	0.08849	0.24230	171.51869	3
2	RMSSEh	234	0.86401	0.95058	0.17553	0.50002	1.00000	0.12447	0.03678	0.13094	202.17780	2
2	AHSIV	234	0.86464	0.95063	0.17614	0.50002	1.00000	0.12455	0.03848	0.13102	202.32523	1
3	ERA	234	0.73672	0.72654	0.14449	0.50002	0.99713	0.17699	0.07830	0.24361	172.39181	3
3	RMSSEh	234	0.86942	0.95092	0.17662	0.50001	0.99945	0.10967	0.03704	0.11533	203.44345	2
3	AHSIV	234	0.86953	0.95235	0.17712	0.50001	0.99973	0.11858	0.03730	0.12451	203.46942	1
4	ERA	234	0.73571	0.72721	0.14467	0.50002	0.99984	0.16615	0.08063	0.22848	172.15657	3
4	RMSSEh	234	0.87576	0.96071	0.17804	0.50001	0.99994	0.09733	0.02980	0.10131	204.92800	2
4	AHSIV	234	0.87761	0.96409	0.17911	0.50001	0.99994	0.09049	0.02651	0.09386	205.36067	1
5	ERA	234	0.73557	0.72755	0.14420	0.50001	0.99404	0.16873	0.07331	0.23192	172.12250	3
5	RMSSEh	234	0.87686	0.96158	0.17844	0.50001	0.99974	0.09728	0.02976	0.10117	205.18504	2
5	AHSIV	234	0.87866	0.96404	0.17937	0.50001	0.99973	0.08733	0.02664	0.09059	205.60711	1
6	ERA	234	0.73521	0.72592	0.14349	0.50001	0.99874	0.16837	0.07600	0.23193	172.03935	3
6	RMSSEh	234	0.87802	0.96170	0.17855	0.50000	0.99978	0.09634	0.02848	0.10018	205.45595	2
6	AHSIV	234	0.87966	0.96461	0.17949	0.50000	0.99970	0.09176	0.02743	0.09513	205.84047	1
7	ERA	234	0.73475	0.72280	0.14319	0.50001	1.00000	0.16556	0.07577	0.22905	171.93205	3
7	RMSSEh	234	0.87767	0.96159	0.17841	0.50000	0.99996	0.09249	0.02737	0.09619	205.37450	2
7	AHSIV	234	0.87911	0.96316	0.17920	0.50000	0.99963	0.09313	0.02778	0.09669	205.71073	1
8	ERA	234	0.73499	0.72560	0.14356	0.50001	0.99834	0.16562	0.08091	0.22825	171.98682	3
8	RMSSEh	234	0.87827	0.96408	0.17865	0.50000	0.99995	0.09083	0.02694	0.09422	205.51488	2
8	AHSIV	234	0.87962	0.96708	0.17947	0.50000	0.99982	0.09074	0.02433	0.09383	205.83023	1
9	ERA	234	0.73450	0.72783	0.14255	0.50001	0.99908	0.16709	0.07803	0.22957	171.87344	3

9	RMSSEh	234	0.87732	0.96210	0.17836	0.50000	0.99976	0.09531	0.02821	0.09907	205.29356	2
9	AHSIV	234	0.87857	0.96768	0.17930	0.50000	0.99964	0.09470	0.02330	0.09786	205.58496	1
10	ERA	234	0.73380	0.72805	0.14220	0.50001	0.99912	0.16642	0.07821	0.22858	171.70811	3
10	RMSSEh	234	0.87771	0.96224	0.17850	0.50000	0.99996	0.09221	0.02840	0.09583	205.38439	2
10	AHSIV	234	0.87843	0.96687	0.17924	0.50000	0.99996	0.09325	0.02388	0.09645	205.55208	1
11	ERA	234	0.73320	0.72709	0.14128	0.50001	0.99629	0.16488	0.07404	0.22677	171.56938	3
11	RMSSEh	234	0.87761	0.96182	0.17849	0.50000	0.99983	0.09252	0.02844	0.09620	205.35993	1
11	AHSIV	234	0.87760	0.96422	0.17895	0.50000	0.99967	0.09324	0.02656	0.09670	205.35859	2
12	ERA	234	0.73280	0.72518	0.14079	0.50001	0.99872	0.16485	0.07516	0.22733	171.47633	3
12	RMSSEh	234	0.87666	0.96000	0.17815	0.50000	0.99997	0.09124	0.03027	0.09505	205.13729	2
12	AHSIV	234	0.87753	0.96396	0.17881	0.50000	0.99997	0.08975	0.02676	0.09311	205.34315	1

M3

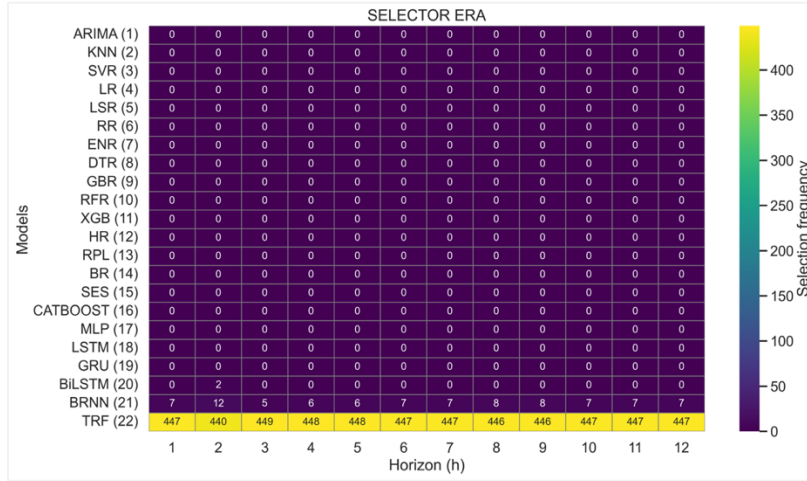


Figure F10. Model Selection Frequency by Forecast Horizon (ERA, M3, 70:30).

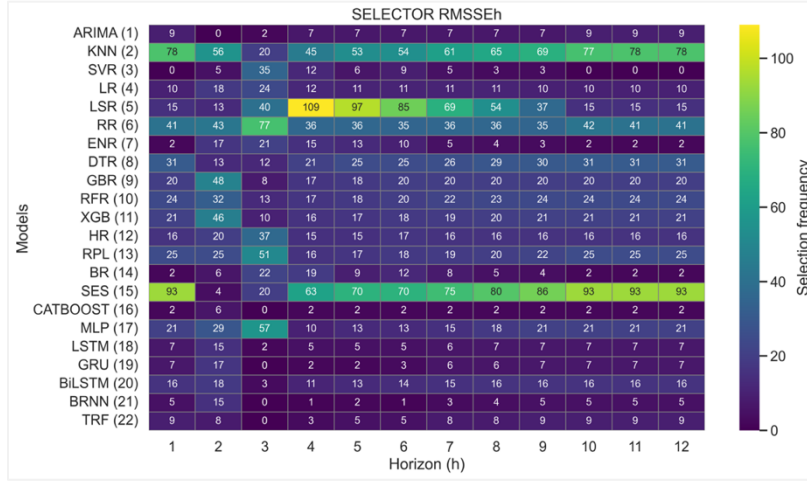


Figure F11. Model Selection Frequency by Forecast Horizon (RMSSEh, M3, 70:30).

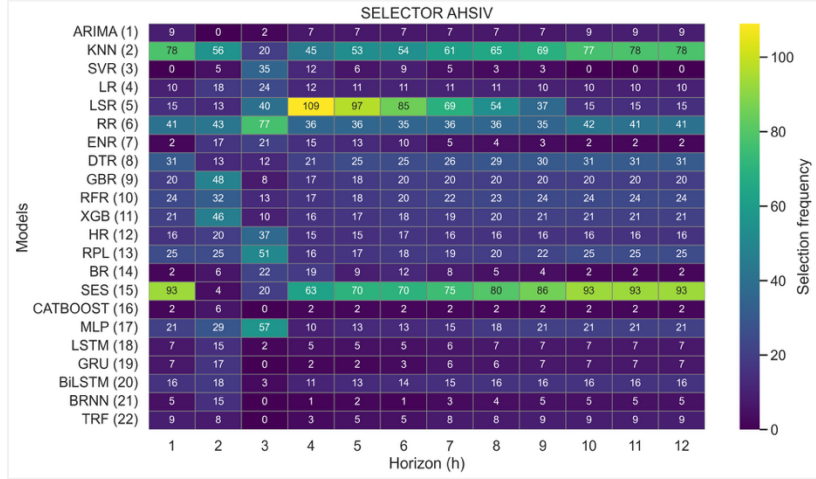


Figure F12. Model Selection Frequency by Forecast Horizon (AHSIV, M3, 70:30).

Table F16. Normality (Shapiro–Wilk) – M3 - Training 70% and Testing 30%

Horizon	ERA (result)	ERA (W, p)	RMSSEh (result)	RMSSEh (W, p)	AHSIV (result)	AHSIV (W, p)
h = 1	Not normal	0.8660, 2.63e-19	Not normal	0.7630, 4.72e-25	Not normal	0.7511, 1.39e-25
h = 2	Not normal	0.8817, 3.73e-18	Not normal	0.7753, 1.76e-24	Not normal	0.7727, 1.33e-24
h = 3	Not normal	0.8794, 2.49e-18	Not normal	0.7823, 3.82e-24	Not normal	0.7776, 2.26e-24
h = 4	Not normal	0.8921, 2.47e-17	Not normal	0.7657, 6.28e-25	Not normal	0.7637, 5.09e-25
h = 5	Not normal	0.8900, 1.66e-17	Not normal	0.7681, 8.08e-25	Not normal	0.7575, 2.68e-25
h = 6	Not normal	0.8916, 2.23e-17	Not normal	0.7652, 5.95e-25	Not normal	0.7585, 2.95e-25
h = 7	Not normal	0.8926, 2.70e-17	Not normal	0.7661, 6.54e-25	Not normal	0.7613, 3.94e-25
h = 8	Not normal	0.8917, 2.30e-17	Not normal	0.7564, 2.38e-25	Not normal	0.7587, 3.03e-25
h = 9	Not normal	0.8912, 2.08e-17	Not normal	0.7722, 1.26e-24	Not normal	0.7758, 1.87e-24
h = 10	Not normal	0.8882, 1.20e-17	Not normal	0.7790, 2.63e-24	Not normal	0.7798, 2.90e-24
h = 11	Not normal	0.8796, 2.58e-18	Not normal	0.7785, 2.49e-24	Not normal	0.7777, 2.29e-24
h = 12	Not normal	0.8813, 3.43e-18	Not normal	0.7843, 4.79e-24	Not normal	0.7829, 4.08e-24

Table F17. Kruskal–Wallis, Dunn – M3 - Training 70% and Testing 30%

Horizon	Kruskal–Wallis			Test post-hoc de Dunn		
	Result	H	p-value	ERA vs RMSSEh	ERA vs AHSIV	RMSSEh vs AHSIV
h = 1	Significant differences	117.4760	3.0932e-26	Significant (p = 0.00000)	Significant (p = 0.00000)	Not significant (p = 1.00000)
h = 2	Significant differences	88.8977	4.9671e-20	Significant (p = 0.00000)	Significant (p = 0.00000)	Not significant (p = 1.00000)
h = 3	Significant differences	103.5313	3.2996e-23	Significant (p = 0.00000)	Significant (p = 0.00000)	Not significant (p = 1.00000)
h = 4	Significant differences	137.1619	1.6431e-30	Significant (p = 0.00000)	Significant (p = 0.00000)	Not significant (p = 1.00000)
h = 5	Significant differences	136.1000	2.7942e-30	Significant (p = 0.00000)	Significant (p = 0.00000)	Not significant (p = 1.00000)
h = 6	Significant differences	132.4504	1.7328e-29	Significant (p = 0.00000)	Significant (p = 0.00000)	Not significant (p = 1.00000)
h = 7	Significant differences	116.2744	5.6406e-26	Significant (p = 0.00000)	Significant (p = 0.00000)	Not significant (p = 1.00000)
h = 8	Significant differences	118.5966	1.7664e-26	Significant (p = 0.00000)	Significant (p = 0.00000)	Not significant (p = 1.00000)
h = 9	Significant differences	106.6944	6.7859e-24	Significant (p = 0.00000)	Significant (p = 0.00000)	Not significant (p = 1.00000)
h = 10	Significant differences	98.1991	4.7461e-22	Significant (p = 0.00000)	Significant (p = 0.00000)	Not significant (p = 1.00000)
h = 11	Significant differences	89.9121	2.9912e-20	Significant (p = 0.00000)	Significant (p = 0.00000)	Not significant (p = 1.00000)
h = 12	Significant differences	93.3195	5.4442e-21	Significant (p = 0.00000)	Significant (p = 0.00000)	Not significant (p = 1.00000)

Table F18. Global Synthesis of Descriptive Statistics by Forecast Horizon and Selector – M3 - Training 70% and Testing 30%

Horizon	Selector	count	mean	median	std	min	max	IQR	MAD	Robust CV	GRA global	Final ranking
1	ERA	454	0.90300	0.92859	0.08466	0.52998	0.99985	0.10446	0.04298	0.11250	409.96342	3
1	RMSSEh	454	0.94099	0.96823	0.07176	0.53893	0.99980	0.07301	0.02508	0.07541	427.20932	2

1	AHSIV	454	0.94199	0.96897	0.07161	0.53893	0.99980	0.06968	0.02422	0.07192	427.66125	1
2	ERA	454	0.90693	0.93205	0.08022	0.57696	0.99965	0.09991	0.04356	0.10719	411.74514	3
2	RMSSEh	454	0.93824	0.96756	0.07330	0.59293	1.00000	0.07833	0.02570	0.08096	425.96156	2
2	AHSIV	454	0.93974	0.96765	0.07184	0.59293	1.00000	0.07218	0.02593	0.07459	426.64335	1
3	ERA	454	0.91148	0.93274	0.07583	0.58624	0.99954	0.09622	0.04231	0.10316	413.81129	3
3	RMSSEh	454	0.94323	0.97065	0.06660	0.57184	0.99974	0.06737	0.02460	0.06941	428.22632	2
3	AHSIV	454	0.94568	0.97324	0.06418	0.57164	0.99986	0.06505	0.02150	0.06684	429.33696	1
4	ERA	454	0.91141	0.93259	0.07425	0.58245	0.99996	0.10118	0.04277	0.10849	413.77985	3
4	RMSSEh	454	0.95004	0.97523	0.06033	0.61376	0.99994	0.06161	0.02138	0.06318	431.31639	2
4	AHSIV	454	0.95121	0.97538	0.05842	0.61376	0.99994	0.05517	0.02087	0.05657	431.84830	1
5	ERA	454	0.91186	0.93274	0.07332	0.58238	0.99886	0.09376	0.04142	0.10053	413.98540	3
5	RMSSEh	454	0.94862	0.97512	0.06157	0.62451	0.99995	0.06367	0.02081	0.06530	430.67506	2
5	AHSIV	454	0.95063	0.97567	0.05966	0.62451	0.99995	0.05386	0.02005	0.05520	431.58672	1
6	ERA	454	0.91115	0.93040	0.07374	0.57883	0.99899	0.09553	0.04305	0.10268	413.66111	3
6	RMSSEh	454	0.94762	0.97296	0.06291	0.62719	0.99998	0.06253	0.02150	0.06427	430.22096	2
6	AHSIV	454	0.94965	0.97322	0.06041	0.67737	0.99992	0.05573	0.02091	0.05727	431.14185	1
7	ERA	454	0.91313	0.93343	0.07364	0.58003	0.99993	0.09328	0.04295	0.09993	414.56199	3
7	RMSSEh	454	0.94837	0.97319	0.06167	0.63607	0.99996	0.06204	0.02172	0.06375	430.56175	2
7	AHSIV	454	0.94973	0.97346	0.06010	0.68301	0.99993	0.05585	0.02125	0.05738	431.17755	1
8	ERA	454	0.91428	0.93401	0.07302	0.57444	0.99973	0.09712	0.04220	0.10398	415.08382	3
8	RMSSEh	454	0.94959	0.97311	0.06133	0.64001	0.99999	0.05991	0.02125	0.06156	431.11392	2
8	AHSIV	454	0.95068	0.97447	0.05943	0.64968	0.99999	0.05868	0.02000	0.06022	431.60833	1
9	ERA	454	0.91499	0.93499	0.07248	0.57135	0.99999	0.09357	0.04235	0.10008	415.40459	3
9	RMSSEh	454	0.94875	0.97341	0.06029	0.64890	1.00000	0.06136	0.02126	0.06303	430.73442	2
9	AHSIV	454	0.94977	0.97335	0.05786	0.66488	1.00000	0.05835	0.02029	0.05994	431.19540	1
10	ERA	454	0.91560	0.93644	0.07258	0.57118	0.99996	0.09568	0.04123	0.10218	415.68236	3
10	RMSSEh	454	0.94851	0.97208	0.05968	0.64699	1.00000	0.06201	0.02207	0.06379	430.62292	2
10	AHSIV	454	0.94907	0.96987	0.05798	0.67820	1.00000	0.05602	0.02227	0.05776	430.87615	1
11	ERA	454	0.91722	0.93892	0.07243	0.57238	0.99959	0.09159	0.03972	0.09755	416.41612	3
11	RMSSEh	454	0.94845	0.97246	0.05930	0.64378	0.99998	0.05950	0.02194	0.06118	430.59576	2
11	AHSIV	454	0.94893	0.97155	0.05793	0.66470	0.99994	0.05589	0.02128	0.05752	430.81306	1
12	ERA	454	0.91602	0.93754	0.07221	0.57355	1.00000	0.08913	0.04038	0.09507	415.87450	3
12	RMSSEh	454	0.94736	0.97131	0.05991	0.64085	1.00000	0.06097	0.02240	0.06277	430.10188	2
12	AHSIV	454	0.94795	0.96929	0.05823	0.67604	1.00000	0.05805	0.02213	0.05989	430.37027	1

References

Abadi, M., Barham, P., Chen, J., Chen, Z., Davis, A., Dean, J., . . . others. (2016). TensorFlow: a system for Large-Scale machine learning. In *12th USENIX symposium on operating systems design and implementation (OSDI 16)* (pp. 265-283).

Abdallah, M., Rossi, R. A., Mahadik, K., Kim, S., Zhao, H., & Bagchi, S. (2025). Evaluation-free time-series forecasting model selection via meta-learning. *ACM Transactions on Knowledge Discovery from Data*, 19(3), 1-41. <https://dl.acm.org/doi/epdf/10.1145/3715149>.

Abolghasemi, M., Beh, E., Tarr, G., & Gerlach, R. (2020). Demand forecasting in supply chain: The impact of demand volatility in the presence of promotion. *Computers & Industrial Engineering*, 142, 106380. <https://doi.org/10.1016/j.cie.2020.106380>.

Aidoo-Anderson, A., Polychronakis, Y., Sapountzis, S., & Kelly, S. (2025). Investigating demand forecasting practices and challenges in Ghana's Manufacturing Pharmaceutical (MPharma) small and medium enterprises (SMEs): insights and recommendations. *International Journal of Production Research*, 1-22. <https://doi.org/10.1080/00207543.2025.2508335>.

Akiba, T., Sano, S., Yanase, T., Ohta, T., & Koyama, M. (2019). Optuna: A next-generation hyperparameter optimization framework. *Proceedings of the 25th ACM SIGKDD international conference on knowledge discovery & data mining* (pp. 2623-2631). <https://doi.org/10.1145/3292500.3330701>.

Altman, N. S. (1992). An introduction to kernel and nearest-neighbor nonparametric regression. *The American Statistician*, 46(3), 175-185. <https://doi.org/10.2307/2685209>.

Armstrong, J. S. (2001). *Principles of forecasting: a handbook for researchers and practitioners* (Vol. 30). Springer Science & Business Media.

Badulescu, Y., Hameri, A.-P., & Cheikhrouhou, N. (2021). Evaluating demand forecasting models using multi-criteria decision-making approach. *Journal of advances in management research*, 18(5), 661-683. <https://doi.org/10.1108/JAMR-05-2020-0080>.

Bandeira, S. G., Alcalá, S. G., Vita, R. O., & Barbosa, T. M. (2020). Comparison of selection and combination strategies for demand forecasting methods. *Production*, 30, e20200009. <https://doi.org/10.1590/0103-6513.20200009>.

Bassiouni, M. M., Chakrabortty, R. K., Sallam, K. M., & Hussain, O. K. (2024). Deep learning approaches to identify order status in a complex supply chain. *Expert Systems with Applications*, 250, 123947. <https://doi.org/10.1016/j.eswa.2024.123947>.

Box, G. E., Jenkins, G. M., Reinsel, G. C., & Ljung, G. M. (2015). *Time series analysis: forecasting and control*. John Wiley & Sons.

Breiman, L. (2001). Random forests. *Machine learning*, 45, 5-32. <https://doi.org/10.1023/A:1010933404324>.

Breiman, L., Friedman, J., Olshen, R. A., & Stone, C. J. (1984). *Classification and regression trees (1st ed.)*. New York: Chapman and Hall/CRC. <https://doi.org/10.1201/9781315139470>.

Brown, R. G. (1959). *Statistical forecasting for inventory control*. McGraw-Hill.

Carboneau, R., Laframboise, K., & Vahidov, R. (2008). Application of machine learning techniques for supply chain demand forecasting. *European journal of operational research*, 184(3), 1140-1154. <https://doi.org/10.1016/j.ejor.2006.12.004>.

Chatfield, C. (2000). *Time-series forecasting*. Chapman and Hall/CRC.

Chen, T., & Guestrin, C. (2016). Xgboost: A scalable tree boosting system. *Proceedings of the 22nd ACM SIGKDD international conference on knowledge discovery and data mining* (pp. 785-794). ACM. <https://doi.org/10.1145/2939672.2939785>.

Cho, K., Van Merriënboer, B., Gulcehre, C., Bahdanau, D., Bougares, F., Schwenk, H., & Bengio, Y. (2014). Learning phrase representations using RNN encoder-decoder for statistical machine translation. In *Proceedings of the 2014 Conference on Empirical Methods in Natural Language Processing (EMNLP)* (pp. 1724-1734). Doha, Qatar: Association for Computational Linguistics. <https://doi.org/10.3115/v1/D14-1179>.

Chollet, F. (2015). *Keras*. Retrieved from <https://github.com/fchollet/keras>

Clements, M. P., & Hendry, D. F. (2005). Evaluating a model by forecast performance. *Oxford Bulletin of Economics and Statistics*, 67, 931-956. <https://doi.org/10.1111/j.1468-0084.2005.00146.x>.

Clements, M., & Hendry, D. F. (1998). *Forecasting economic time series*. Cambridge University Press.

Coello, C. C. (2006). Evolutionary multi-objective optimization: a historical view of the field. *IEEE computational intelligence magazine*, 1(1), 28-36. <https://doi.org/10.1109/MCI.2006.1597059>.

Deb, K. (2011). Multi-objective optimisation using evolutionary algorithms: an introduction. *Multi-objective Evolutionary Optimisation for Product Design and Manufacturing*, 3-34. https://doi.org/10.1007/978-0-85729-652-8_1.

Demizu, T., Fukazawa, Y., & Morita, H. (2023). Inventory management of new products in retailers using model-based deep reinforcement learning. *Expert Systems with Applications*, 229, 120256. <https://doi.org/10.1016/j.eswa.2023.120256>.

Doszyń, M., & Dudek, A. (2024). Outliers in intermittent demand forecasting. *Procedia Computer Science*, 246, 4114-4122. <https://doi.org/10.1016/j.procs.2024.09.250>.

Efendigil, T. a., & Kahraman, C. (2009). A decision support system for demand forecasting with artificial neural networks and neuro-fuzzy models: A comparative analysis. *Expert systems with applications*, 36(3), 6697-6707. <https://doi.org/10.1016/j.eswa.2008.08.058>.

Erjiang, E., Yu, M., Tian, X., & Tao, Y. (2022). Dynamic Model Selection Based on Demand Pattern Classification in Retail Sales Forecasting. *Mathematics*, 10(17), 1-16. <https://doi.org/10.3390/math10173179>.

Flyckt, J., & Lavesson, N. (2025). Navigating demand forecasting in make-to-order manufacturing: The role of global models and intermittent time-series. *Proceedings of the Swedish AI Society Workshop 2025*, 4037, 12–25.

Friedman, J. H. (2001). Greedy function approximation: a gradient boosting machine. *Annals of statistics*, 1189-1232. <https://doi.org/10.1214/aos/1013203451>.

Gardner Jr, E. S. (2006). Exponential smoothing: The state of the art—Part II. *International journal of forecasting*, 22(4), 637-666. <https://doi.org/10.1016/j.ijforecast.2006.03.005>.

Garred, W., Oger, R., & Lauras, M. (2026). Automatic demand forecast model selection in supply chains: a forecast value-added analysis of selection strategies, machine learning, and hyperparameter optimisation. *International Journal of Production Research*, 1-20. <https://doi.org/10.1080/00207543.2026.2623194>.

Giannopoulos, P. G., Dasaklis, T. K., Tsantilis, I., & Patsakis, C. (2025). Machine learning algorithms in intermittent demand forecasting: a review. *International Journal of Production Research*, 1-43. <https://doi.org/10.1080/00207543.2025.2578701>.

Goltsos, T. E., Syntetos, A. A., Glock, C. H., & Ioannou, G. (2022). Inventory-forecasting: Mind the gap. *European journal of operational research*, 299(2), 397-419. <https://doi.org/10.1016/j.ejor.2021.07.040>.

González, A. (2020). Un modelo de gestión de inventarios basado en estrategia competitiva. *Ingeniare. Revista chilena de ingeniería*, 28(1), 133-142. <http://dx.doi.org/10.4067/S0718-33052020000100133>.

González, A., & Parada, V. (2026). Hierarchical evaluation function: a multi-metric approach for optimizing demand forecasting models. *Expert Systems with Applications*, 131289. <https://doi.org/10.1016/j.eswa.2026.131289>.

Goodwin, P., Hoover, J., Makridakis, S., Petropoulos, F., & Tashman, L. (2023). Business forecasting methods: Impressive advances, lagging implementation. *Plos one*, 18(12), e0295693. <https://doi.org/10.1371/journal.pone.0295693>.

Graves, A., & Schmidhuber, J. (2005). Framewise phoneme classification with bidirectional LSTM and other neural network architectures. *Neural networks*, 18(5-6), 602-610. <https://doi.org/10.1016/j.neunet.2005.06.042>.

Hammam, I. M., El-Kharbotly, A. K., & Sadek, Y. M. (2025). Adaptive demand forecasting framework with weighted ensemble of regression and machine learning models along life cycle variability. *Scientific Reports*, 15(1), 38482. <https://doi.org/10.1038/s41598-025-23352-w>.

Harris, C. R., Millman, K. J., Van Der Walt, S. J., Gommers, R., Virtanen, P., Cournapeau, D., . . . others. (2020). Array programming with NumPy. *Nature*, 585(7825), 357-362. <https://doi.org/10.1038/s41586-020-2649-2>.

Haykin, S. (1994). *Neural networks: a comprehensive foundation*. Prentice Hall PTR.

Hendry, D. F., & Pretis, F. (2023). Analysing differences between scenarios. *International Journal of Forecasting*, 39(2), 754-771. <https://doi.org/10.1016/j.ijforecast.2022.02.004>.

Hochreiter, S. a. (1997). Long short-term memory. *Neural computation*, 9(8), 1735-1780. <https://doi.org/10.1162/neco.1997.9.8.1735>.

Hoerl, A. E., & Kennard, R. W. (1970). Ridge regression: Biased estimation for nonorthogonal problems. *Technometrics*, 12(1), 55-67. <https://doi.org/10.1080/00401706.1970.10488634>.

Huber, J., Gossmann, A., & Stuckenschmidt, H. (2017). Cluster-based hierarchical demand forecasting for perishable goods. *Expert systems with applications*, 76, 140-151. <https://doi.org/10.1016/j.eswa.2017.01.022>.

Huber, P. J. (1992). Robust estimation of a location parameter. *Breakthroughs in statistics: Methodology and distribution* (pp. 492-518). Springer. <https://doi.org/10.1214/aoms/1177703732>.

Hunter, J. D. (2007). Matplotlib: A 2D graphics environment. *Computing in science & engineering*, 9(03), 90-95. <https://doi.org/10.1109/MCSE.2007.55>.

Hyndman, R. J., & Athanasopoulos, G. (2021). *Forecasting: Principles and Practice (3rd ed.)*. OTexts. <https://otexts.com/fpp3/>.

Hyndman, R. J., & Koehler, A. B. (2006). Another look at measures of forecast accuracy. *International journal of forecasting*, 22(4), 679-688. <https://doi.org/10.1016/j.ijforecast.2006.03.001>.

Katrakis, C., & Daskalaki, S. (2015). Comparing forecasting approaches for Internet traffic. *Expert systems with applications*, 42(21), 8172-8183. <https://doi.org/10.1016/j.eswa.2015.06.029>.

Khan, N. T., & Al Hanbali, A. (2025). Machine Learning Approaches for Disaggregated and Intermittent Demand Forecasting for Last-mile Logistics. *Transportation Research Procedia*, 84, 307-314. <https://doi.org/10.1016/j.trpro.2025.03.077>.

Kolassa, S., & Schütz, W. (2007). Advantages of the MAD/Mean Ratio over the MAPE. *Foresight: The International Journal of Applied Forecasting*(6), 40-43.

Kourentzes_1, N., Barrow, D. K., & Crone, S. F. (2014). Neural network ensemble operators for time series forecasting. *Expert Systems with Applications*, 41(9), 4235-4244. <https://doi.org/10.1016/j.eswa.2013.12.011>.

Kumar, V. D., Maheswari, S., Raman, Y. S., Iniyavan, S., & Hashim, S. A. (2025). Inventory Optimization and Demand Forecasting Using Machine Learning. *International Conference on Intelligent Systems and Digital Transformation (ICISD 2025)* (pp. 760-773). https://doi.org/10.2991/978-94-6463-866-0_62. Atlantis Press.

Lazcano, A., Sandubete, J. E., & Jaramillo-Morán, M. A. (2025). A Comparative Framework for Multi-Horizon Time Series Forecasting: Neural Networks with Adaptive Preprocessing. *Machine Learning with Applications*, 100781. <https://doi.org/10.1016/j.mlwa.2025.100781>.

MacKay, D. J. (1992). Bayesian interpolation. *Neural computation*, 4(3), 415-447. <https://doi.org/10.1162/neco.1992.4.3.415>.

Makridakis, S., & Hibon, M. (2000). The M3-Competition: results, conclusions and implications. *International journal of forecasting*, 16(4), 451-476. [https://doi.org/10.1016/S0169-2070\(00\)00057-1](https://doi.org/10.1016/S0169-2070(00)00057-1).

Makridakis, S., & Petropoulos, F. (2020). The M4 competition: Conclusions. *International journal of forecasting*, 36(1), 224-227. <https://doi.org/10.1016/j.ijforecast.2019.05.006>.

Makridakis, S., Spiliotis, E., & Assimakopoulos, V. (2018). Statistical and Machine Learning forecasting methods: Concerns and ways forward. *PloS one*, 13(3), e0194889. <https://doi.org/10.1371/journal.pone.0194889>.

Makridakis, S., Spiliotis, E., & Assimakopoulos, V. (2018). The M4 Competition: Results, findings, conclusion and way forward. *International Journal of forecasting*, 34(4), 802-808. <https://doi.org/10.1016/j.ijforecast.2018.06.001>.

Makridakis, S., Spiliotis, E., & Assimakopoulos, V. (2022). M5 accuracy competition: Results, findings, and conclusions. *International Journal of Forecasting*, 38(4), 1346-1364. <https://doi.org/10.1016/j.ijforecast.2021.11.013>.

Makridakis, S., Spiliotis, E., & Assimakopoulos, V. (2022). M5 accuracy competition: Results, findings, and conclusions. *International journal of forecasting*, 38(4), 1346-1364. <https://doi.org/10.1016/j.ijforecast.2021.11.013>.

Makridakis, S., Spiliotis, E., Hollyman, R., Petropoulos, F., Swanson, N., & Gaba, A. (2025). The M6 forecasting competition: Bridging the gap between forecasting and investment decisions. *International Journal of Forecasting*, 41(4), 1315-1354. <https://doi.org/10.1016/j.ijforecast.2024.11.002>.

Mancuso, A. C., & Werner, L. (2019). A comparative study on combinations of forecasts and their individual forecasts by means of simulated series. *Acta Scientiarum. Technology*, 41, e41452. <https://doi.org/10.4025/actascitechnol.v41i1.41452>.

Mentzer, J. T., & Moon, M. A. (2004). *Sales forecasting management: a demand management approach*. Sage Publications.

Montgomery, D. C., Peck, E. A., & Vining, G. G. (2021). *Introduction to linear regression analysis, 6th Edition*. John Wiley & Sons.

Negre, P., Alonso, R. S., Prieto, J., García, Ó., & de-la-Fuente-Valentín, L. (2024). Prediction of footwear demand using Prophet and SARIMA. *Expert Systems with Applications*, 255, 124512. <https://doi.org.ezproxy.usach.cl/10.1016/j.eswa.2024.124512>.

Nguyen, T. N., Nguyen, T. X., Tran, N. T., Nguyen, T. H., Nguyen, P. A., & Vu, H. A. (2026). Optimizing supply chain operations using advanced Time-Series Mixer models for demand forecasting and inventory under uncertain demand. *Expert Systems with Applications*, 296, 128955. <https://doi.org/10.1016/j.eswa.2025.128955>.

Nowotarski, J., & Weron, R. (2015). Computing electricity spot price prediction intervals using quantile regression and forecast averaging. *Computational Statistics*, 30(3), 791-803. <https://doi.org/10.1007/s00180-014-0523-0>.

Paranthaman, N., Perera, H. N., Thalagala, N. T., & Kosgoda, D. (2025). Evaluating intermittent demand forecasting techniques for spare part supply chains. *IFAC-PapersOnLine*, 59(10), 136-141. <https://doi.org/10.1016/j.ifacol.2025.09.025>.

Pedregosa, F., Varoquaux, G., Gramfort, A., Michel, V., Thirion, B., Grisel, O., . . . others. (2011). Scikit-learn: Machine learning in Python. *the Journal of machine Learning research*, 12, 2825-2830.

Peláez-Rodríguez, C., Pérez-Aracil, J., Fister, D., Torres-López, R., & Salcedo-Sanz, S. (2024). Bike sharing and cable car demand forecasting using machine learning and deep learning multivariate time series approaches. *Expert Systems with Applications*, 238, 122264. <https://doi.org/10.1016/j.eswa.2023.122264>.

Peng, T., Gan, M., Ou, Q., Yang, X., Wei, L., Ler, H. R., & Yu, H. (2024). Railway cold chain freight demand forecasting with graph neural networks: A novel GraphARMA-GRU model. *Expert Systems with Applications*, 255, 124693. <https://doi.org/10.1016/j.eswa.2024.124693>.

Pesendorfer, M., Schiraldi, P., & Silva-Junior, D. (2023). Omitted budget constraint bias in discrete-choice demand models. *International Journal of Industrial Organization*, 86, 102889. <https://doi.org/10.1016/j.ijindorg.2022.102889>.

Petropoulos, F., Apiletti, D., Assimakopoulos, V., Babai, M. Z., Barrow, D. K., Taieb, S. B., . . . others. (2022). Forecasting: theory and practice. *International Journal of forecasting*, 38(3), 705-871. <https://doi.org/10.1016/j.ijforecast.2021.11.001>.

Petropoulos, F., Kourentzes, N., Nikolopoulos, K., & Siemsen, E. (2018). Judgmental selection of forecasting models. *Journal of Operations Management*, 60, 34-46. <https://doi.org/10.1016/j.jom.2018.05.005>.

Petropoulos, F., Wang, X., & Disney, S. M. (2019). The inventory performance of forecasting methods: Evidence from the M3 competition data. *International Journal of Forecasting*, 35(1), 251-265. <https://doi.org/10.1016/j.ijforecast.2018.01.004>.

Poler, R., & Mula, J. (2011). Forecasting model selection through out-of-sample rolling horizon weighted errors. *Expert Systems with Applications*, 38(12), 14778-14785. <https://doi.org/10.1016/j.eswa.2011.05.072>.

Porter, M. (1998). *Competitive Advantage: Creating and Sustaining Superior Performance*. Nueva York, Estados Unidos: Free Press.

Prokhorenkova, L., Gusev, G., Vorobev, A., Dorogush, A. V., & Gulin, A. (2018). CatBoost: unbiased boosting with categorical features. *Advances in neural information processing systems*, 31, 6638–6648. <https://dl.acm.org/doi/10.5555/3327757.3327770>.

Riachy, C., He, M., Joneidy, S., Qin, S., Payne, T., Boulton, G., . . . Angione, C. (2025). Enhancing deep learning for demand forecasting to address large data gaps. *Expert Systems with Applications*, 268, 126200. <https://doi.org/10.1016/j.eswa.2024.126200>.

Sanders, N. R., & Graman, G. A. (2016). Impact of bias magnification on supply chain costs: The mitigating role of forecast sharing. *Decision Sciences*, 47(5), 881-906. <https://doi.org/10.1111/deci.12208>.

Santa Cruz, R., & Corrêa, C. (2017). Intermittent demand forecasting with time series methods and artificial neural networks: A case study. *DYNA: revista de la Facultad de Minas. Universidad Nacional de Colombia. Sede Medellín*, 84(203), 9-16. <https://doi.org/10.15446/dyna.v84n203.63141>.

Sayed, H. E., Gabbar, H. A., & Miyazaki, S. (2009). A hybrid statistical genetic-based demand forecasting expert system. *Expert Systems with Applications*, 36(9), 11662-11670. <https://doi.org/10.1016/j.eswa.2009.03.014>.

Schuster, M., & Paliwal, K. K. (1997). Bidirectional recurrent neural networks. *IEEE transactions on Signal Processing*, 45(11), 2673-2681. <https://doi.org/10.1109/78.650093>.

Seabold, S., Perktold, J., & others. (2010). Statsmodels: econometric and statistical modeling with python. *SciPy*, 7(1), 92-96.

Semenoglou, A.-A., Spiliotis, E., Makridakis, S., & Assimakopoulos, V. (2021). Investigating the accuracy of cross-learning time series forecasting methods. *International Journal of Forecasting*, 37(3), 1072-1084. <https://doi.org/10.1016/j.ijforecast.2020.11.009>.

Sepúlveda-Rojas, J. P., Rojas, F., Valdés-González, H., & San Martín, M. (2015). Forecasting models selection mechanism for supply chain demand estimation. *Procedia Computer Science*, 55, 1060-1068. <https://doi.org/10.1016/j.procs.2015.07.068>.

Shi, Y., Ding, J., Qu, T., & Xie, B. (2026). Beverage manufacturing demand forecasting system driven by multi-stage machine learning model pool. *Applied Soft Computing*, 114254. <https://doi.org/10.1016/j.asoc.2025.114254>.

Silver, E. A., Pyke, D. F., Peterson, R., & others. (1998). *Inventory management and production planning and scheduling* (Vol. 3). Wiley New York.

Smola, A. J., & Schölkopf, B. (2004). A tutorial on support vector regression. *Statistics and computing*, 14, 199-222. <https://doi.org/10.1023/B:STCO.0000035301.49549.88>.

Song, X., Chang, D., Gao, Y., Huang, Q., & Ye, Z. (2025). An aggregate--disaggregate framework for forecasting intermittent demand in fast fashion retailing. *Advanced Engineering Informatics*, 64, 103069. <https://doi.org/10.1016/j.aei.2024.103069>.

Sousa, M. a., & Miguéis, V. (2025). Predicting demand for new products in fashion retailing using censored data. *Expert systems with applications*, 259, 125313. <https://doi.org/10.1016/j.eswa.2024.125313>.

Syntetos, A. A., & Boylan, J. E. (2005). The accuracy of intermittent demand estimates. *International Journal of forecasting*, 21(2), 303-314. <https://doi.org/10.1016/j.ijforecast.2004.10.001>.

Syntetos, A. A., Boylan, J. E., & Croston, J. (2005). On the categorization of demand patterns. *Journal of the operational research society*, 56(5), 495-503. <https://doi.org/10.1057/palgrave.jors.2601841>.

Taghiyeh, S., Lengacher, D. C., & Handfield, R. B. (2020). Forecasting model selection using intermediate classification: Application to MonarchFx corporation. *Expert Systems with Applications*, 151, 113371. <https://doi.org/10.1016/j.eswa.2020.113371>.

Tashman, L. J. (2000). Out-of-sample tests of forecasting accuracy: an analysis and review. *International journal of forecasting*, 16(4), 437-450. [https://doi.org/10.1016/S0169-2070\(00\)00065-0](https://doi.org/10.1016/S0169-2070(00)00065-0).

Team, T. P. (2020). pandas-dev/pandas: Pandas. *Zenodo*, <https://doi.org/10.5281/zenodo.3509134>.

Theodorou, E., Spiliotis, E., & Assimakopoulos, V. (2025). Forecast accuracy and inventory performance: Insights on their relationship from the M5 competition data. *European Journal of Operational Research*, 322(2), 414-426. <https://doi.org/10.1016/j.ejor.2024.12.033>.

Tibshirani, R. (1996). Regression shrinkage and selection via the lasso. *Journal of the Royal Statistical Society Series B: Statistical Methodology*, 58(1), 267-288.
<https://academic.oup.com/jrssb/article/58/1/267/7027929>.

Ulrich, M., Jahnke, H., Langrock, R., Pesch, R., & Senge, R. (2022). Classification-based model selection in retail demand forecasting. *International Journal of Forecasting*, 38(1), 209-223. <https://doi.org/10.1016/j.ijforecast.2021.05.010>.

Vaswani, A. a. (2017). Attention is all you need. *Advances in neural information processing systems*, 30.

Virtanen, P., Gommers, R., Oliphant, T. E., Haberland, M., Reddy, T., Cournapeau, D., . . . others. (2020). SciPy 1.0: fundamental algorithms for scientific computing in Python. *Nature methods*, 17(3), 261-272. <https://doi.org/10.1038/s41592-019-0686-2>.

Wang, X., Hyndman, R. J., Li, F., & Kang, Y. (2023). Forecast combinations: An over 50-year review. *International Journal of Forecasting*, 39(4), 1518-1547.
<https://doi.org/10.1016/j.ijforecast.2022.11.005>.

Waskom, M. L. (2021). Seaborn: statistical data visualization. *Journal of open source software*, 6(60), 3021. <https://doi.org/10.21105/joss.03021>.

Yasser, H. (2021). *Walmart Sales Prediction - (Best ML Algorithms)*. Retrieved Mayo 2024, from Kaggle: <https://www.kaggle.com/code/yasserh/walmart-sales-prediction-best-ml-algorithms>

Zhao, S., Xie, T., Ai, X., Yang, G., & Zhang, X. (2023). Correcting sample selection bias with model averaging for consumer demand forecasting. *Economic Modelling*, 123, 106275.
<https://doi.org/10.1016/j.econmod.2023.106275>.

Zou, H., & Hastie, T. (2005). Regularization and variable selection via the elastic net. *Journal of the Royal Statistical Society Series B: Statistical Methodology*, 67(2), 301-320.
<https://doi.org/10.1111/j.1467-9868.2005.00503.x>.